BICTAM-CISM Symposium on Dispersed Multiphase Flows: From Measuring to Modeling

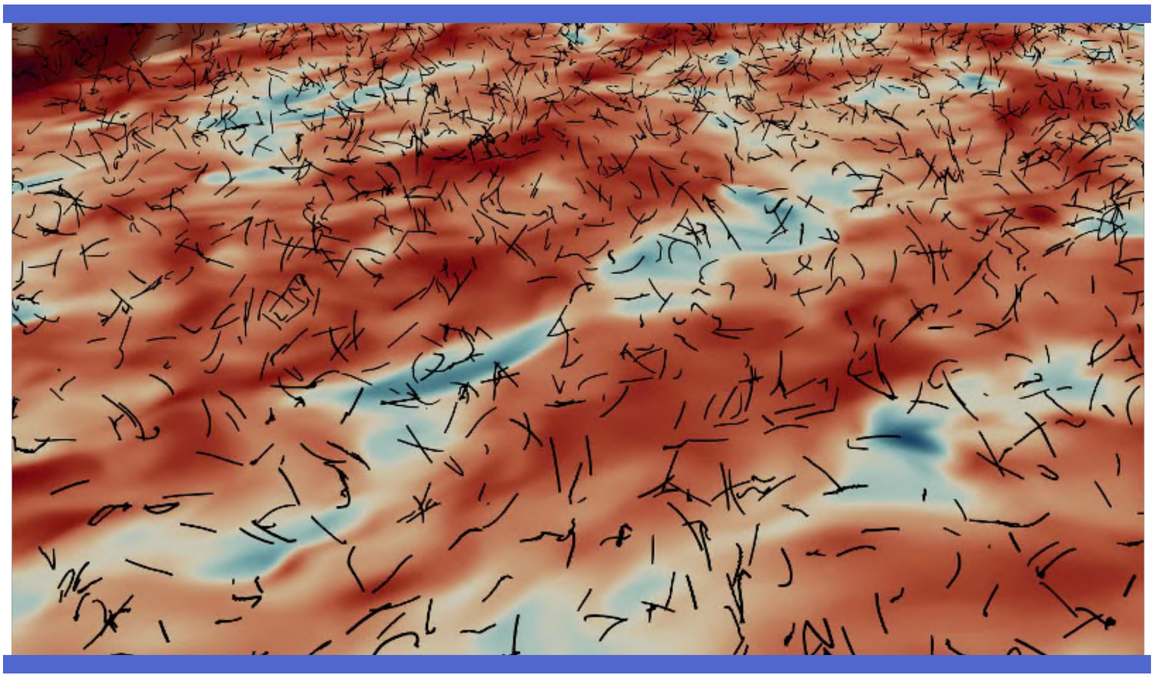

Udine, Italy

July 22-24, 2026

http://calliope.dem.uniud.it/BICTAM-CISM-2026/

Cover image: Flexible fibers dispersed in turbulent channel flow

Image credits: Davide Di Giusto, Cristian Marchioli

SYMPOSIUM SCHEDULE-AT-A-GLANCE

Wednesday, July 22, 2026

Time	
8:30 - 9:00	Registration & Opening Remarks
9:00 - 9:40	Keynote Lecture: Chao Sun, CHN
9:45-10:30	Session #1-1 (regular talks)
10:30-11:00	Coffee break
11:00-12:45	Session #1-2 (regular talks)
12:45-14:00	Lunch
14:00-14:40	Keynote Lecture: Omar Matar, UK
14:45-16:00	Session #2-1 (regular talks)
16:00-16:30	Coffee break
16:30-18:15	Session #2-2 (regular talks)

Thursday, July 23, 2026

Time	
8:45 - 9:25	Keynote Lecture: Gholamhossein Bagheri, GER
9:30-10:30	Session #3-1 (regular talks)
10:30-11:00	Coffee break
11:00-12:45	Session #3-2 (regular talks)
12:45-14:00	Lunch
14:00-14:40	Keynote Lecture: Kun Xue, CHN
14:45-16:00	Session #4-1 (regular talks)
16:00-16:30	Coffee break
16:30-18:15	Session #4-2 (regular talks)

Friday, July 24, 2026

Time	
8:45 - 9:25	Keynote Lecture: Yantao Yang, CHN
9:30-10:30	Session #5-1 (regular talks)
10:30-11:00	Coffee break
11:00-12:45	Session #5-2 (regular talks)
12:45-14:00	Lunch
14:00-14:40	Keynote Lecture: Julien Chauchat, FRA
14:45-16:00	Session #6-1 (regular talks)
16:05-16:15	Closing

WELCOME

On behalf of the Scientific and Organizing Committee, we warmly welcome you to the 3rd BICTAM-CISM Symposium on Dispersed Multiphase Flows: From Measuring to Modeling.

The Symposium brings together experts from Europe and China working across the complementary fields of physics, applied mathematics, chemistry and engineering, with the shared goal of presenting and discussing recent advances in research, development and applications related to dispersed multiphase flows. By gathering graduate students, postdoctoral researchers, faculty and industry scientists under one roof, the Symposium fosters the cross-pollination of new ideas, methods and results across generations and communities.

To sustain a long-lasting scientific dialogue between the two communities, the Symposium is organized every two years, alternating between China and Europe. The 1st edition was held in 2021, organized by BICTAM and Tsinghua University; owing to the Covid-19 pandemic, it took place in virtual mode. The 2nd edition returned to an in-person format in 2024, again organized by BICTAM and Tsinghua University in Beijing. This 3rd edition, organized by the University of Udine, marks a further step in the growth of the Symposium: we have received contributions from 11 countries, and the scientific program features 6 keynote lectures and 62 regular presentations spanning the full breadth of the field.

We hope that the coming days will offer all participants rich scientific exchanges, fruitful collaborations, and a memorable experience in Udine.

Lihao Zhao

Lihao Zhao, BICTAM & Tsinghua University
Chairman of the Symposium

Cristian Marchioli

Cristian Marchioli, CISM & University of Udine
Chairman of the Symposium

SYMPOSIUM SCOPE

The Symposium will provide the opportunity to compare and contrast the different available approaches, giving a global overview of the most significant advancements in the field. It will also serve the purpose of identifying the main open issues and research pathways that the community should focus on in the future. To these aims the Symposium will bring together internationally renowned scientists from all horizons (analytical, numerical, and experimental) to foster scientific exchange and strengthen interdisciplinary work among engineers, applied mathematicians, and physicists through invited keynote lectures and contributed talks.

TOPICS

The Symposium spans a wide selection of topics in the broad area of dispersed multiphase flows. The focus will be on generic aspects and physics of particulate flows (both viscous and turbulent), be it computer simulations, laboratory or field measurements, and theoretical studies. The topics included in the program are: Particle dynamics in turbulence, bubble dynamics, droplet and interfacial flows, fiber and elongated particle dynamics, multiphase turbulence, stochastic and continuum modelling, DNS, LES and CFD of multiphase flows, experimental methods and diagnostics, particle interactions and fragmentation, reactive and thermal multiphase flows, biofluid dynamics, sediment transport and environmental flows.

ORGANIZATION

The Symposium's physical venue will be the Auditorium Sgorlon (via Monsignor Pasquale Margreth 3, 33100 Udine).

ACKNOWLEDGEMENT

The Symposium is sponsored by IUTAM, BICTAM, CISM, Institute of Mechanics of Chinese Academy of Sciences and School of Aerospace Engineering of Tsinghua University.

SYMPOSIUM CHAIRMEN

- Professor Lihao Zhao, BICTAM & Tsinghua University (CHN)
- Professor Cristian Marchioli, CISM & University of Udine (Italy)

SCIENTIFIC COMMITTEE

- Carlo Massimo Casciola, University of Roma “La Sapienza” (ITA)
- Eric Climent, ABEL CNRS / Imperial (FRA/UK)
- Gaetano D’Avino, University of Napoli Federico II (ITA)
- Elisabetta De Angelis, University of Bologna (ITA)
- Xiqiao Feng, Tsinghua University (CHN)
- Weixi Huang, Tsinghua University (CHN)
- Guodong Jin, Chinese Academy of Sciences (CHN)
- Jianzhong Lin, Zhejiang University (CHN)
- Kun Luo, Zhejiang University (CHN)
- Cristian Marchioli, University of Udine (ITA)
- Marco Mazzuoli, University of Genova (ITA)
- Ming-Jiu Ni, University of Chinese Academy of Sciences (CHN)
- Francesco Picano, University of Padova (ITA)
- Christian Poelma, TU Delft (NED)
- Wolfgang Schröder, RWTH Aachen (GER)
- Alfredo Soldati, TU Wien (AUT)
- Chao Sun, Tsinghua University (CHN)
- Markus Uhlmann, Karlsruhe Institute of Technology (GER)
- Bing Wang, Tsinghua University (CHN)
- Lianping Wang, Southern University of Science and Technology (CHN)
- Chunxiao Xu, Tsinghua University (CHN)
- Haitao Xu, Tsinghua University (CHN)
- Zhaosheng Yu, Zhejiang University (CHN)
- Lihao Zhao, Tsinghua University (CHN)
- Xiaojing Zheng, Xidian University (CHN)

ORGANIZING COMMITTEE

- Cristian Marchioli, University of Udine (ITA)
- Alessio Roccon (Scientific Secretary), University of Udine (ITA)
- Lihao Zhao, Tsinghua University (CHN)
- Jie Chen, BICTAM (CHN)

SYMPOSIUM VENUE

Auditorium Sgorlon
Address: via Monsignor Pasquale Margreth 3, 33100 Udine
The auditorium is walking distance from all hotels in downtown Udine.

Maps:

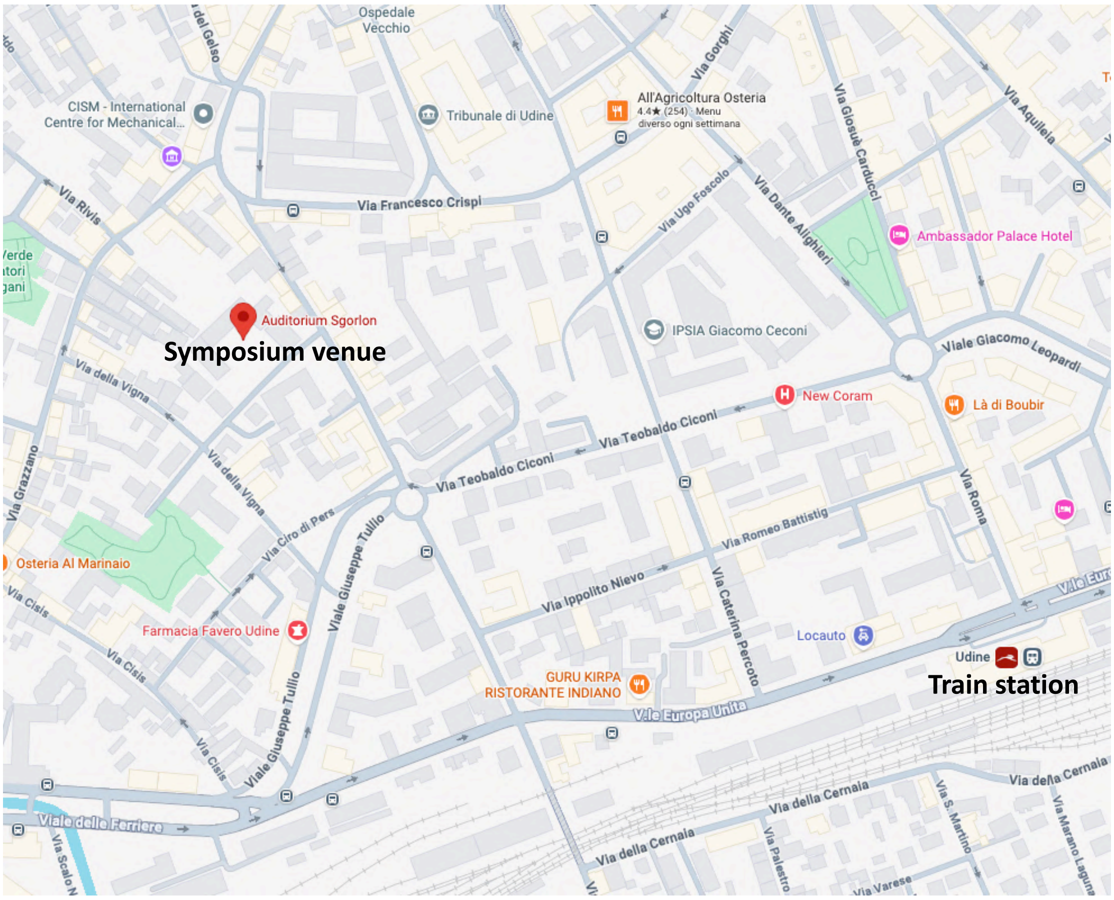

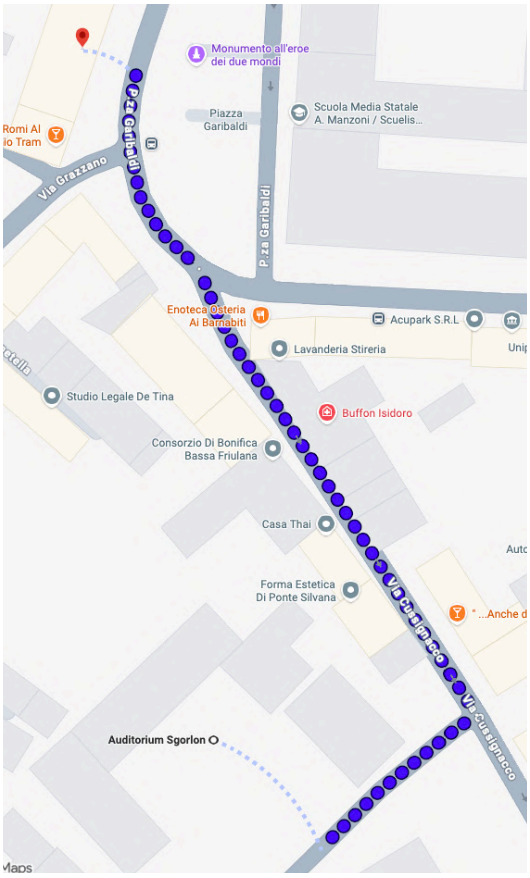

From Auditorium Sgorlon to CISM (240 m, 3-minute walk).

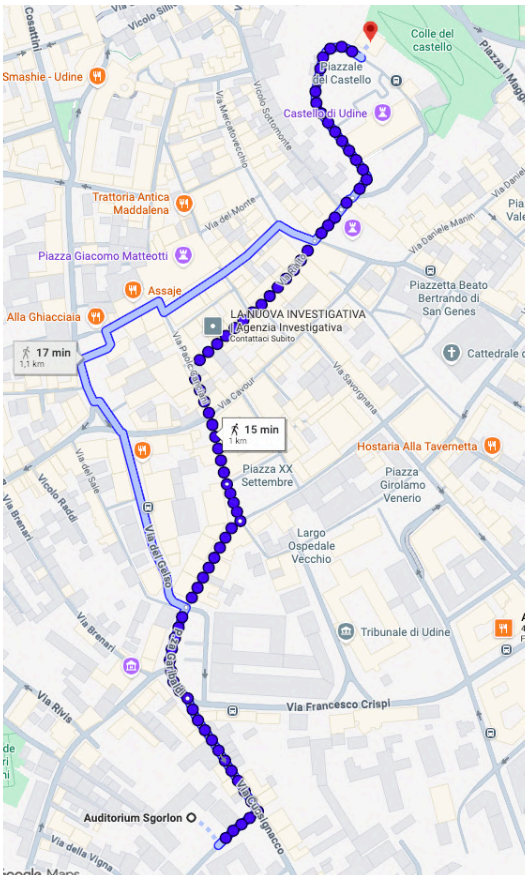

From Auditorium Sgorlon to Casa della Contadinanza (venue of the social dinner, 1 km, 15-minute walk).

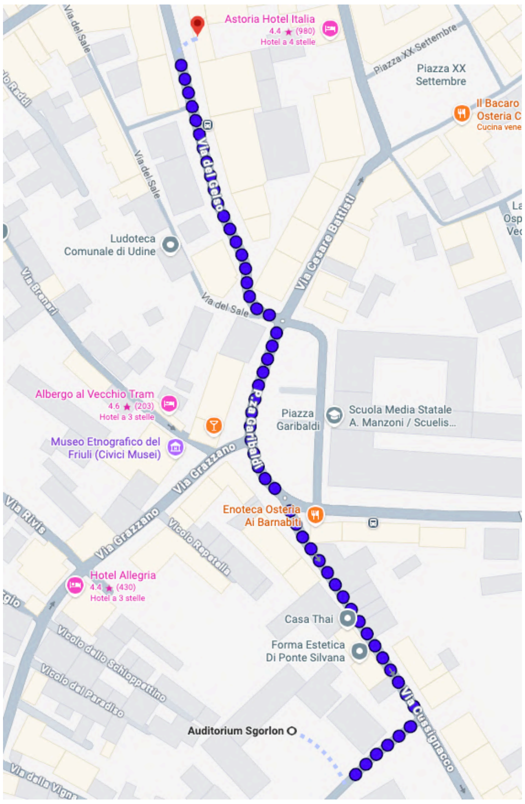

From Auditorium Sgorlon to Pizzeria al Gelso (venue of the pizza dinner, 450 m, 6-minute walk).

USEFUL INFORMATION

Registration Desk Hours

Wednesday, July 22, 8:30 am – 11:00 am
Thursday, July 23, 8:45 am – 11:00 am
Friday, July 24, 8:45 am – 11:00 am

The registration desk is located at the symposium venue, Auditorium Sgorlon (address: via Monsignor Pasquale Margreth 3, 33100 Udine)

Pizza Dinner and Social Dinner

The Pizza Dinner (which includes 1 pizza + 1 drink) will be held on Wednesday, July 22 (19:45 -21:45), at Ristorante Pizzeria Al Gelso (Via del Gelso 10, Udine).

The Social Dinner (which includes a fixed menu) will be held on Thursday, July 23 (20:00-22:30), at the restaurant Casa della Contadinanza (Piazzale della Patria del Friuli 2, Udine).

Admission to both dinners will be limited to registered participants (please, bring your badge) and to registered accompanying persons.

Pizzeria Al Gelso

Casa della Contadinanza

Wi-Fi
Participants may access Internet via Eduroam.

Public transportation in Udine
For detailed information on public transportation in Udine, click HERE.

INVITED SPEAKERS

Wednesday, July 22, 2026

Professor Chao Sun
Tsinghua University (CHN)

The physics of flowing dense emulsions in wall-bounded turbulence

Professor Omar Matar
Imperial College London (UK)

Numerical simulations of complex multiphase flows

Thursday, July 23, 2026

Professor Gholamhossein (Mohsen) Bagheri
Max Planck Institute for Dynamics and Self-Organization (GER)

The mystery of the lucky droplet: can turbulence trigger rain in warm clouds?

Professor Kun Xue
Beijing Institute of Technology (CHN)

Engineering method for cross-scale evolution of supersonic droplet cloud

Friday, July 24, 2026

Professor Yantao Yang
Peking University (CHN)

A numerical framework for multi-medium and multi-component incompressible flows and its applications in natural and engineering systems

Professor Julien Chauchat
INRAE Grenoble (FRA)

From turbulence to ripples: a two-fluid perspective on sediment transport

INSTRUCTIONS FOR SPEAKERS AND SESSION CHAIRS

1. Keynote talks are assigned 35 minutes for presentation, plus additional 5 minutes for questions and change of speaker.
2. Regular contributed talks are assigned 12 minutes for presentation, plus additional 3 minutes for questions and change of speaker.
3. Chairpersons are kindly asked to maintain the schedule, even in the case of no-show.
4. The conference room will be equipped with a PC (capable of displaying PDF, Keynote and Powerpoint presentations), an LCD projector and a laser presentation pointer.
5. Speakers may use their own laptop. However, in order to minimize technical difficulties, they are also kindly invited to upload their presentation in the conference PC and test the presentation well beforehand.
6. Please prepare a good quality portable PDF version of the presentation in the case other formats are not supported by the PC.

Symposium Program

Wednesday July 22nd (Day 1)

	Time			CHAIRPERSON
	From	To		
	8:50	9:00	Opening Remarks	Cristian Marchioli Lihao Zhao
Keynote #1	9:00	9:40	**The physics of flowing dense emulsions in wall-bounded turbulence** **Speaker: Chao Sun, Tsinghua University, China**	Lihao Zhao Tsinghua University
Session #1-1 Theory and Stochastic Modelling	9:45	10:00	Modelling of particle diffusion in turbulence using the kinetic PDF approach Speaker: Chris Stafford, University of Manchester, UK	Thomas Pähtz Zhejiang University
	10:00	10:15	Unified Lagrangian stochastic modelling for acceleration and velocity gradient in isotropic turbulence Speaker: Ramiro Ezequiel Castro Torre, IMFT Toulouse, France	
	10:15	10:30	In the footsteps of Albert Einstein – A kinetic theory for the dispersion and clustering of turbulent gas particle suspensions Speaker: Mike Reeks, Newcastle University, UK	
	10:30	11:00	Coffee break	
Session #1-2 Multiphase Modelling and Numerical Methods	11:00	11:15	Pair dispersion by intermittent wavelet-based stochastic fields Speaker: Clément Morhain, Université Paris-Saclay, France	Ping Wang Lanzhou University & Chris Stafford Iowa State University
	11:15	11:30	Eulerian-Lagrangian framework for simulations of dispersed multiphase flows with interacting particles and/or polymers Speaker: Francesco Serafini, University of Rome "La Sapienza", Italy	
	11:30	11:45	Euler-Lagrange LES of turbulent bubble plumes with a new lift force model Speaker: Mohammad Karimi Zand, Metallurgical Competence Center Linz, Austria	
	11:45	12:00	A unified mesoscopic framework for two-phase flows via inverse design Speaker: Jun Lai, Guangzhou Maritime University, China	
	12:00	12:15	A wall-modeled LES framework for particle-laden turbulent flows in complex geometries Speaker: Francesco Picano, University of Padova, Italy	
	12:15	12:30	The effect of electrostatic interactions on bidisperse charged particles transported by a homogeneous isotropic turbulence Speaker: Clovis Schoeck, IMFT Toulouse, France	
	12:30	12:45	On the buoyancy force density in two-fluid continuum models Speaker: Thomas Pähtz, Zhejiang University, China	
	12:45	14:00	Lunch	
Keynote #2	14:00	14:40	**Numerical simulations of complex multiphase flows** **Speaker: Omar Matar, Imperial College London, UK**	Andrea Mazzino University of Genova

Session #2-1 Fibers and Elongated Particles I	14:45	15:00	Tomographic PIV study of fiber-flow interaction in a turbulent channel flow Speaker: Dominic S. Sebastian, Technion, Israel	Mohsen Bagheri Max Planck Institute for Dynamics and Self-Organization
	15:00	15:15	Optical activity-based measurements of fiber-flow interaction in the near-wall region of a turbulent channel flow Speaker: Vlad Rinsky, Technion, Israel	
	15:15	15:30	Direct numerical simulations of a dilute turbulent jet laden with spheroidal particles Speaker: Jietuo Wang, Tsinghua University, China	
	15:30	15:45	Fiber fragmentation in turbulence Speaker: Harishankar Muppirala, University of Udine, Italy	
	15:45	16:00	Dynamics of long flexible fibers turbulent flow Speaker: Darish Jeswin Dhas, University of Udine, Italy	
	16:00	16:30	Coffee break	
Session #2-2 Particle Dynamics in Turbulence	16:30	16:45	Inertial particle clustering in the transitional wake of a normal flat plate Speaker: Deekshith I. Poojary, IIT Madras, India	Mike Reeks Newcastle University & Francesco Picano University of Padova
	16:45	17:00	Decoupling between inertial and gravitational effects in the dynamics of particles in turbulence Speaker: Jérémie Auzoux, ENS Lyon, University of Lyon, France	
	17:00	17:15	Settling velocity of Kolmogorov-size and finite-size particles in homogeneous isotropic turbulence Speaker: Zhaosheng Yu, Zhejiang University, China	
	17:15	17:30	Slip and unsteady drag dynamics of finite-size inertial particles in homogeneous turbulence under micro-gravity Speaker: Facundo Cabrera-Booman, University of Nevada, Reno, USA	
	17:30	17:45	Inertial particle settling in turbulence under gravity: the roles of preferential sampling and loitering Speaker: Hugo Pradel, ENS Lyon, University of Lyon, France	
	17:45	18:00	Stochastic resonance of rotating particles in turbulence Speaker: Ziqi Wang, Eindhoven University of Technology, The Netherlands	
	18:00	18:15	Particle-resolved simulations of many spherical particles settling in an inflow/outflow configuration Speaker: Manuel Moriche, Wien University of Technology, Austria	

	19:45	21:45	Pizza Dinner @ Ristorante Pizzeria Al Gelso (Via del Gelso 10, Udine)	

Thursday July 23rd (Day 2)

	Time			CHAIRPERSON
	From	To		
Keynote #3	8:45	9:25	**The mystery of the lucky droplet: Can turbulence trigger rain in warm clouds?**	Dominik Krug RWTH Aachen
			Speaker: Gholamhossein (Mohsen) Bagheri, Max Planck Institute for Dynamics and Self-Organization, Germany	
Session #3-1 Bubble Dynamics I	9:30	9:45	Influence of dissolved gas concentration on the lifetime of surface bubbles in volatile liquids	Maike Baltussen Eindhoven University of Technology
			Speaker: Yanshen Li, University of Chinese Academy of Sciences, China	
	9:45	10:00	Capillary migration of floating bubbles at a free surface	
			Speaker: Kuntal Patel, Max Planck Institute Gottingen, Germany	
	10:00	10:15	Why a pair of bubbles rising in-line becomes more stable with the shape oblateness	
			Speaker: Jie Zhang, Xi'an Jiaotong University, China	
	10:15	10:30	Predicting the bubble-particle collision rate in turbulence	
			Speaker: Dominik Krug, RWTH Aachen, Germany	
	10:30	11:00	Coffee break	
Session #3-2 Droplets, Interfaces and Marangoni Flows	11:00	11:15	Spatiotemporal analysis of single droplet under HIT	Eric Climent ABEL CNRS / Imperial & Chao Sun Tsinghua University
			Speaker: Arda Safak, Johannes Kepler University, Austria	
	11:15	11:30	Solutal-Marangoni-driven freezing dynamics of supercooled ethanol-water droplets	
			Speaker: Feng Wang, Tsinghua University, China	
	11:30	11:45	A one-half law relating viscous-pressure and viscous-stress forces on a spherical droplet in incompressible flow	
			Speaker: Tian Long, Xi’an Jiaotong University, China	
	11:45	12:00	Dynamics of polymer-laden drops on inclined surfaces	
			Speaker: Jessica Wilson, Tsinghua University, China	
	12:00	12:15	Droplets in HIT: 3D internal flow measurement	
			Speaker: Fabio Sortini, Wien University of Technology, Austria	
	12:15	12:30	Marangoni instabilities of thin cylindrical drops vertically immersed in stratified liquids	
			Speaker: Li-Chen Huang, University of Chinese Academy of Sciences, China	
	12:30	12:45	The multifractal structure of energy dissipation in multiphase turbulence	
			Speaker: Marco Crialesi-Esposito, University of Modena and Reggio Emilia, Italy	
	12:45	14:00	Lunch	
Keynote #4	14:00	14:40	**Engineering method for cross-scale evolution of supersonic droplet cloud**	Chiyu Xie Beihang University
			Speaker: Kun Xue, Beijing Institute of Technology, China	

Session #4-1 Fibers and Elongated Particles II	14:45	15:00	Interface-resolved DNS studies of flexible fiber dynamics in a fluid using an LBM-DEM method Speaker: Junjie Chen, Zhejiang University, China	Cristian Marchioli University of Udine
	15:00	15:15	Modelling of elongated particles in channel flows with realistic rough walls Speaker: Manuel A. Taborda, Otto-von-Guericke University Magdeburg, Germany	
	15:15	15:30	Numerical simulation of a long flexible fibre in a lid-driven fluid cavity Speaker: Subhadrakutty (Subbu) Radhakrishnakumar, Dresden University of Technology, Germany	
	15:30	15:45	Length effect on rigid fiber dynamics in turbulent channel flow Speaker: Defa Sun, Université Côte d'Azur, CNRS, France	
	15:45	16:00	Fragmentation of slender fibres by inertial-range turbulence: Quasi-static mechanics, hazard scaling and intermittency effects Speaker: Andrea Mazzino, University of Genova, Italy	
	16:00	16:30	Coffee break	
Session #4-2 Turbulence, Complex Flows and Biofluid Dynamics	16:30	16:45	Numerical investigation of drag enhancement by interfacial tension in Taylor–Couette turbulence Speaker: Jinghong Su, China University of Petroleum (Beijing), China	Elisabetta De Angelis University of Bologna & Ruifeng Hu Lanzhou University
	16:45	17:00	Length scales and interphase energy transfer in turbulent gas-particle flows Speaker: Simon Schneiderbauer, Johannes Kepler University, Austria	
	17:00	17:15	A sharp interface multiphase method for shock-induced reactive droplets with phase change Speaker: Shucheng Pan, Northwestern Polytechnical University, China	
	17:15	17:30	The dynamics of copepods in turbulence: how micro-swimmers can adapt their behaviour Speaker: Eric Climent, ABEL CNRS / Imperial, France / UK	
	17:30	17:45	Swimmer-resolving simulations on the biogenic hydrodynamic transport of cruising copepods Speaker: Rui Zhu, Dresden University of Technology, Germany	
	17:45	18:00	Lagrangian angular velocity of fluid elements in homogeneous isotropic turbulence Speaker: Zhiwen Cui, Hunan University, China	
	18:00	18:15	Time-reversal-symmetry breaking in free-surface turbulence Speaker: Yaxing Li, Zhejiang University, China	

	19:45	23:00	Social Dinner Casa della Contadinanza (P.le della Patria del Friuli 2, Udine)	

Friday July 24th (Day 3)

	Time			CHAIRPERSON
	From	To		
Keynote #5	8:45	9:25	**A numerical framework for multi-medium and multi-component incompressible flows and its applications in natural and engineering systems**	Zhaosheng Yu Zhejiang University
			Speaker: Yantao Yang, Peking University, China	
Session #5-1 Bubble Dynamics II	9:30	9:45	Bubble-generated turbulent convection in a liquid vessel	Marco Crialesi-Esposito University of Modena and Reggio Emilia
			Speaker: Ron Shnapp, Ben-Gurion University of the Negev, Israel	
	9:45	10:00	Preferential flow control by non-coalescing multi-bubble systems in pore-doublet channels	
			Speaker: Caoxing Mo, Beihang University, China	
	10:00	10:15	Eliminating spurious currents in the simulation of hydrogen micro-bubbles for electrolysis	
			Speaker: Maike Baltussen, Eindhoven Univ. Technology, The Netherlands	
	10:15	10:30	Dynamics of a large spherical bubble in a turbulent flow	
			Speaker: Elisabetta De Angelis, University of Bologna, Italy	
	10:30	11:00	Coffee break	
Session #5-2 Reactive, Thermal and Industrial Flows	11:00	11:15	Numerical simulation of powder melting and multiphase keyhole dynamics in laser powder bed fusion	Yaxing Li Zhejiang University & Simon Schneiderbauer Johannes Kepler University
			Speaker: Zhiyuan Yang, Zhejiang University, China	
	11:15	11:30	Asymmetric particle transport in turbulent flows within concentric annular ducts	
			Speaker: Chi Zhang, Peking University, China	
	11:30	11:45	Numerical investigation of cohesive iron powder fluidization in metal energy storage systems	
			Speaker: Bingchen Li, Zhejiang University, China	
	11:45	12:00	Wall-bounded turbulence driven by heat-releasing particles	
			Speaker: Yuhang Du, Hebei University, China	
	12:00	12:15	Active control of bubbling fluidized bed by coupling deep reinforcement learning with reduced-order model	
			Speaker: Junjie Lin, Zhejiang University, China	
	12:15	12:30	Release of ice-entrapped bubbles accelerates melting	
			Speaker: Jin Hu, Tsinghua University, China	
	12:30	12:45	Direct numerical simulation of boiling	
			Speaker: Alessio Roccon, University of Udine, Italy	
	12.45	14:00	Lunch	
Keynote #6	14:00	14:40	**From turbulence to ripples: A two-fluid perspective on sediment transport**	Kun Xue Beijing Institute of Technology
			Speaker: Julien Chauchat, INRAE Grenoble, France	
	14:45	15:00	Simulating aeolian sand transport with a turbulence-informed stochastic particle force model	
			Speaker: Ruifeng Hu, Lanzhou University, China	

Session #6-1 Sediment Transport and Environmental Flows	15:00	15:15	Sediment transport in a half-channel turbulent flow: The effect of density	Julien Chauchat INRAE Grenoble
			Speaker: Xinyu Jiang, Polytechnic University of Torino, Italy	
	15:15	15:30	Numerical study of the randomness of single particle entrainment in wall turbulence on rough bed	
			Speaker: Ping Wang, Lanzhou University, China	
	15:30	15:45	Wave-induced transport of neutrally buoyant particles over a shallow rippled seabed	
			Speaker: Karthikeyan Jagadeesan, University of Genova, Italy	
	15:45	16:00	Wall-resolved large-eddy simulation of electrification of wind-blown sand flows	
			Speaker: Huan Zhang, Lanzhou University, China	
Closing	16:05	16:15	Closing Remarks	Lihao Zhao, Cristian Marchioli

ABSTRACTS

Modelling of particle diffusion in turbulence using the kinetic PDF approach

C.P. Stafford[1], D.C. Swailes[2] and M.W. Reeks[3]
[1] Department of Mechanical and Aerospace Engineering, University of Manchester, Manchester, UK
[2] School of Mathematics, Statistics & Physics, Newcastle University, Newcastle upon Tyne, UK
[3] School of Engineering, Newcastle University, Newcastle upon Tyne, UK

Diffusion is a dominant factor affecting dispersion within particle-laden flows, and naturally appears within continuum models for such systems. The associated diffusion coefficient in these formulations is usually a mean-field description however, and does not take into account the effect of the structures that are inherent to the turbulent carrier flow. To address this, models exist that describe the diffusion coefficient in terms of the carrier flow velocity correlations. The analysis of Tchen (1947) concluded that in homogeneous isotropic turbulence the particle and carrier flow diffusion coefficients are equal in the long-time limit,

$$D_{ij}^{\infty} = \int_0^{\infty} \langle u_i'(0) u_j'(t) \rangle \, dt \tag{1}$$

where $\boldsymbol{u}'$ is the fluctuating carrier flow velocity. In contrast, the effective diffusion coefficient appearing in the kinetic PDF approach is (Reeks, 2021)

$$\epsilon_{ij}^{\infty} = \frac{1}{\beta} \left(\overline{v_i' v_j'}^{\infty} + \overline{\lambda_{ij}}^{\infty} \right) \tag{2}$$

in which dependence on both the long-time particle kinetic stresses $\overline{\boldsymbol{v}'\boldsymbol{v}'}^{\infty}$ and kinetic dispersion coefficient $\overline{\boldsymbol{\lambda}}^{\infty}$ is exhibited, with β being the particle inertia. The present work uses the analysis previously applied to particle clustering (Stafford, 2025) to investigate the importance of $\overline{\boldsymbol{\lambda}}^{\infty}$ within Eq. (2). It is shown that using a local homogeneous approximation to model $\overline{\boldsymbol{\lambda}}^{\infty}$ results in $\boldsymbol{\epsilon}^{\infty}$ reducing to Eq. (1), whilst retaining the correlation structure of the turbulence that naturally appears within $\overline{\boldsymbol{\lambda}}$ results in an additional contribution to $\boldsymbol{\epsilon}^{\infty}$. The role of this additional contribution to the particle diffusion is demonstrated using kinematic simulation, from which it is seen that Eq. (1) is only accurate in the fluid-point limit, whilst the importance of the turbulent flow structures to the particle diffusion becomes apparent at increased particle inertia. This highlights the capability of the kinetic PDF framework for capturing the influence of the turbulence within a continuum model for the particle phase, through its intrinsic description of the spatiotemporal structure of the carrier flow.

References

C.M. Tchen. *Mean Value and Correlation Problems Connected with the Motion of a small Particle suspended in a Turbulent Fluid.* Thesis Univ. of Delft, 1947.

M.W. Reeks. *The development and application of a kinetic theory for modeling dispersed particle flows.* J. Fluids Eng., **143**, 080803, 2021.

C.P. Stafford, D.C. Swailes, and M.W. Reeks. *Kinetic theory based solutions for particle clustering in turbulent flows.* Phys. Fluids, **37**, 043303, 2025.

Unified Lagrangian stochastic modelling for acceleration and velocity gradient in isotropic turbulence

R. E. Castro Torre[1], R. Zamansky[1], P. Fede[1], and O. Simonin[1]

[1] *Institut de Mécanique des Fluides de Toulouse (IMFT), Université de Toulouse, INPT, CNRS, Allée Camille Soula, Toulouse, 31400, France*

Since G. I. Taylor's pioneering article in 1921, the description of Lagrangian statistics of turbulence has attracted considerable interest. The accurate prediction of the evolution of a dispersed phase in highly turbulent flows can significantly depend on the small scales of the flow, which are discarded in LES or RANS methods. To alleviate this problem, it has been proposed to supplement the Eulerian simulations with a Lagrangian model for the sub-grid scales. In that respect, stochastic models were proposed to reproduce the Lagrangian evolution of the fluid velocity (Fede and Simonin[1] and Fede et al.[2]), for the acceleration (Gorokhovski and Zamansky[3] and Zamansky[6]) or for the velocity gradient (Johnson and Meneveau[4] and Pereira et al.[5]). However, despite considerable progress, the consistent Lagrangian modelling of small-scale intermittency (e.g. multifractality, non-Gaussianity, long-range correlations) remains an open issue. To date, no model simulating the joint evolution of acceleration, velocity and velocity gradients has been proposed in the literature.

In this work we proposed such a model of stochastic differential equations:

$$
\begin{aligned}
dG_{ij} &= f_{ij}(\mathbb{G}, \mathbf{a}, \mathbf{u})dt + g_{ijkl}(\mathbb{G}, \mathbf{a}, \mathbf{u})dW_{kl}(t) \\
da_i &= h_i(\mathbb{G}, \mathbf{a}, \mathbf{u})dt + k_{ij}(\mathbb{G}, \mathbf{a}, \mathbf{u})dW_j(t) \\
du_i &= a_i dt
\end{aligned}
$$

where $\mathbb{G}$ is the velocity gradient tensor, $\mathbf{a}$ the acceleration, $\mathbf{u}$ the velocity and dW_j and dW_{kl} are the increments of Wiener processes. The main novelty of the work lies in the modelling of functions f_{ij}, g_{ijkl}, h_i and k_{ij} reproducing the consistent correlation between velocity and velocity gradient and acceleration. They are based on the conditional averages obtained from DNS of homogeneous isotropic turbulence (HIT) up to $Re_\lambda = 200$. While our multiplicative model is able to reproduce non-Gaussian statistics of the acceleration and the velocity gradient, we also report that it gives the correct alignment of the acceleration with the velocity gradient eigenframe, which is of interest for reproducing the preferential sampling of inertial particles in turbulence.

References

[1] Fede, P. and Simonin, O. (2006). Numerical study of the subgrid fluid turbulence effects on the statistics of heavy colliding particles. *Physics of Fluids*, 18(4):045103.

[2] Fede, P., Simonin, O., Villedieu, P., and Squires, K. (2006). *Stochastic modeling of turbulent subgrid fluid velocity along inertia particle trajectories*, pages 247–258.

[3] Gorokhovski, M. and Zamansky, R. (2018). Modeling the effects of small turbulent scales on the drag force for particles below and above the Kolmogorov scale. *Physical Review Fluids*, 3(3):034602.

[4] Johnson, P. L. and Meneveau, C. (2018). Predicting viscous-range velocity gradient dynamics in large-eddy simulations of turbulence. *Journal of Fluid Mechanics*, 837:80–114.

[5] Pereira, R. M., Moriconi, L., and Chevillard, L. (2018). A multifractal model for the velocity gradient dynamics in turbulent flows. *Journal of Fluid Mechanics*, 839:430–467.

[6] Zamansky, R. (2022). Acceleration scaling and stochastic dynamics of a fluid particle in turbulence. *Physical Review Fluids*, 7(8):084608.

In The Foot Steps of Albert Einstein

A KINETIC THEORY FOR THE DISPERSION AND CLUSTERING OF TURBULENT GAS PARTICLE SUSPENSIONS

Reeks, M. W [1], Swailes, D. C,[2], Stafford C. P.[3]
[1]*School of Engineering, Newcastle University, Newcastle upon Tyne, NE1 7RU, mike.reeks@ncl.ac.uk*
[2]*School of Maths, Stats & Physics, Newcastle University, Newcastle upon Tyne, NE1 7RU, d.c.swailes@ncl.ac.uk*
[3] *Dept of Engineering, Iowa State University, Iowa, USA,cs9@iastate.edu*

Abstract

Theoretical predictions are presented for the dispersion and clustering of small particles in a turbulent gas flow based on a kinetic theory for turbulent gas-particle suspensions, Reeks [3]. Solutions for the dispersion by the large scales of the turbulence indicate that the long term particle diffusion coefficient in a KS generated isotropic homogeneous stationary flow $\geq$ the local flow by a small amount that depends upon the particle Stokes number. The clustering of particles by the small scales of the turbulence is measured by the concentration of particle pairs at equilibrium which is shown to be a balance of convective and diffusive fluxes arising from the kinetic and turbulent stresses and body forces associated with the aerodynamic driving forces acting on the particles that reflect the inhomogeneity in the flow field for particle pairs. Results for the particle pair concentration versus separation agree well with simulation measurements

Introduction

We present theoretical predictions for the dispersion and clustering of small particles in a turbulent gas flow based on a kinetic equation for the suspended particles in their response to both the large and small scales of the underlying carrier flow turbulence. For the case of the large scales we calculate the long time diffusion coefficient for particles in a fully mixed unbounded isotropic homogeneous and stationary flow and consider how it depends upon the particle Stokes number. For the clustering of particles by the small scales we calculate the particle pair concentration of mono disperse particles as a function of particle pair separation and particle Stokes number St_E. A crucial element of the kinetic equation for both scales is the form of the net driving force Reeks [3] in particle in phase space (per unit particle phase space volume) and given by

$$\langle f_i W \rangle = -\left(\frac{\partial}{\partial x_j} \lambda_{ji} \langle W \rangle + \frac{\partial}{\partial \mathrm{v}_j} \mu_{ji} \langle W \rangle - \kappa_i \langle W \rangle \right) \tag{1}$$

where $\boldsymbol{f}(\mathbf{x},t)$ is the force acting on an individual particle at time t. $\mathrm{W}(\mathbf{x}, \mathbf{v}, t)$ is the instantaneous phase space particle number density at time t for a particle with spatial position $\boldsymbol{x}$ and velocity $\mathbf{v}$.

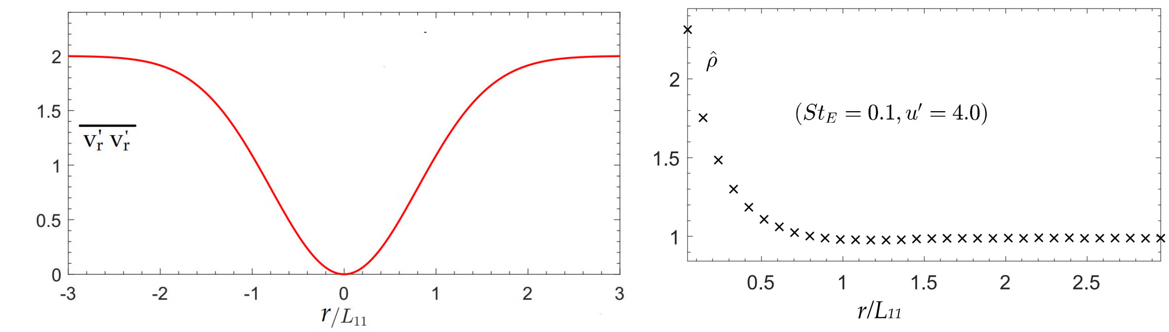

Figure 1: (a) Mean square fluctuating flow velocity profile as a function of separation r / distance from stagnation point; (b) Radial normalized steady state particle number concentration $\widehat{\rho}$

$\langle ... \rangle$ is the average value over all realizations of the carrier flow field, so $\langle W(\boldsymbol{x}, \mathbf{v}, t) \rangle$ is the average particle phase space density or pdf . See Reeks [3] for details. λ_{ji} and μ_{ji} are the components of stress tensors and κ_i the component of a body force per unit particle mass.

The particle mass flux the mass flux is not entirely diffusive (as in homogeneous turbulence) so that in inhomogeneous turbulence there is a convective component in addition to the convection due to the body force $\boldsymbol{\kappa}$. A similar relation exists for particle pairs where $\mathbf{x}$ and $\mathbf{v}$ refer respectively to the particle pair separation and relative velocity between pairs. Their contribution to the total mass flux is revealed more transparently in the expression for the particle mass flux $\langle \rho \rangle \overline{\mathbf{v}}$

$$\langle \rho \rangle \overline{\mathbf{v}} = \underbrace{\langle \rho \rangle \left(\langle \mathbf{u} \rangle + \mathbf{v}_g + \beta^{-1} \left\{ \underbrace{\left[\overline{\boldsymbol{\kappa}} - \nabla \cdot \overline{\boldsymbol{\lambda}} \right]}_{(1)} \underbrace{- \nabla \cdot \overline{\mathbf{v}' \mathbf{v}'}}_{(2)} - \underbrace{\frac{D_p}{Dt} \overline{\mathbf{v}}}_{(3)} \right\} \right)}_{\text{convective flux}} \underbrace{- \beta^{-1} \left(\overline{\mathbf{v}' \mathbf{v}'} + \boldsymbol{\lambda}^{\dagger} \right) \cdot \nabla \langle \rho \rangle}_{\text{diffusive flux}} \tag{2}$$

where the mass flux has been separated into convective and diffusive fluxes. For completeness, the gravitational settling velocity $\mathbf{v}_g$ is included. Term (1) refers to the convective velocity derived from the net turbulent driving force as the sum of (the body force per unit particle mass) and the divergence of a turbulent stress (per unit particle mass). Term (2) is the turbophoretic force (per unit particle mass)Reeks [2] derived from the divergence of the particle kinetic stresses. Term (3) is the inertial acceleration of the suspended particles which at equilibrium/steady-state conditions is zero or very small for weakly interacting inertial particles. We note that for particle pairs the turbulence associated with carrier flow is inhomogeneous so the convective flux contains contributions from all 3 sources.

Numerical Simulation Results

Particle diffusion coefficient in homogeneous isotropic stationary turbulence

We have measured the long term diffusion coefficient of particles in a KS generated homogeneous isotropic unbounded flow field. From Eq(2) the particle flux $\langle \rho \rangle \overline{\mathbf{v}}$ contains no convective contribution and is entirely diffusive with a diffusion coefficient given by

$$D(\infty) = \beta^{-1} \left(\langle \mathrm{v}^2 \rangle + \overline{\lambda} \right) \tag{3}$$

We have compared values for $D(\infty)$ with the exact result involving the integral timescale of the carrier flow along a particle trajectory in the KS turbulent flow field for a range of values of the particle Stokes number St. are consistent with the fact that $D(\infty)\succ$ the equivalent diffusion coefficient of the local fluid. [4].In particular for Stokes drag reduces to the well known formula given in [1]

$$D(\infty) = \int_0^\infty \langle \boldsymbol{u}(0).\boldsymbol{u}(t)\rangle \, dt \tag{4}$$

where $u(t)$ refers to the carrier flow velocity along a particle trajectory

Particle clustering/ particle pair concentration in homogeneous isotropic turbulence

The relative velocity between fluid point pairs as a function of separation for the KS flow filed is shown in Figure 1 (a), with the corresponding simulation results for the particle pair concentration as a function of separation in Fig 1 (b) showing the build up of concentration near the point of zero relative velocity between fluid particle pairs. Figure 2(b) shows the corresponding contribution of the convective terms to the particle mass flux for the small Stokes number in Figure 1

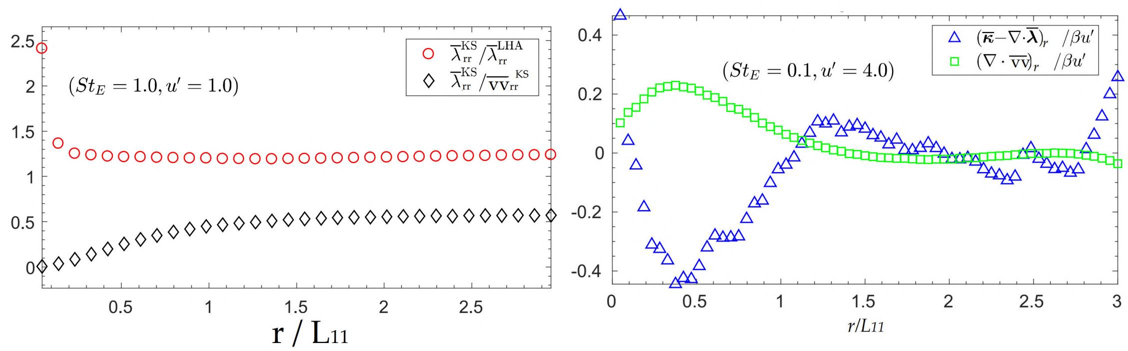

Figure 2: (a)Ratio of diffusive flux contributions as a function of separation distance r for monodisperse particles in inhomogeneous turbulence (see Figure 1 for mean sq. velocity profile) (b); kinetic and turbulent convective fluxes (including the body force $\overline{\kappa}$ for particle pairs in inhomogeneous turbulence (See Figure 1) derived from KS isotropic homogeneous stationary flow field.

We consider how the individual convective and diffusive fluxes depend upon the Stokes number St_E and pair separation and their combined contribution to the predictions of the particle pair concentration based on the force balance of the turbulent and kinetic stresses and body forces associated with the mean turbulent driving forces.

References

[1] M. W. Reeks. On the dispersion of small particles in an isotropic turbulent flow. *J. Fluid Mech.*, 83:529–546, 1977.

[2] M. W Reeks. The transport of discrete particles in inhomogeneous turbulence. *J. Aerosol Sci.*, 14(6):729–739, 1983.

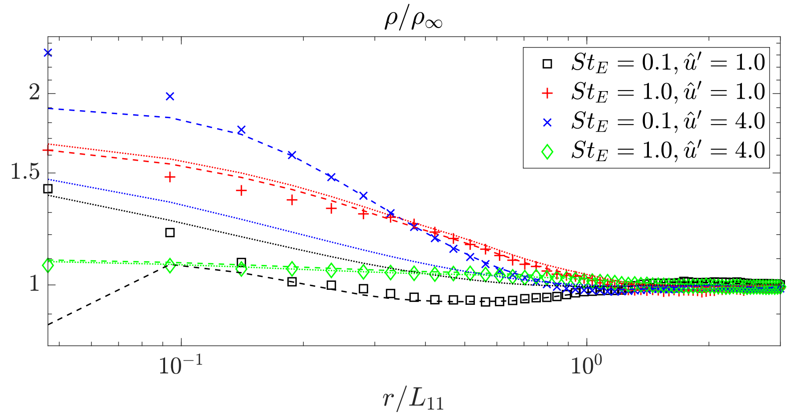

Figure 3: Radial profiles of the steady-state normalised particle concentration obtained using KS: black□ $St_E = 0.1, \hat{u}' = 1.0$, red+ $St_E = 1.0, \hat{u}' = 1.0$, blue× $St_E = 0.1, \hat{u}' = 4.0$, green◇ $St_E = 1.0, \hat{u}' = 4.0$. The pair concentration solution is represented by the dashed lines, whilst accounting for only the turbophoresis is shown by the dotted lines.

[3] M. W. Reeks. The development and application of a kinetic theory for modeling dispersed particle flows, freeman scholar paper. *J. Fluids Eng.*, 143:080803–1,53, 2021.

[4] K. D. Squires and J. K. Eaton. Measurements of particle dispersion obtained from direct numerical simulations of isotropic turbulence. *Journal of Fluid Mechanics*, 226:1–35, 1991.

Pair dispersion by intermittent wavelet-based stochastic fields

C. Morhain[1,2], R. Zamansky[3], M. Massot[4] and A. Vié[1,2]
[1]EM2C laboratory, CNRS-UPR288, CentraleSupélec, Université Paris-Saclay, 3 rue Joliot Curie, 91192 Gif-sur-Yvette cedex, France
[2]Fédération de Mathématiques de CentraleSupélec, CNRS FR-3487, 9 rue Joliot Curie, 91192 Gif-sur-Yvette cedex, France
[3]IMFT, CNRS-UMR5502, 2 Allée du Pr. Camille Soula, 31400 Toulouse cedex, France
[4]CMAP, École Polytechnique, Route de Saclay, 91128 Palaiseau cedex, France

To accurately predict particle statistics, LES of turbulent particle-laden flows requires the description of the unresolved velocity field in the subgrid scale models (1). Recently, we have developed a synthetic homogeneous isotropic turbulence (HIT) model that reconciles two-point spatial correlations and intermittency effects. Using a basis of divergent wavelets, we constructed spatially and temporally correlated velocity fields. In (2), we showed that the transport of inertial particles by these synthetic fields reproduces the segregation and dispersion phenomena of the particles. More recently, intermittency has been incorporated through a multiplicative cascade process embedded in the random wavelet coefficients (3).

In this work, HIT is generated using the proposed model with a sufficiently extended inertial range. The intermittency parameter is varied to control deviations from Kolmogorov (1941) self-similarity. Particle-pair dispersion statistics are then investigated. We first assess the ability of the model to recover the superdiffusive regime, and contrast it with Fourier Kinematic Simulation results, i.e. non-intermittent synthetic velocity fields for which the emergence of a clear Richardson regime has been questioned, e.g. (4). We subsequently examine the probability density function of particle separation over a prescribed range of initial separations. Finally, we analyse the scaling exponents of the moments of particle-pair separation as a function of moment order and quantify their deviation from the linear Richardson prediction, which provides a direct measure of intermittency effects on dispersion.

Overall, the intermittent wavelet-based model is assessed from a particle-dispersion perspective, and its ability to capture anomalous scaling behaviour is critically evaluated. Perspectives for further developments will be discussed, including the incorporation of large-scale sweeping effects on small wavelet modes.

References

[1] C. Marchioli. Large-eddy simulation of turbulent dispersed flows: a review of modelling approaches. *Acta Mechanica*, 228, pp. 741-771, 2017.

[2] C. Morhain, R. Letournel, M. Massot, and A. Vié. Stochastic-structural reduced-order modelling of particle-laden turbulent flows based on wavelet reconstruction. *Submitted to Computers & Fluids*

[3] C. Morhain, M. Massot, and A. Vié. Synthesizing turbulence from divergence free wavelets and random multiplicative cascades: an intermittent HIT model. *In preparation*

[4] G.E. Elsinga, T. Ishihara, and J.C.R. Hunt, Non-Local Dispersion and the Reassessment of Richardson's t^3 -Scaling Law, *Journal of Fluid Mechanics*, 932, A17, 2022,

Eulerian-Lagrangian framework for simulations of dispersed multiphase flows with interacting particles and/or polymers

F. Serafini, I. Silvestrini, A. Costabile, P. Gualtieri, F. Battista and C. M. Casciola
Department of Mechanical and Aerospace Engineering, Sapienza University of Rome, Via Eudossiana 18 00184 Rome, Italy

We present a high-performance computational framework for the simulation of point-wise particle, bead-spring, and bead-rod polymers, two-way coupled with the solvent phase through the Exact Regularised Point Particle (ERPP) method (Gualtieri et al., 2015). The framework includes short-range interactions between neighbouring particles and beads, and the possibility of particle aggregation/de-aggregation and of chain scission/recombination. These ingredients are essential for a comprehensive study of multiphase, eventually turbulent, flows, widespread over many technological applications, environmental, and biological flows. As a few examples, we can cite supramolecular polymer dynamics for drag reduction and misting control (Wei et al., 2015) or microplastic aggregates in high-shear oceanic environment (Hidalgo-Ruz et al., 2012). Hybrid MPI-GPU parallelisation is employed to handle the huge computational demand, to guarantee large scalability on High Performance Computing (HPC) architectures.

Methodological details and applications to polymer drag reduction by supramolecular polymers and buoyant particle dispersions will be discussed during the oral presentation. The figure below shows two snapshots of two possible applications of the proposed framework: an instantaneous visualisation of polymer bead-spring chains in a turbulent channel flow at $Re = 3000$ (left) and of buoyant particles on the free surface of an open channel flow at $Re = 3000$ (right).

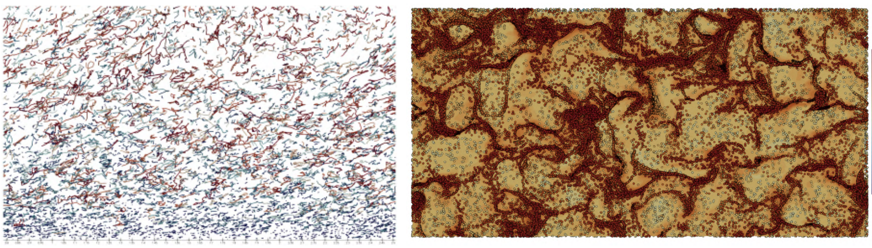

References

P Gualtieri, F Picano, G Sardina, and CM Casciola. Exact regularized point particle method for multiphase flows in the two-way coupling regime. *Journal of Fluid Mechanics*, 773: 520–561, 2015.

V Hidalgo-Ruz, L Gutow, RC Thompson, and M Thiel. Microplastics in the marine environment: a review of the methods used for identification and quantification. *Environmental science & technology*, 46(6):3060–3075, 2012.

M-H Wei, B Li, RLA David, SC Jones, V Sarohia, JA Schmitigal, and JA Kornfield. Megasupramolecules for safer, cleaner fuel by end association of long telechelic polymers. *Science*, 350(6256):72–75, 2015.

Euler-Lagrange LES of turbulent bubble plumes with a new lift force model

Mohammad Karimi Zand[1,2], Stefan Puttinger[2], Mahdi Saeedipour[2]
[1]K1-MET Metallurgical Competence Center, Linz, Austria
[2]Department of Particulate Flow Modelling Johannes Kepler University, Linz, Austria
mohammad.zand@k1-met.com mahdi.saeedipour@jku.at

Bubble plumes are widely encountered in industrial and environmental systems, where their macroscopic behavior is strongly governed by bubble liquid interactions. Among the interfacial forces acting on rising bubbles, the lateral lift force plays a key role in controlling bubble dispersion, plume spreading, and liquid entrainment. In Euler Lagrange simulations, the lift force is typically modeled using closures derived from single bubble hydrodynamics under laminar or weakly sheared conditions. However, such models often fail to predict the lateral distribution of bubbles and gas holdup in turbulent plumes, leading to discrepancies in velocity fields and plume dynamics. These limitations highlight the need for lift closures that explicitly account for the turbulent characteristics of the carrier phase.

In this work, a physics-based lift force model is proposed for Euler Lagrange large eddy simulation (LES) of turbulent bubble plumes. The formulation introduces a new dimensionless parameter based on the ratio of two resolved time scales: a turbulence decay time scale, related to turbulent kinetic energy and dissipation, and a vorticity based time scale associated with local rotational motion. This parameter characterizes the balance between coherent jet-like transport and turbulence-induced lateral dispersion within the plume and is used to adapt the lift coefficient accordingly. The model is assessed against established closures, including the Tomiyama et al. (2002) and Hessenkemper et al. (2021) lift models, using the well documented bubble plume experiments of Deen (2001) as a benchmark. Results demonstrate improved prediction of plume spreading and liquid velocity profiles, indicating that incorporating resolved turbulence scales enhances the accuracy of lift modeling in turbulent bubbly flows.

References

Tomiyama, A., Tamai, H., Zun, I., and Hosokawa, S. : Transverse migration of single bubbles in simple shear flows. *Chemical Engineering Science*, **57**, 1849–1858 (2002).

Hessenkemper, H., Ziegenhein, T., Rzehak, R., Lucas, D., and Tomiyama, A. : Lift force coefficient of ellipsoidal single bubbles in water. *International Journal of Multiphase Flow*, **138**, 103587 (2021).

Deen, N. G. : *An Experimental and Computational Study of Fluid Dynamics in Gas–Liquid Chemical Reactors*. PhD thesis, Aalborg University, Denmark (2001).

A unified mesoscopic framework for two-phase flows via inverse design

J. Lai[1], C. Peng[2], X. Chen[3], L.-P. Wang[3] and S. Wang[1]
[1] Guangzhou Maritime University, Guangzhou, Guangdong, China
[2] Shandong University, Jinan, Shandong, China
[3] Southern University of Science and Technology, Shenzhen, Guangdong, China

This study presents a unified inverse design framework for mesoscopic modeling of two-phase flows within the phase-field method. Traditional mesoscopic approaches often require case-specific formulations for different phase-field evolution equations (*e.g.*, Cahn-Hilliard, Allen-Cahn, and their variants), leading to fragmented model development. To address this, we propose a generalized formulation for the order parameter equation that encapsulates both conservative and non-conservative forms. By predetermining the equilibrium distribution functions and inversely designing the source terms in the Boltzmann equations via Chapman-Enskog analysis, we derive constraints that ensure recovery of macroscopic governing equations for mass, momentum, and interface evolution. This framework accommodates diverse phase-field models within a single numerical structure, enhancing flexibility, consistency, and design efficiency. Numerical results demonstrate the validity of the proposed inverse design framework. The approach offers a robust foundation for future extensions to broader fluid dynamics applications.

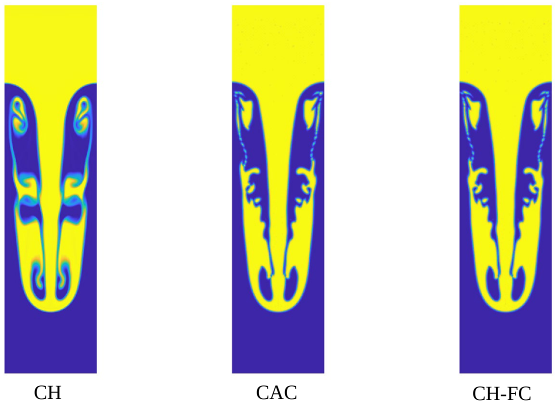

Figure 1: Snapshots of the 2D Rayleigh-Taylor instability simulated by Cahn-Hilliard (CH), conservative Allen-Cahn (CAC), and CH flux-corrected (CH-FC) methods at $t/T_0 = 3.7$.

References

J. W. Cahn and J. E. Hilliard. *Free energy of a nonuniform system. I. Interfacial free energy.* J. Chem. Phys., **28**, 258-267, 1958.

P.-H. Chiu and Y.-T. Lin. *A conservative phase field method for solving incompressible two-phase flows.* J. Comput. Phys., **230**, 185-204, 2011.

Y. Zhang and W. Ye. *A flux-corrected phase-field method for surface diffusion.* Commun. Comput. Phys., **22**, 422-440, 2016.

A wall-modeled LES framework for particle-laden turbulent flows in complex geometries

F. Dalla Barba[1,2], A. Bottacin Busolin [1,2] and F. Picano[1,2]
[1] Department of Industrial Engineering, University of Padova, Padova, Italy
[2] CISAS, University of Padova, Padova, Italy

Particle-laden turbulent flows are ubiquitous in both natural and industrial environments, playing a key role in processes such as aerosol transport, sediment dynamics and combustion systems. Predicting the behavior of these multiphase flows remains challenging due to the complex interactions between turbulence and dispersed particles. Large-Eddy Simulation (LES) has emerged as a powerful framework to capture turbulent dynamics while modeling the effect of unresolved small scales. However, in wall-bounded configurations LES still requires extremely fine near-wall resolution. Wall-modeled LES (WM-LES) offers a practical alternative by modeling near-wall turbulence, significantly alleviating computational requirements. When complex geometries are considered, the problem becomes even more challenging.

In this work, we present a numerical approach aimed at representing the transport of solid particles in turbulent flows confined by complex geometrical boundaries. The dispersed phase is tracked using the classical point-particle formulation. A semi-stochastic approach, based on the model originally developed in Kong (2025), is adopted to reproduce near-wall particle behavior and statistics. Complex boundaries are represented through an immersed-boundary-method-like algorithm. The method relies on modifying the near-wall diffusive fluxes through an algebraic equilibrium wall model in order to impose the correct wall stress reconstructed from the LES velocity at the matching location.

Preliminary results show good agreement with canonical configurations such as turbulent channel flow and turbulent pipe flow. Applications to more complex geometries will be presented and discussed at the conference.

We acknowledge financial support from the SID project "Wall-modeled LES of particle-laden flows for environmental applications" funded by the Department of Industrial Engineering, University of Padova.

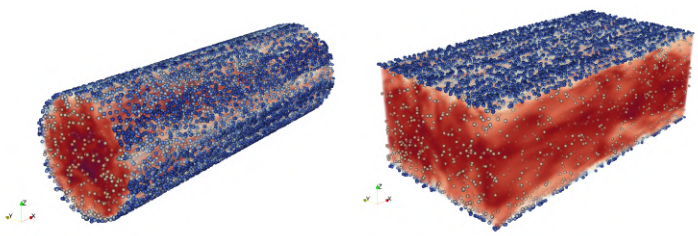

Figure 1: Snapshot of WM-LES of particles dispersed in turbulent pipe and channel flows.

References

Kong, X., Picano, F., & Dalla Barba, F. *A semi-stochastic approach for point-particle dispersion in Wall-Modelled Large Eddy Simulation of particle-laden turbulent flows,* International Journal of Multiphase Flow, 2025

The effect of electrostatic interactions on bidisperse charged particles transported by a homogeneous isotropic turbulence

C. Schoeck[1*], P. Fede[1] and O. Simonin[1]
[1] Institut de Mécanique des Fluides de Toulouse, France
*clovis.schoeck@imft.fr

The interactions between inertial particles and turbulent flows are crucial. In many industrial or natural situations [1, 2], particles transported by turbulent flows can get electrically charged through the phenomenon of triboelectrification. These electric charges have non negligible effects on the dynamics of inertial particles. The first effect comes from the competition between the drag and the electrostatic forces that leads to decrease the self-particle dispersion [3, 4] through the modification of the fluid-particle velocity correlation. Another effect is the modification of the preferential concentration. Indeed, inertial particles transported by a turbulent fluid flow tend to cluster in low vorticity regions of the flow (preferential concentration). These previous works considered like-charged particles whereas in practical applications the particle charges are not equal. Hence, in the present, the dispersion of binary charged —but of same sign— particles is investigated.

The presentation will focus on the recent results of 3D Direct Numerical Simulations for bidisperse charged particles in HIT, using an Euler-Lagrange approach. The effects of the electrostatic forces on the dispersion of the particles will be presented. One considers a dilute suspension of the particles, then collisions are neglected and one does one-way coupling simulations. Also, one considers that the particles are already charged (as a result of triboelectrification), and they do not exchange together or lose any part of their charges.

References

[1] B. Chide et al., “Detection of triboelectric discharges during dust events on Mars,” Nature, vol. 647, no. 8091, pp. 865–869, Nov. 2025, doi: 10.1038/s41586-025-09736-y.

[2] M. Di Renzo and J. Urzay. Aerodynamic generation of electric fields in turbulence laden with charged inertial particles. *Nat. Commun.* **9**, 1676, 2018.

[3] A. Boutsikakis, P. Fede, A. Pedrono, and O. Simonin, “Numerical Simulations of Short- and Long-Range Interaction Forces in Turbulent Particle-Laden Gas Flows,” *Flow, Turbulence and Combustion*, vol. 105, no. 4, pp. 989–1015, Feb. 2020, doi: 10.1007/s10494-020-00115-3.

[4] A. Boutsikakis, P. Fede and O. Simonin. Effect of electrostatic forces on the dispersion of like-charged solid particles transported by homogeneous isotropic turbulence. *J. Fluid Mech.*, **938**, 2022.

On the buoyancy force density in two-fluid continuum models

Thomas Pähtz[1], Rui Zhu[1], Yulan Chen[1], Katharina Tholen[2] and Zhiguo He[1]
[1] Institute of Port, Coastal and Offshore Engineering, Zhejiang University
[2] Institute for Theoretical Physics, Leipzig University

Two-fluid continuum models for disperse two-phase flow tend to be ill-posed due to unbounded growth of infinitesimally-small-wavelength, small-amplitude perturbations of a given initial state described by the system of PDEs, a so-called Hadamard instability (Langham et al., 2025; Lhuillier et al., 2013). Those models that are subject to this pathology are necessarily missing or misrepresenting physics, since the underlying microscopic problems they intend to describe are obeying Newton's equations of motion and/or the Navier-Stokes equations, for both of which growth is bounded. In practice, this means that numerical algorithms solving such ill-posed models do not converge upon grid refinement, making their predictions inherently unreliable. Here, we show that the primary cause for the ill-posedness of many two-fluid models is the mismodeling of the buoyancy force density in the coupled fluid phase and dispersed-phase momentum balance equations. We summarize a rigorous mathematical analysis that demonstrates that existing buoyancy expressions are self-contradictory for fluid-particle systems at complete rest. There is only one way to fix this problem, and applying the fix automatically resolves the ill-posedness issue as a byproduct. In addition, using DNS-DEM simulations of two simple systems—sediment transport driven by laminar flow and a single particle in pressure-driven free-surface flow without gravity—we also tackle a long-standing question regarding the contribution of shear stresses and pseudo-stresses, such as the Reynolds stress, to the buoyancy force density closure. In many two-fluid models, the buoyancy force density is modeled as the dispersed-phase volume fraction times the negative pressure gradient. Many other models add to this the divergence of the average viscous shear stress. Our simulations clearly indicate that both normal and shear stresses matter and that the stress divergence should also include the pseudo-stress that emerges from fluid-particle interactions, which is the stress that gives rise to mixture viscosity and other effects. By contrast, the Reynolds stress divergence does not contribute. The latter result seems to falsify the widespread modeling of buoyancy after Jackson (2000), who argued in favor of including all stresses and pseudo-stressed in the stress divergence.

References

R. Jackson. *The Dynamics of Fluidized Particles.* Cambridge University Press, New York, 2000.

J. Langham, X. Meng, J. P. Webb, C. G. Johnson, and J.M.N.T. Gray. Ill posedness in shallow multi-phase debris-flow models. *Journal of Fluid Mechanics*, 1015:A52, 2025. doi:10.1017/jfm.2025.10297.

D. Lhuillier, C. H. Chang, and T. G. Theofanous. On the quest for a hyperbolic effective-field model of disperse flows. *Journal of Fluid Mechanics*, 731:184–194, 2013. doi:10.1017/jfm.2013.380.

Tomographic PIV study of fiber-flow interaction in a turbulent channel flow

Dominic S. Sebastian[1], Vladislav Rinsky[1] and René van Hout[1]
[1] Faculty of Mechanical Engineering, Technion - Israel Institute of Technology, Haifa City, Haifa, Israel

The dynamics of inertial fibers in wall-bounded turbulent flows are central to many industrial and environmental processes, yet their near-wall kinematics and interactions with coherent turbulence structures remain incompletely understood (Shaik and van Hout, 2023). The present study presents an experimental investigation of fiber-flow interaction in a fully developed turbulent water channel flow using Tomographic Particle Image Velocimetry (Tomo-PIV). Measurements were conducted using a four-camera system arranged in a linear configuration at an acquisition rate of 15 Hz. The volume of interest (VOI) was 38 $\times$ 38 $\times$ 27 mm^3. The local flow field around fibers is analyzed to evaluate its effect on fiber motion, with particular focus on the near-wall region where strong velocity gradients and anisotropic turbulence dominate fiber-flow interactions.Two nylon fiber types with lengths of 2917 μm, and 3840 μm, and diameters of 62 μm, and 38.5 μm were dispersed in the flow under complementary experimental conditions by varying the Stokes and Reynolds numbers. By independently controlling Reynolds number and particle inertia, this study provides new experimental insight into fiber-turbulence interactions in wall-bounded flows. Experimental limitations of Tomo-PIV in near-wall measurements are also addressed, including wall reflections from intense laser illumination and speckle effects due to laser coherence.

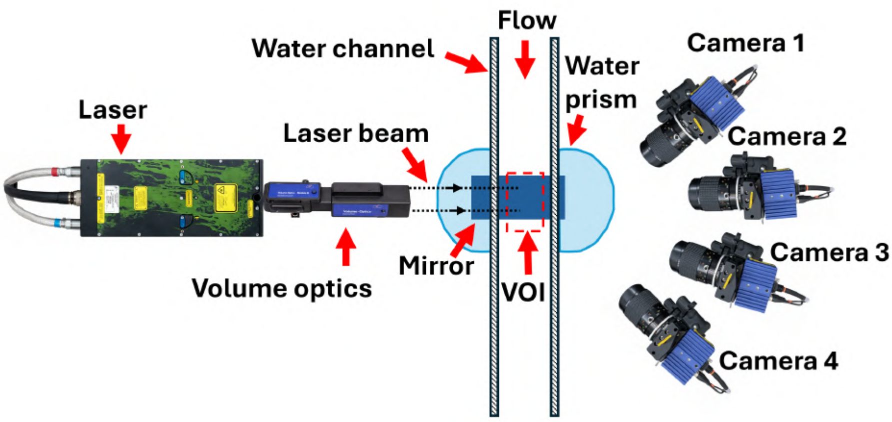

Figure 1: Schematic of experimental steup with Tomo-PIV.

References

S. Shaik, and R. van Hout. Kinematics of rigid fibers in a turbulent channel flow. *International Journal of Multiphase Flow*, 158:104262, 2023.

Optical activity based measurements of fiber-flow interaction in the near-wall region of a turbulent channel flow

Vlad Rinsky, Dominic S. Sebastian and René van Hout
Technion – Israel Institute of Technology,
Technion city, Haifa, Israel

Understanding fiber–turbulence interactions in wall-bounded flows requires phase-resolved volumetric measurements in the near-wall region where deposition, resuspension, and turbulence modulation occur. However, conventional laser-based tomographic particle image velocimtery (tomo-PIV) faces intrinsic limitations. Strong scattering from fibers combined with wall reflections causes saturation and glare (Fig. 1), while weak tracer signals demand high laser power, resulting in dynamic range imbalance and reduced reconstruction fidelity.

We propose a tomographic optically active PIV (tomo-OAPIV) approach that leverages polarization-modified forward-transmitted light through optically active tracers and fibers. A crossed-polarizer configuration suppresses background illumination and wall reflections, enabling selective detection of optically active particles (Rinsky et al., 2023). The use of high-current pulsed light emitting diode (LED) illumination instead of lasers eliminates speckle and enhances phase brightness parity between tracers and fibers (van Hout, 2025).

Implemented in a turbulent channel flow, the method is directly compared with conventional tomo-PIV. Initial results show substantial improvement in SNR which is expected to lead to improved volumetric reconstruction quality, enabling reliable simultaneous measurement of carrier-flow structures and fiber dynamics in the near-wall region. This polarization-based tomographic approach opens new experimental possibilities for quantifying turbulence modulation, fiber orientation statistics, and near-wall transport mechanisms in particle-dispersed boundary layers.

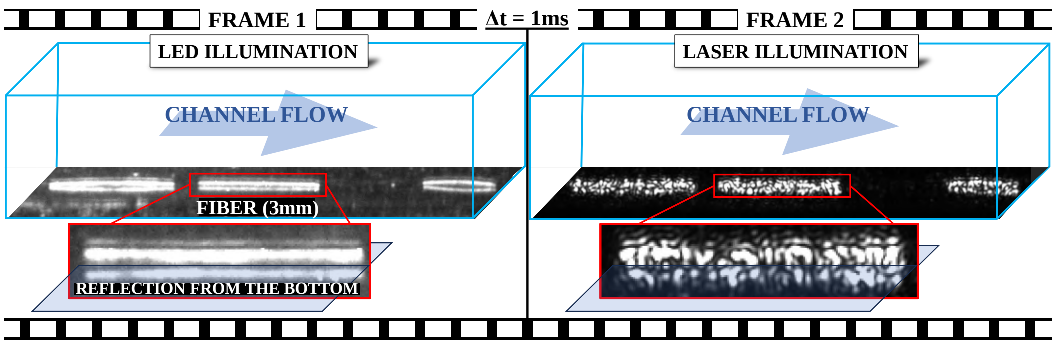

Figure 1: Laser versus LED (optical-activity-based) illumination in near-wall tomo-PIV, showing reduced glare and improved fiber visibility with LED. The image presents two frames captured with a 1ms interval: frame 1 acquired with LED and frame 2 with laser.

References

V. Rinsky, S. Shaik, and R. van Hout. Leveraging optical activity in visualizing particle-laden flows. *Experiments in Fluids*, 64(2):36, 2023.

R. van Hout. Full-field optical visualization techniques in "dilute" particle-laden flows. *Acta Mechanica*, pages 1–26, 2025.

Direct numerical simulations of a dilute turbulent jet laden with spheroidal particles

J. Wang[1] and L. Zhao[1]
[1] AML, Department of Engineering Mechanics, Tsinghua University, 100084 Beijing, China

The present work aims at understanding the transport and orientation dynamics of spheroidal particles within a dilute turbulent round jet at a bulk Reynolds number of $Re = 6000$. Understanding the behavior of non-spherical particles in turbulent shear flows is essential in applications such as biomass combustion, volcanic ash dispersion, and airborne pathogen transport, where particle shape strongly influences settling, alignment, and dispersion. In this study, the carrier phase is fully resolved by DNS in a cylindrical coordinate system using an in-house Fortran-based solver Wang et al. (2021), while the dispersed phase is treated using a Lagrangian point-particle approach. The rotational dynamics and orientation of the non-spherical particles are modeled following the established framework of Zhao et al (2016), ensuring an accurate description of the torque and angular momentum evolution. The primary objective is to elucidate how the particle aspect ratio and inertia influence their spatial distribution and alignment relative to the jet's turbulent structures. Preliminary analysis focuses on the preferential orientation of spheroids within the shear layer and the jet core. These findings will provide fundamental insights into the anisotropic particle dynamics in high-speed turbulent shear flows, with implications for industrial spray systems or pollutant dispersion.

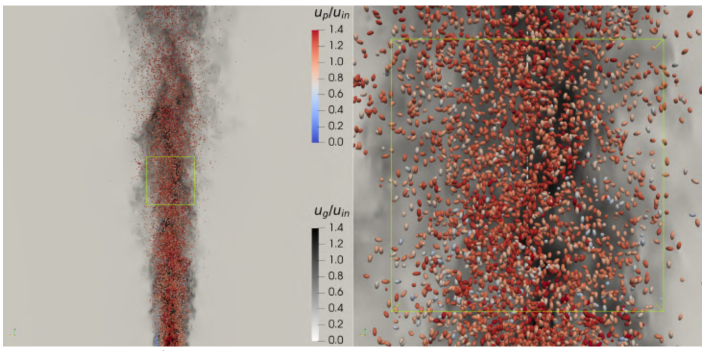

Figure 1: Radial-axial slices of the a turbulent spray laden with elliptical particles at $Re = 6,000$. Both carrier phase and dispersed phase are contoured according to the instantaneous velocity field normalized with the inlet value. For the sake of concise visualization, only particles located within a distance $\Delta/R = 0.1$ to the slice plane is presented.

References

J. Wang, F. Dalla Barba, F. Picano. *Direct numerical simulation of an evaporating turbulent diluted jet-spray at moderate reynolds number.* Int. J. Multiph. Flow., **137**, 103567, 2021.

L. Zhao, HI. Andersson. *Why spheroids orient preferentially in near-wall turbulence.* J. Fluid. Mech., **807**, 221-234, 2016.

Fiber Fragmentation in Turbulence

H. Muppirala[1], D.J Dhas[1], A. Roy[2] and C. Marchioli[1]
[1] Dept. of Engineering and Architecture, University of Udine, Italy
[2] Dept. of Applied Mechanics and Biomedical Engineering, IIT Madras, India

Long, slender fiber-like particles are ubiquitous, most notably encountered in the form of microplastic pollutants. These pollutants originate from the breakdown of larger plastic debris, and subsequently undergo continuous deformation by hydrodynamic stresses in natural flows leading to further fragmentation. To this end, we perform large scale Euler-Lagrange direct numerical simulations of flexible fibers in a channel. These fibers are constructed by constraining sub-Kolmogorov rods using a rod-chain model. Through these simulations, we show how turbulent structures and intermittent shear fluctuations generate large deformations along the fiber, promoting conditions conducive to breakage. We identify such breakage events by monitoring the cumulative strain experienced along the fiber over time, using it as a physically motivated indicator for their fragmentation. We subsequently quantify the resulting breakage statistics as a function of the fiber and fluid flow properties without explicitly modeling physical fracture.

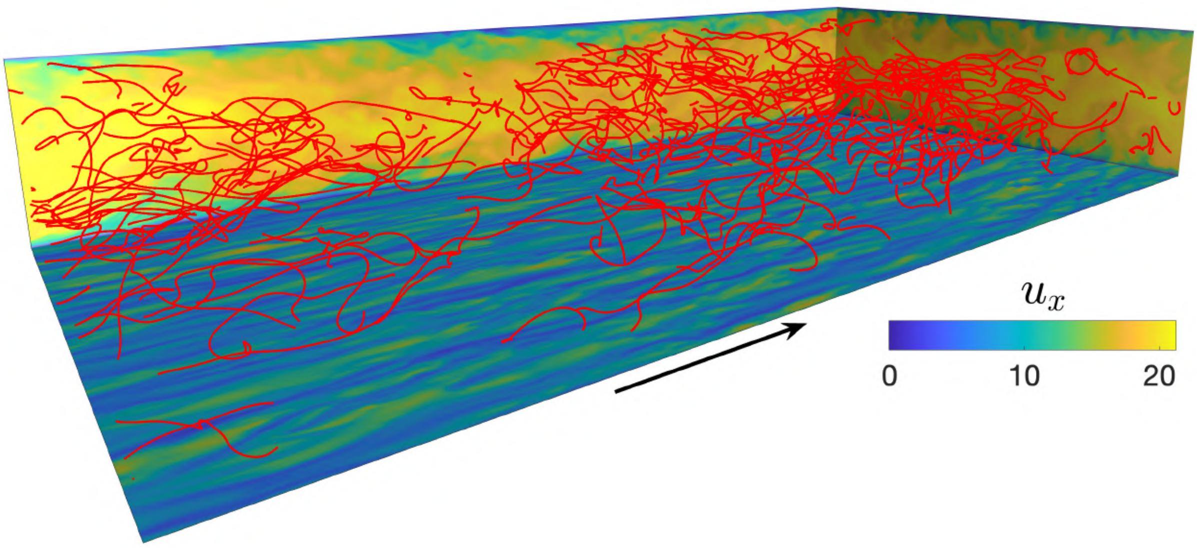

Figure 1: Instantaneous distribution of a random collection of flexible fibers of length $L_0^+ = 380$ in a turbulent channel flow with shear Reynolds number 300. The side and bottom panels display the stream-wise component of the velocity (u_x), with the bottom cut at $z^+ = 10$. The fiber thickness is magnified for better visualization.

Dynamics of long flexible fibers in wall-bounded turbulent flows

Darish Jeswin Dhas[1] and Cristian Marchioli[1]
[1] Department of Engineering and Architecture, University of Udine, Italy

The canonical picture of inertial particle transport in wall turbulence is one of turbophoretic drift toward the wall and accumulation in the viscous sublayer. Using direct numerical simulations of flexible fibers in turbulent channel flow, we show that fiber length fundamentally alters this picture. Short fibers behave like inertial point particles and accumulate at the wall through classical turbophoresis, whereas long fibers migrate in the opposite direction. This reversal arises from a tug of war between two competing mechanisms with distinct parameter dependencies: turbophoresis, which strengthens with particle inertia and draws fibers toward the wall along gradients of turbulent velocity fluctuations, and a geometric effect that strengthens with fiber length, by which a long fiber straddling the strongly sheared near-wall region is levered away from the wall. Because the two tendencies scale oppositely, with inertia and with length, the outcome is set by their interplay: the transition from wall accumulation to bulk migration traces a boundary in the length-Stokes number plane, along which the wall-ward and bulk-ward drifts cancel. More inertial fibers require greater lengths to escape the wall, so the critical length increases with Stokes number. These results identify the joint role of fiber length and inertia as decisive for the dispersion and deposition of elongated particles in wall turbulence, with direct implications for the transport of microplastic fibers and other slender contaminants in natural and industrial flows.

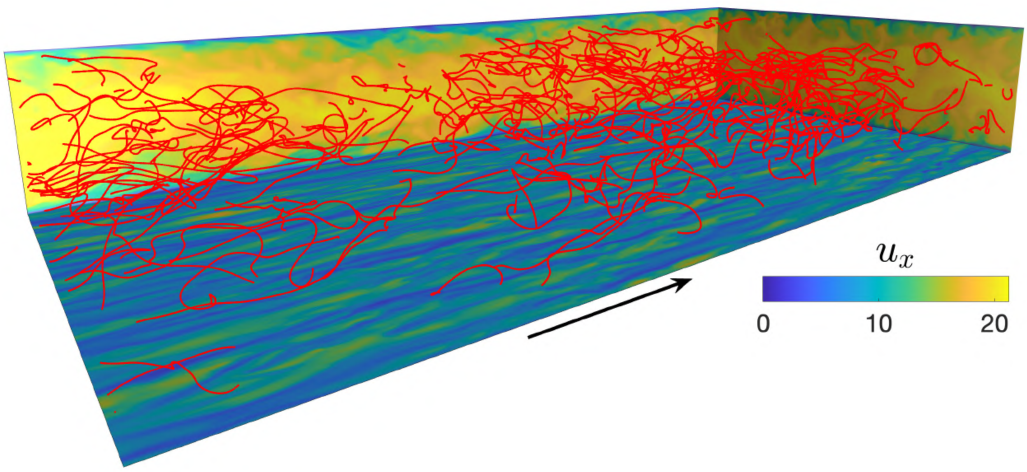

Figure 1: Instantaneous distribution of a random collection of flexible fibers of length $L_0^+ = 380$ in a turbulent channel flow with shear Reynolds number 300. The side and bottom panels display the stream-wise component of the velocity (u_x), with the bottom cut at $z^+ = 10$. The fiber thickness is magnified for better visualization.

Inertial particle clustering in the transitional wake of a normal flat plate

Deekshith I. Poojary[1], Lihao Zhao[2] and Vagesh D. Narasimhamurthy[1]
[1] Department of Applied Mechanics & Biomedical Engineering,
Indian Institute of Technology Madras, Chennai 600036, India
[2] Department of Engineering Mechanics, Tsinghua University, Beijing 100084, China

Clustering of inertial particles in multiphase flows strongly affects mixing, transport, and dispersion. In transitional wakes, deformed von Kármán and streamwise vortices create strong spatial variations in particle concentration, especially for Stokes number $St \approx 1$. The objective of this study is to quantify how Kármán and streamwise vortices drive preferential concentration across different St and to compare two cluster-detection methods. This is investigated using one-way coupled Eulerian-Lagrangian simulations with MGLET-LaParT (Mahamure et al., 2026). The clusters are then identified using two techniques. The first is Voronoï tessellation, which measures local concentration from normalized cell volumes and uses a parameter-free statistical threshold based on deviations from a Poisson random process; spatial connectivity is then applied to form coherent clusters. The second is a multi-stage DBSCAN method that employs a stability-based sweep over ϵ (search radius) and $MinPts$ to extract particle groups that persist across parameter choices. Cluster geometry is analyzed using principal component analysis. Results show that particles with $St = 1$ exhibit the strongest accumulation. Streamwise vortices eject particles from braid regions, creating voids, while particles trapped between Kármán cells form dense inner clusters with strong spanwise variability. Voronoï tessellation captures the overall clustering footprint, whereas DBSCAN isolates compact high-density cores (cf. Figure 1). Overall, the results show how particle inertia and wake vortex topology govern preferential concentration.

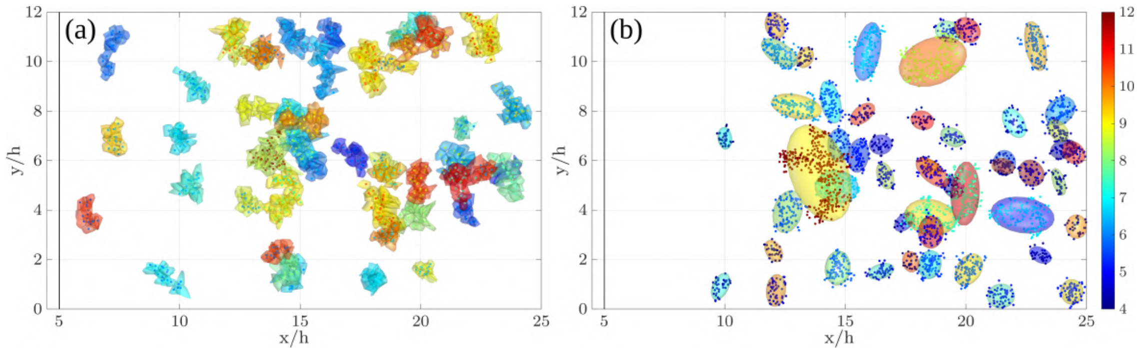

Figure 1: Top 50 clusters identified by (a) the Voronoï method and (b) the DBSCAN method for $St = 1$. Each cluster is colored by the mean z-position of its particles. Particles within clusters colored by size (blue = small, red = large clusters)

References

H. P. Mahamure, D. I. Poojary, V. D. Narasimhamurthy, and L. Zhao. *An Eulerian-Lagrangian parallel algorithm for simulation of particle-laden turbulent flows.* Acta Mech. Sin., **42**(1), 724946, 2026.

Decoupling between inertial and gravitational effects in the dynamics of particles in turbulence

J. Auzoux[1,2], F. Cabrera-Booman[1,2,3], C. Wang[2], K. Cardin[1,4], R. Pedurand[2], R. Volk[2], N. Plihon[2], M. Bourgoin[2] and R. B. Cal[1]
[1]Department of Mechanical & Materials Engineering, Portland State University, Portland, OR, USA
[2]Laboratoire de Physique de l'École Normale Supérieure de Lyon, CNRS & Université de Lyon, Lyon, France
[3]Department of Mechanical Engineering, University of Nevada, Reno, NV 89557, USA
[4]Aix Marseille Université, CNRS, Centrale Méditerranée, IRPHE, Marseille, France

Volcanic ash transport, atmospheric pollution, and aeolian dust are examples of turbulent flows laden with particles. Understanding the dynamics of heavy inertial particles in turbulence remains a major challenge, particularly due to the coupling between inertial and gravitational effects. In this study, we experimentally investigate the dynamics of heavy spherical particles in turbulence by exploring several particle-to-fluid density ratios and particle diameters, corresponding to different Stokes numbers. To isolate inertial effects from gravitational settling, experiments are conducted under micro-gravity conditions. A dedicated experimental facility was designed and implemented in the Dryden Drop Tower at Portland State University, providing 2.1 seconds of micro-gravity. Particle Tracking Velocimetry (PTV) enables simultaneous measurement of inertial and tracer particle trajectories, allowing direct access to one-point and two-point statistics as well as slip velocity dynamics. This approach provides new insight into the role of inertia in particle–turbulence interactions in the absence of gravitational bias.

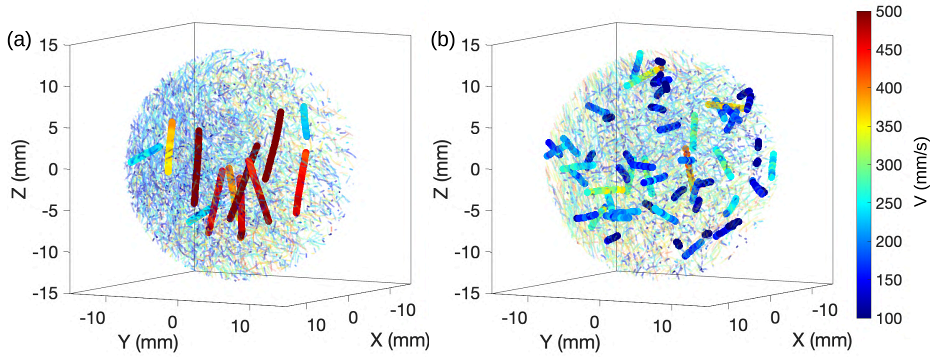

Figure 1: Simultaneous 3D trajectories of inertial particles (large spheres) and tracer particles (small spheres). Panel (a) shows terrestrial gravity and panel (b) micro-gravity, both over 50 time steps (16 ms). Colours indicate the magnitude of particle velocity.

References

Cabrera, F, *Settling of particles in quiescent and turbulent flows. from ground conditions to micro-gravity.* PhD thesis, École Normale Supérieure de Lyon. (2021).

Settling velocity of Kolmogorov-size and finite-size particles in homogeneous isotropic turbulence

T. Wang and Z. Yu
Department of Mechanics, Zhejiang University, Hangzhou 310027, China

It has been well recognized that turbulence can generally enhances the settling velocity of sub-Kolmogorov particles, while reducing the settling velocity of finite size particles. How the turbulence affects the settling velocity of particles with size comparable to the Kolmogorov scale, however, remains unclear. In the present study, particle-resolved direct numerical simulations are performed to investigate the settling velocity of spherical particles in homogeneous isotropic turbulence at the ratio of particle diameter to Kolmogorov length scale ranging from 0.87 to 13.7, Stokes number based on Kolmogorov time scale ranging from 0.0077 to 18.9, and particle volume fraction ranging from 0.0004 to 0.05. Our results show that the settling enhancement of Kolmogorov-size particles is due to preferential sweeping, while the reduction occurs when the loitering dominates preferential sweeping. A criterion for the turbulence-induced enhancement or reduction of particle settling velocity for the dilute case is proposed, based on the data from both the present simulations and the literature.

References

L. Brandt and F. Coletti. Particle-laden turbulence: progress and perspectives. *Annual Review of Fluid Mechanics*, 54(1), 159-189, 2022.

G. H. Good, P. J. Ireland, G. P. Bewley, E. Bodenschatz, L. R. Collins and Z.Warhaft, Settling regimes of inertial particles in isotropic turbulence. *Journal of Fluid Mechanics*, 759, R3, 2014.

C. Peng, K. Karzhaubayev, L. P. Wang, S. Chen and Z. Niu. Settling of finite-size particles in homogeneous isotropic turbulence: the influence of particle inertia and a unified predictive model. *Journal of Fluid Mechanics*, 1016, A63, 2025.

Slip and unsteady drag dynamics of finite-size inertial particles in homogeneous turbulence under micro-gravity

F. Cabrera-Booman[1,2,3], J. Auzoux[1,2], K. Cardin[1], R. Pedurand[2], P. Metz[2], R. Volk[2], N. Plihon[2], M. Bourgoin[2] and R.B. Cal[1]

[1]Department of Mechanical and Materials Engineering, Portland State University, OR, United States of America.
[2]Univ Lyon, ENS de Lyon, CNRS, Laboratoire de Physique, F-69342 Lyon, France.
[3]Department of Mechanical Engineering, University of Nevada, Reno, NV, United States of America.

We present an experiment in micro-gravity where sustained settling is suppressed and particle-fluid relative motion is driven primarily by turbulent fluctuations. A water facility generated quasi-homogeneous isotropic turbulence at $Re_\lambda = 170$ and was operated in the Dryden Drop Tower at Portland State University (USA). Four-dimensional Lagrangian particle tracking simultaneously measured neutrally buoyant tracers and finite-size inertial particles, enabling direct estimation of the locally sampled coarse-grained flow velocity $\vec{u}_R(t)$ and the slip velocity $\vec{SV}(t) = \vec{u}_R(t) - \vec{v}(t)$.

Micro-gravity suppresses persistent settling (see Figure 1) and shifts slip events toward lower particle Reynolds number. Particle accelerations remain strongly intermittent and much broader than quasi-steady Maxey–Riley–Gatignol predictions; both Stokes and non-linear drag closures under-predict acceleration variance in micro-gravity by up to a factor of two and show poor instantaneous and statistical agreement with measurements.

To study this discrepancy, wake unsteadiness is assessed by comparing vortex-shedding and particle-scale turbulent fluctuation time scales, which are found to be comparable in both gravity conditions. Turbulence therefore modulates slip before the wake can equilibrate, breaking the quasi-steady wake assumption implicit in steady-drag models and motivating drag formulations that include finite-time wake evolution.

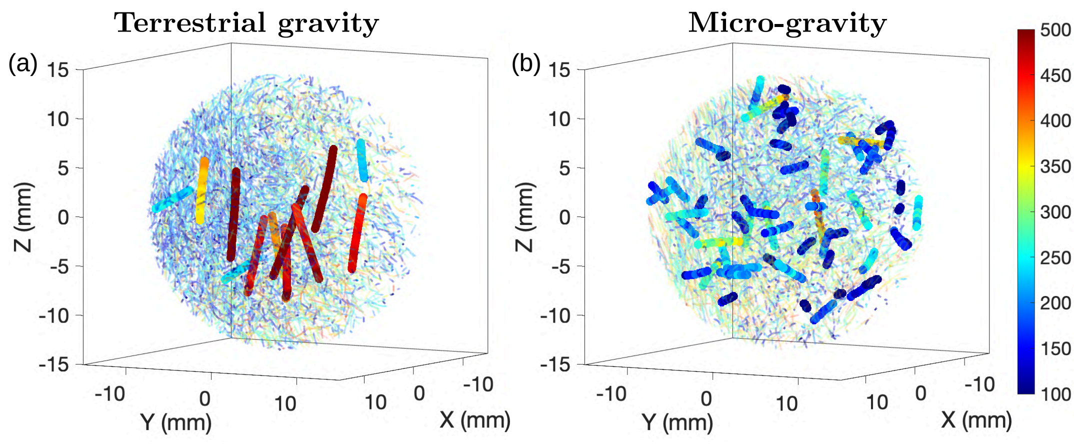

Figure 1: Simultaneous 3D trajectories of inertial particles (large spheres) and tracer particles (small spheres). Colors indicate velocity.

Inertial particle settling in turbulence under gravity: the roles of preferential sampling and loitering

H. Pradel[1], C. Wang[1], B. Laplace[1], N. Plihon[1], R. Volk[1] and M. Bourgoin[1]
[1] Ens de Lyon, CNRS, Laboratoire de physique, UMR 5672, F-69342 Lyon, France

We report experimental measurements of inertial particle settling in turbulence, in which both enhanced and hindered settling velocities are observed. Simultaneous volumetric Lagrangian particle tracking is performed for finite-size inertial particles and tracer particles. A particle Froude number defined for finite-size inertial particles is identified as a key dimensionless parameter governing the transition between enhanced and hindered settling. Particles of moderate density and small size, corresponding to moderate inertial and small finite-size effects, exhibit enhanced settling in turbulence owing to increased slip velocity and preferential sampling of downward flow. As finite-size effects increase with particle size, particles continue to preferentially sample downward flow but experience a reduction in slip velocity, resulting in hindered settling. For heavy particles with strong inertial effects, settling is consistently hindered by turbulence and is associated with reduced slip velocity and preferential sampling of upward flow.

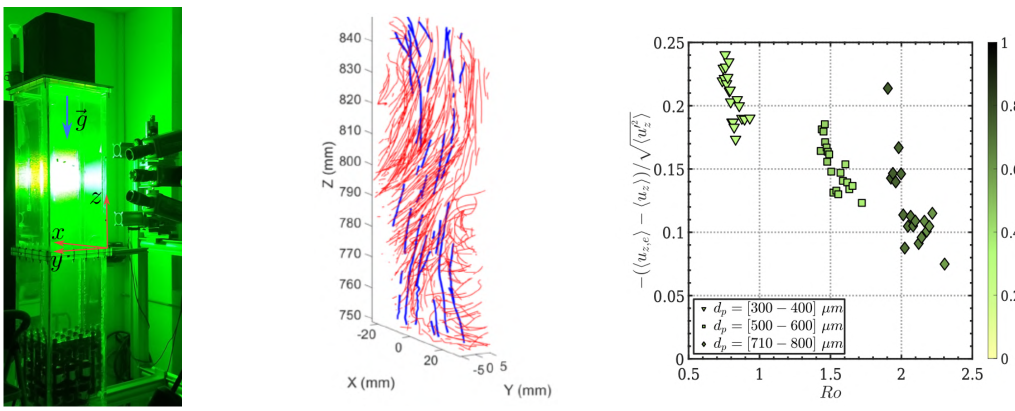

a) b) c)

Figure 1: a: Photograph of the water tower with the pumps at the bottom, the 3 high speed cameras and laser sheet. b: 3-D trajectories of settling particles and tracers. Inertial particles are plotted in blue and tracers trajectories are plotted in red. b: Mean settling speed of the small glass particles with respect to the fluid normalized by quiescent settling speed. $\langle v_z \rangle$ is the particle mean vertical velocity, $\langle u_z \rangle$ is the fluid mean vertical velocity in the field of view, and v_s the particle settling velocity measured in quiescent water. Ro is the Rouse number $v_s/\sqrt{\langle u_z'^2 \rangle}$, where $\sqrt{\langle u_z'^2 \rangle}$ is the turbulent velocity fluctuations.

References

B. Laplace. *Etude expérimentale de la sédimentation de particules inertielles en turbulence.* PhD thesis, Université de Lyon, 2022.

C. Peng, K. Karzhaubayev, L-P. Wang, S. Chen and Z. Niu. *Settling of finite-size particles in homogeneous isotropic turbulence: the influence of particle inertia and a unified predictive model.* Journal of Fluid Mechanics. 2025;1016:A63.

Stochastic resonance of rotating particles in turbulence

Z. Wang[1], X. M. de Wit[1], R. Benzi[2,3], C. Wu[1],
R. P. J. Kunnen[1], H. J. H. Clercx[1], and F. Toschi[1,4]

[1]Fluids and Flows group and J. M. Burgers Center for Fluid Mechanics, Department of Applied Physics and Science Education, Eindhoven University of Technology, 5600 MB Eindhoven, The Netherlands
[2]Sino-Europe Complex Science Center, School of Mathematics, North University of China, Taiyuan 030051, Shanxi, China
[3]Department of Physics and Istituto Nazionale di Fisica Nucleare, University of Rome Tor Vergata, I-00133 Rome, Italy
[4]Consiglio Nazionale delle Ricerche – Istituto per le Applicazioni del Calcolo, I-00185 Rome, Italy

The chaotic dynamics of small-scale vorticity plays a key role in understanding and controlling turbulence, with direct implications for energy transfer, mixing, and coherent structure evolution. However, measuring or controlling its dynamics remains a major conceptual and experimental challenge due to its transient and chaotic nature. Here we use a combination of experiments, theory, and simulations to show that small magnetic particles of different densities, exploring flow regions of distinct vorticity statistics, can act as effective probes for measuring and forcing turbulence at its smallest scale . The interplay between the magnetic torque, from an externally controllable magnetic field, and hydrodynamic stresses, from small-scale turbulent vorticity, uncovers an extremely rich phenomenology. Notably, we present the first experimental and numerical observation of stochastic resonance for particles in turbulence, where turbulent fluctuations, remarkably acting as an effective noise, enhance the particle rotational response to external forcing. We identify a pronounced resonant peak in the particle rotational phase lag when the applied rotating magnetic field matches the characteristic intensity of small-scale turbulent vortices. Furthermore, we reveal a novel symmetry-breaking mechanism: an oscillating magnetic field with zero mean angular velocity can counterintuitively induce net particle rotation in zero-mean vorticity turbulence. Our findings pave the way to developing flexible techniques for manipulating particle dynamics in complex flows. The discovered mechanism enables a novel magnetic resonance-based approach to be developed for measuring turbulent vorticity. In this approach, particles act as probes, emitting a detectable magnetic field that can characterize turbulence even under conditions that are optically inaccessible.

References

Z. Wang, X. M. de Wit, R. Benzi, C. Wu, R. P. J. Kunnen, H. J. H. Clercx, and F. Toschi. *Stochastic resonance of rotating particles in turbulence.* Nat. Commun., **16**, 10376, 2025.

Particle-resolved simulations of many spherical particles settling in an inflow/outflow configuration

Manuel Moriche[1], Manuel García-Villalba[1] and Markus Uhlmann[2]
[1] Institute of Fluid Mechanics and Heat Transfer ,TU Wien, Austria
[2] Karlsruhe Institute of Technology, Germany

We analyze the flow fluctuations generated by a set of particles settling under gravity in an inflow/outflow configuration. This new setup allows for a more realistic configuration in which the energy of the fluctuating flow is introduced at the small and large scales, namely the boundary layers of the particles and the large columnar clusters, respectively. We recover some results observed previously for triply periodic configurations (for example the anisotropy in the fluctuating flow, see Uhlmann and Doychev, 2014), and obtain new results like the decay of the perturbations downstream of the particle clusters The figure shows results for a parametric point $Ga = U_g D/\nu = 178, \tilde{\rho} = 1.5$, where $U_g = \sqrt{(\tilde{\rho}-1)\, gD}$ is a gravitationally scaled velocity and $\tilde{\rho}$ is the density ratio between the particles and the fluid.

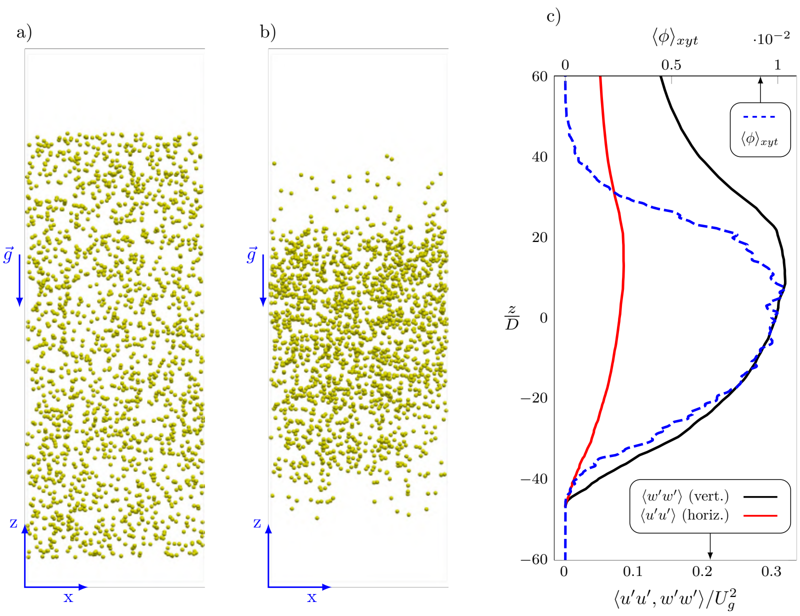

Figure 1: Visualization of the a) initial and b) converged particle distribution. c) Averaged solid volume fraction ($\langle\phi\rangle_{xy}$) and vertical (w') and horizontal (u') flow fluctuations.

References

M. Uhlmann and T. Doychev. Sedimentation of a dilute suspension of rigid spheres at intermediate Galileo numbers: the effect of clustering upon the particle motion. *J. Fluid Mech.*, 752:310–348, 2014. doi:10.1017/jfm.2014.330.

Influence of dissolved gas concentration on the lifetime of surface bubbles in volatile liquids

Xin Li[1] and Yanshen Li[1]
[1] School of Engineering Science, University of Chinese Academy of Sciences, Beijing 101408, PR China

Bubbles at the air-liquid interface are important for many natural and industrial processes, including climate change, food and household industry. Factors influencing the lifetime of such surface bubbles have been investigated extensively. However, the impact of dissolved gas concentration has not been explored, even though it is strongly relevant in the food industry. Here we investigate how the surface bubble lifetime t_l in volatile liquids depends on the dissolved gas concentration c.

The dissolved gas concentrations are varied by depressurizing or pressurizing the liquid. Dissolved oxygen concentrations are measured to calculate the gas oversaturation $\zeta = (c - c_{\text{sat}})/c_{\text{sat}} = (c_{\text{o}} - c_{\text{o,sat}})/c_{\text{o,sat}}$. Surface bubbles are generated by injecting a certain volume of air into the bulk liquid and let it rise. High speed recordings reveal that microbubbles are responsible for the film rupture, see Fig. 1(a). Further, it is found that larger microbubbles at increased gas concentration trigger bubble bursting at earlier times, thus leading to a decrease in the bubble lifetime. Assuming the growth of the microbubble is dictated by diffusion, we obtain the average diameter of the microbubble $\overline{d} \sim c$ according to Epstein and Plesset (1950). The bubble cap will rupture if $\overline{d}$ is larger than the film thickness at spontaneous rupture h_r by a certain factor, i.e., $\overline{d} \sim h_r$. Then we have $h_r \sim c$. For volatile liquids, it has been found that the film thickness of a surface bubble follows $h \sim t^{-2/3}$ (Poulain et al., 2018). At the instant when the film ruptures, $h_r \sim t_l^{-2/3}$, thus we obtain $t_l \sim c^{-3/2} \sim (\zeta + 1)^{-3/2}$. This scaling fits well with the experimental results (see Fig. 1(b)) and is found to be independent of factors like container type, pool depth and bubble size. Our findings may provide new insight on surface bubble lifetime and foam stability.

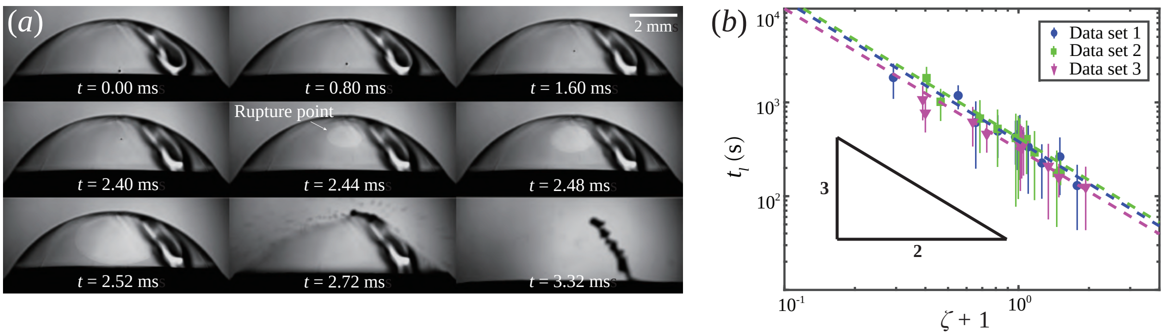

Figure 1: (a) Snapshots of a rupture event for an isopropanol surface bubble. The oversaturation of the liquid is $\zeta = 0.12$. (b) Dependence of surface bubble lifetime t_l on dissolved gas concentration represented by the gas oversaturation ζ. The three data sets are obtained with different pool depths and bubble sizes.

References

Epstein, P. S., Plesset, M. S. *On the stability of gas bubbles in liquid-gas solutions.* J. Chem. Phys. **18**, 1505–1509, 1950.

Poulain, S., Villermaux, E., Bourouiba, L. *Ageing and burst of surface bubbles.* J. Fluid Mech. **851**, 636 – 671, 2018.

Capillary migration of floating bubbles at a free surface

Kuntal Patel[1] and Xiaojue Zhu[1]
[1] Max Planck Institute for Solar System Research, 37077 Göttingen, Germany

Floating bubbles at a free surface sense one another through the deformation they imprint on the interface. Under the influence of deformation-induced capillary forces, initially separated floating bubbles migrate, align, and organize into ordered structures resembling bubble rafts. Despite their relevance to foams, whitecaps, and interfacial transport processes, this capillary-driven self-organization in floating bubbles remains poorly quantified.

In this work, we use high-resolution direct numerical simulations (DNS) of non-coalescing floating bubbles to characterize the dynamics of capillary-induced aggregation in both bubble pairs and bubble swarms. To prevent interfacial coalescence, we capture the free surface and each individual bubble using distinct volume-fraction indicators. We find that the interaction strength between two side-by-side floating bubbles is non-monotonic in the Bond (Bo) number. Bubbles at intermediate Bo exhibit the fastest convergence, whereas bubbles at relatively small (surface-tension-dominated) and very large (buoyancy-dominated) Bo interact more weakly and approach one another more slowly. The migration time required to form a two-bubble raft through capillary attraction increases exponentially with initial separation.

We then develop a simplified predictive model for the evolution of bubble spacing in a pair undergoing capillary-driven approach in the small-Bond-number limit. The model is based on linear superposition, approximating the free-surface shape as the sum of the individual deformations produced by each isolated bubble within the pair. The resulting capillary force on each bubble is derived from the gradient of potential energy as it moves along the deformation field generated by its neighbor. Bubble motion is then determined by balancing this capillary attraction with a calibrated hydrodynamic drag. Despite its simplicity, the model accurately reproduces the temporal evolution of bubble spacing observed in the DNS.

Finally, we examine the collective dynamics of floating bubbles arranged in a monolayer configuration. The simulations reveal the formation of transient chain- and island-like structures arising from capillary attraction between neighboring bubbles. These intermediate aggregates progressively reorganize and coalesce into a larger, compact floating raft (see figure 1). The collective behavior is quantified using polar and bond-orientational order parameters, which capture the evolution of spatial organization of floating bubbles during capillary migration.

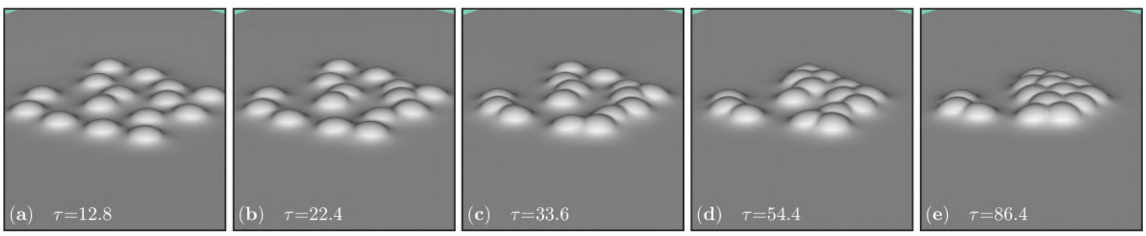

Figure 1: Capillary migration in a monodisperse suspension of floating bubbles at $Bo = 10$.

Why a pair of bubbles rising in-line becomes more stable with the shape oblateness: a linear stability analysis

J. Zhang[1], W. - Q. Liu[1] and J. - M. Jiang[1]
[1] State Key Laboratory for Strength and Vibration of Mechanical Structures, School of Aerospace, Xi'an Jiaotong University, Xi'an, China

The stability of two bubbles rising initially in-line through a viscous liquid is revisited using a global linear stability analysis formulated within an Arbitrary Lagrangian-Eulerian framework. Whereas previous studies (Zhang et al., 2021; Maeda et al., 2021) attributed the promoted in-line stability of oblate bubbles to a deformation-enhanced wake entrainment, the present analysis demonstrates that the dominant stabilizing mechanism arises instead from an inclination-induced rotational feedback generated as the trailing bubble experiences the asymmetric shear of the leading bubble's wake. This inclination-shear coupling, rather than deformation itself, governs the recovery of stability with increasing aspect ratio. Furthermore, the results reveal that the unstable drafting-kissing-tumbling mode originates from short-range, two-way coupling between the bubbles, whereas the asymmetric side-escape mode corresponds to a long-range, one-way interaction dominated by the trailing bubble response. Together, these findings provide a unified framework for interpreting the stationary transitions of rising bubble pairs across a broad range of inertial and deformable regimes.

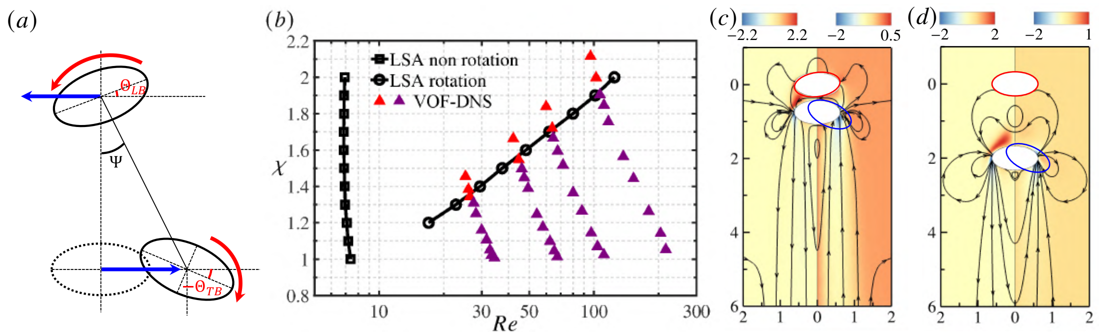

Figure 1: (a) Schematic of the ALE-LSA configuration. (b) Comparison between the present ALE-LSA results with (circles) and without (squares) rotational degrees of freedom suppressed, and the VOF-DNS data (Zhang et al., 2021) (triangles). (c)(d) Structure of the stationary eigenmode for the oblate bubble pair of $\chi = 1.9$ near the critical threshold for different separations.

References

J. Zhang, M.-J. Ni, and J. Magnaudet *Three-dimensional dynamics of a pair of deformable bubbles rising initially in line. Part 1. Moderately inertial regimes.* J. Fluid Mech., **A16**, 920, 2021.

K. Maeda et al. *Viscid-inviscid interactions of pairwise bubbles in a turbulent channel flow and their implications for bubble clustering.* J. Fluid Mech., **A30**, 919, 2021.

Predicting the bubble-particle collision rate in turbulence

Dominik Krug[1,2], Timothy T.K. Chan[2] and Linfeng Jiang[1]
[1] Institute of Aerodynamics, RWTH Aachen University,
Wüllnerstraße 5a, 52062 Aachen, Germany
[2] Physics of Fluids Group, Max Planck Center for Complex Fluid Dynamics,
University of Twente, P.O. Box 217, 7500 AE Enschede, The Netherlands

Bubble-particle collisions are central to the efficiency of industrial separation processes such as froth flotation. Despite their practical importance, a consistent framework to predict collision rates under turbulent conditions remains lacking. In particular, capturing the flow distortion around bubble, which is typically larger than the particles, within turbulence has remained challenging. Building on the frozen-turbulence approach of Jiang et al. (2024), which accounts for turbulent fluctuations of the bubble slip velocity, we develop an *a priori* model for predicting bubble-particle collision rates based solely on bubble, particle, and turbulence parameters.

We validate the model against direct numerical simulations of finite-size bubbles with Stokes numbers $St_b = 2.8$ and 6.3, interacting with particles of Stokes numbers $0.01 \leq St_p \leq 2$ in homogeneous isotropic turbulence at Taylor Reynolds number $Re_\lambda = 64$. Good agreement between model predictions and simulations is obtained for Froude numbers $Fr \leq 0.25$. Beyond this range, we propose a practical criterion for model applicability and discuss its limitations.

Evaluation under typical flotation conditions indicates that particle inertia and gravitational settling effects are generally significant. The model predicts increased collision rates for smaller bubbles, larger particles, and stronger turbulence intensities.

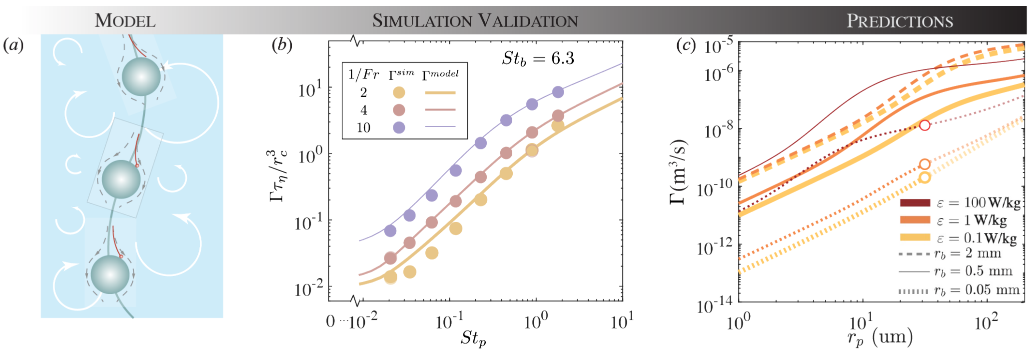

Figure 1: Predicting the bubble-particle collision kernel through modeling and simulation validation. *From: Chan et al., Chem. Eng. Sci., (2026).*

References

L. Jiang, and D. Krug. *How turbulence increases the bubble-particle collision rate.* J. Fluid Mech., **1006**, A19, 2025.

T. Chan, L. Jiang, and D. Krug. *A predictive model for bubble-particle collisions in turbulence.* Chem. Eng. Sci., **321**, 122850, 2026.

Spatiotemporal Analysis of Single Droplet under HIT

A. Safak[1] and M. Saeedipour[1]
[1] Johannes Kepler University, Linz, Austria

A single droplet in homogeneous isotropic turbulence (HIT) is a canonical configuration to investigate how the background turbulence interacts with a fluid-fluid interface and the subsequent interfacial events such as fragmentation and coalescence. This study establishes a well-defined triple-periodic HIT box under various Taylor-scale Reynolds and Weber numbers to serve as groundwork for further explorations on droplet breakups. It has been already shown by Saeedipour and Schneiderbauer (2025) that fragmentation of droplets is controlled by the spectral contribution of enstrophy mechanisms i.e. when vortex stretching surpasses that of surface tension. The present work proceeds this analysis on spatiotemporal scales by replicating Vela-Martin and Avila (2022) for a small ensemble. Moreover, it follows Chen *et al.* (2019) attempting to distinguish between two competing mechanisms attributed to breakups of equal or non-equal split ratios based on turbulent quantities. Figure 1 shows two such instances for one case, yet expressing markedly distinct behaviors. This analysis provides insight for better understanding of turbulent emulsification regimes.

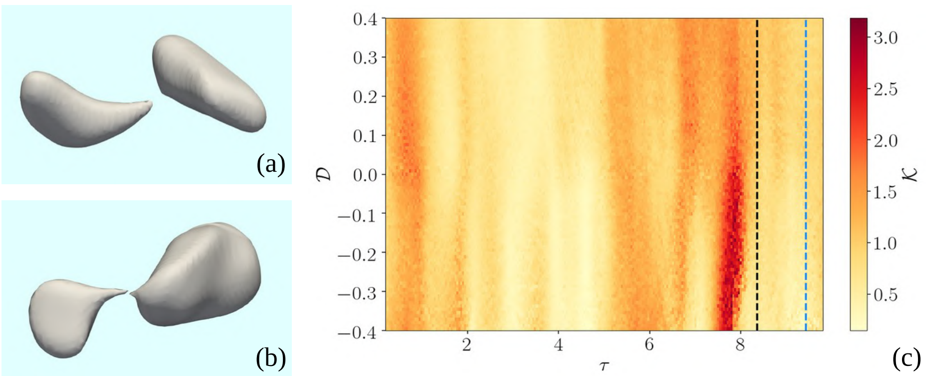

Figure 1 Droplet breakups under HIT with $Re_\lambda = 52$ and We = 1.66: (a) equal, (b) non-equal splits, (c) normalized kinetic energy over the full spatiotemporal field of normalized time and distance to the interface with blue and black vertical dashed lines corresponding to (a) and (b), respectively.

References

M. Saeedipour and S. Schneiderbauer. Enstrophy transport rates determine the Kolmogorov-Hinze scale in turbulent fragmentation of droplets. *Phys. Rev. Fluids*, **10**, 044301, 2025.

A. Vela-Martin and M. Avila. Memoryless drop breakup in turbulence. *Science Advances*, **8**, eabp9561, 2022.

Y. Chen, J. Ding, P. Weng, Z. Lu and X. Li. A theoretical model describing bubble deformability and its effect on binary breakup in turbulent dispersions. *Eur. J. Mech. B Fluids*, **75**, 352-360, 2019.

Solutal-Marangoni-Driven Freezing Dynamics of Supercooled Ethanol-Water Droplets

F. Wang[1], H. Zeng[1], Y. Du[1], X. Tang[1] and C. Sun[1,2]
[1] New Cornerstone Science Laboratory, Department of Energy and Power Engineering, Tsinghua University, Beijing 100084, China
[2] Department of Engineering Mechanics, School of Aerospace Engineering, Tsinghua University, Beijing 100084, China

Solidification of droplets is of great importance to various applications. In the case of multicomponent droplets undergoing solidification, the emergence of concentration gradients may trigger significant interfacial flows that dominate the freezing dynamics. Here, we experimentally investigate the interfacial freezing dynamics of supercooled ethanol-water droplets, accompanied with the migration and growth of massive ice particles. We reveal that this unique freezing dynamics is driven by solidification-induced solutal Marangoni flow within the droplets. Our model, which incorporates the temperature- and concentration-dependent properties of the ethanol-water mixture, quantitatively predicts both the migration velocity and the growth rate of the ice particles. The former is determined by the solutal Marangoni flow velocity, while the latter is governed by a balance between the latent heat release and the enhanced thermal dissipation by the Marangoni flow. Moreover, we show that the final wrapping state of droplets can be modulated by the concentration of ethanol.

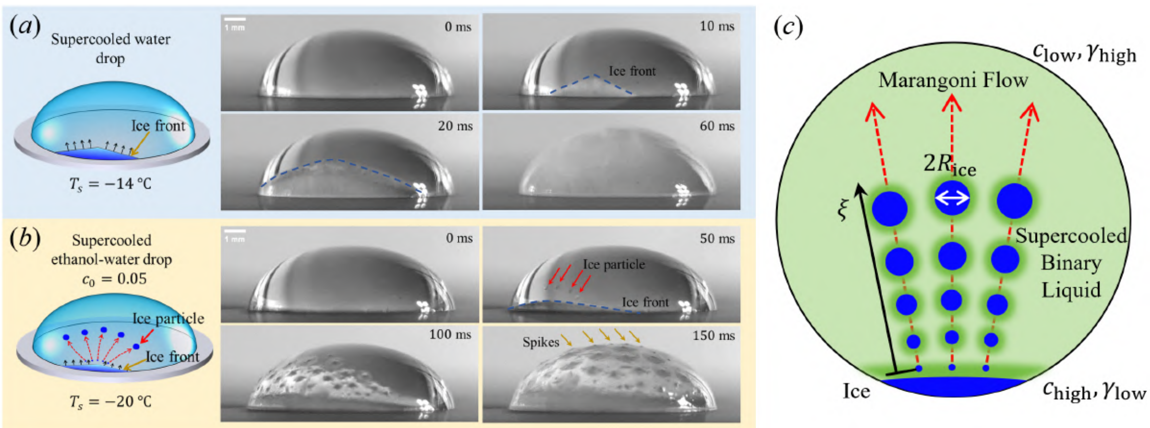

Figure 1: Freezing dynamics of supercooled droplets. **(a)** Side view for recalescence of the supercooled water droplets. **(b)** Side view for ice migration of the supercooled ethanol-water droplets. **(c)** Top-down view of a sketch illustrating ice growth and migration driven by the solutal Marangoni effect, which results from solute rejection during solidification.

References

F. Wang, H. Zeng, Y. Du, X. Tang, and C. Sun. *Marangoni-driven freezing dynamics of supercooled binary droplets.* J. Fluid Mech., **1026**, A11, 2026.

D. Dedovets, C. Monteux, and S. Deville. *Five-dimensional imaging of freezing emulsions with solute effects.* Science, **360**, 303-306, 2018.

A one-half law relating viscous-pressure and viscous-stress forces on a spherical droplet in incompressible flow

Tian Long[1] and Jie Zhang[1]
[1] School of Aerospace, Xi'an jiaotong University, Xi'an, Shaanxi 710049, PR China

For dispersed multiphase flows, the forces acting on an immersed body govern the associated dispersion mechanisms and are commonly decomposed into distinct contributions to clarify the underlying physics. In this work, we investigate the forces acting on a spherical droplet in incompressible flow, with particular emphasis on the pressure component associated with viscosity. In certain limited cases, previous studies found that the net force due to viscous pressure equals one half of that arising from viscous stress. Here we demonstrate that this one-half law is general: it holds for any interfacial slip boundary condition, ranging from fully slip bubbles to no-slip spheres, at any Reynolds number, and in the presence of external body forces (as illustrated in the accompanying figure). We obtain a numerical decomposition of the pressure field by solving auxiliary Poisson equations, and the resulting force components agree closely with theoretical expectations. We further analyze the force distributions by expanding them in Legendre polynomials. For a given viscosity ratio, the ratios of the first modal coefficients fully determine the force relation and remain invariant with Reynolds number. Finally, we provide a rigorous analytical proof based on Force Element Analysis (FEA), demonstrating that the relationship between the forces induced by viscous pressure and viscous stress is determined solely by the spherical geometry and is independent of the flow conditions.

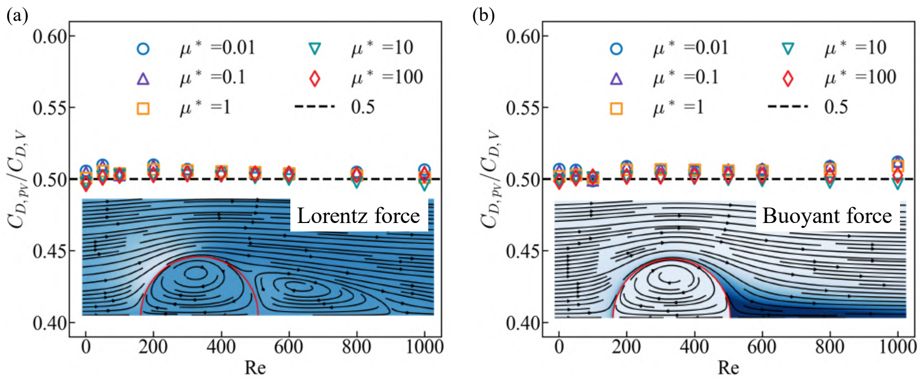

Figure 1: Uniform flow past a viscous droplet with body forces: ratio of viscous pressure drag to viscous stress drag across all Reynolds numbers and viscosity ratios for (a) MHD flows and (b) stratified flows.

References

J. Magnaudet, M. Rivero and J. Fabre. *Accelerated flows past a rigid sphere or a spherical bubble. Part I. Steady straining flow.* J. Fluid Mech., **284**, 97-135, 1995.

C.C. Chang. *Potential flow and forces for incompressible viscous flow.* Proc. R. Soc. Lond. A., **437**(1901), 517-525, 1999.

Dynamics of Polymer-Laden Drops on Inclined Surfaces: Toward Modulation of Pearling Instabilities

J. Wilson[1], Y. Zhang[1], F. Wang[1], and C. Sun[1,2]
[1] Department of Energy and Power Engineering,
Tsinghua University, Beijing 100084, China
[2] Department of Engineering Mechanics, School of Aerospace Engineering,
Tsinghua University, Beijing 100084, China

The motion of liquid drops on surfaces governs a wide range of industrial and natural processes, from coating flows to pesticide deposition. At sufficiently high capillary numbers, drops on an inclined surface develop a corner which at even higher capillary number transitions to a cusp and emits satellite droplets. The contact angle inclines to delay the onset of dynamic wetting, and the "pearling" instability is thus a suitable vehicle for studying the impact of polymers on dynamic wetting and contact line motion. While the hydrodynamics of pure fluids in this regime are well studied, the role of viscoelasticity introduced by dissolved polymers remains largely unexplored. Polymers are known to modify instabilities in other free-surface flows - either suppressing or promoting them depending on the balance of elastic and viscous stresses. Their influence on moving contact lines, however, remains largely unexplored. Here, we present an experimental investigation of aqueous polymer drops sliding down inclined PMMA substrates. Preliminary experiments with pure water establish reproducible baseline behavior, including the onset conditions for pearling. Building on this foundation, we introduce polyethylene oxide (PEO) and quantify the critical capillary number for pearling onset as a function of polymer concentration and molecular weight.

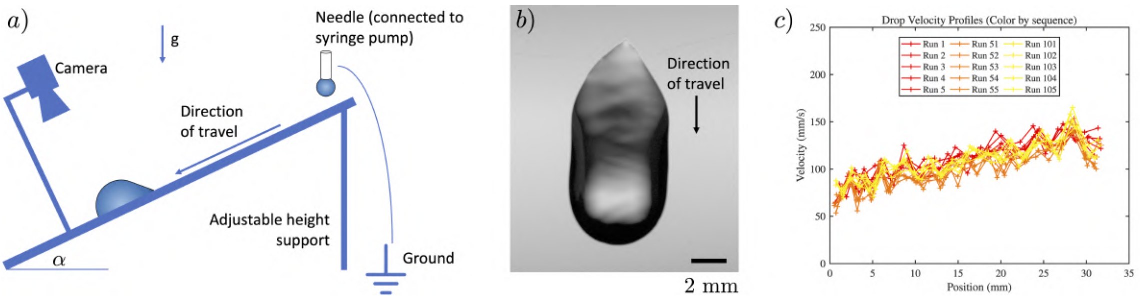

Figure 1: a) Schematic of the experimental setup with high-speed imaging and controlled deposition, b) top view of a water drop on an inclined PMMA surface showing corner formation near pearling threshold, c) early results showing minimal surface aging effects.

References

T. Podgorski, J.-M. Flesselles, and L. Limat. *Corners, Cusps, and Pearls in Running Drops.* Phys. Rev. Lett., **87**, 036102, 2001.

S. Engelnkemper, M. Wilczek, S.V. Gurevich, and U. Thiele. *Morphological transitions of sliding drops: Dynamics and bifurcations.* Phys. Rev. Fluids, **1**, 073901, 2016.

I. Peters, J.H. Snoeijer, A. Daerr, and L. Limat. *Coexistence of Two Singularities in Dewetting Flows: Regularizing the Corner Tip.* Phys. Rev. Lett., **103**, 114501, 2009.

L. Limat, and H.A. Stone. *Three-dimensional lubrication model of a contact line corner singularity.* Europhys. Lett., **65**, 365, 2004.

J.H. Snoeijer, and B. Andreotti. *Moving Contact Lines: Scales, Regimes, and Dynamical Transitions.* Annu. Rev. Fluid Mech., **45**, 269, 2013.

A. Deblais, R. Harich, A. Colin, and H. Kellay. *Taming contact line instability for pattern formation.* Nat. Commun., **7**, 12458, 2016.

A. Varma. *Weak-inertial effects on destabilized receding contact lines.* Phys. Rev. Fluids, **9**, 084006, 2024.

S. Varagnolo, D. Filippi, G. Mistura, M. Pierno, and M. Sbragaglia. *Stretching of viscoelastic drops by steady sliding.* Soft Matter **13**, 3116, 2017.

Droplets in HIT: 3D Internal Flow Measurement

F. Sortini[1], L. E. Beckedorff[2] and A. Soldati[1,2]
[1] Polytechnic Department of Engineering and Architecture,
Universita degli Studi di Udine, 33100 Udine, Italy
[2] Institute of Fluid Mechanics and Heat Transfer, TU Wien, 1060 Vienna, Austria

Abstract

We investigate the internal flow of oil droplets dispersed in homogeneous isotropic turbulence, with the goal of quantifying how the droplet-interior velocity field couples with interface deformation and orientational dynamics. Turbulence is generated in an octagonal horizontal water tank by two opposing jet arrays, producing an energy dissipation rate of $\varepsilon \approx 0.1\ \mathrm{m^2\,s^{-3}}$ and a Taylor-microscale Reynolds number of $Re_\lambda \approx 560$. Five high-speed cameras record the time-resolved droplet interface together with tracer particles in the surrounding liquid, and the velocity field is reconstructed using 3D Particle Tracking Velocimetry (Shake-The-Box). Thanks to refractive-index matching between the droplet and carrier phases, the measurements can be extended also inside the droplet, enabling simultaneous access to the inner and outer flow fields around deforming droplets.

The oil is nearly density-matched with water and has a viscosity of the same order of magnitude. The resulting measurements provide a direct basis to study (i) the structure and time evolution of the internal velocity-gradient field, (ii) its relation to droplet shape and principal-axis orientation, and (iii) the correspondence between interior dynamics and local turbulent strain and rotation in the surrounding flow.

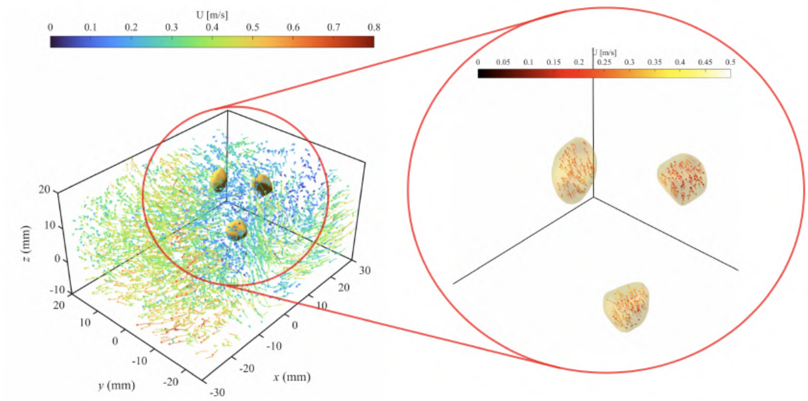

Figure 1: Reconstruction of the inner and outer velocity fields.

References

[1] Beckedorff L., Caridi G. C. A., Soldati A. *Jet-stirred homogeneous isotropic turbulent water tank for bubble and droplet fragmentation.* Rev. Sci. Instrum. 1 February,2025.

[2] Ni R. *Deformation and Breakup of Bubbles and Drops in Turbulence.* Annu. Rev. Fluid Mech., 56, 319-347,2024.

[3] Masuk AUM, Salibindla AKR, Ni R. *The orientational dynamics of deformable finite-sized bubbles in turbulence.* Journal of Fluid Mechanics,2021 .

Marangoni instabilities of thin cylindrical drops vertically immersed in stratified liquids: Influence of the Hele-Shaw cell

Li-Chen Huang[1], Yanshen Li[1]
[1] School of Engineering Science, University of Chinese Academy of Sciences, Beijing 101408, PR China

Marangoni flows in confined geometries are important for bubble/droplet manipulation, micro mixing and drug delivery, etc. The Marangoni instabilities of drops/bubbles in vertical Hele-Shaw cells have been studied previously [1], however, the influence of the Hele-Shaw cell remains unexplored and the underlying physics is not clear. Here we study the onset of Marangoni instabilities of cylindrical drops in a vertical Hele-Shaw cell immersed in linearly stratified ethanol-water mixtures. The parameter space of drop radius R and concentration gradient $\mathrm{d}w_\mathrm{e}/\mathrm{d}y$ are experimentally explored and the concentration field is directly observed by laser interferometry. The flow is found to become unstable when advection is too strong for diffusion to maintain a stable concentration field, but two different instability regimes are found: When the concentration gradient is large (small), the flow becomes unstable when the drop is relatively small (large), and all the flow field around (only the flow field close to the equator of) the drop is unstable, see Fig. 1(a) and (b), respectively.

From Buckingham-PI theory, we know that the controlling parameters of this system include Ma, Ra, and R/d, where $Ma = V_\mathrm{M}R/D$ is the Marangoni number, V_M is the Marangoni flow velocity at the equator of the drop, D is the diffusivity of ethanol, $Ra = -\mathrm{d}\rho/\mathrm{d}y \cdot gR^4/(\mu D)$ is the Rayleigh number and d is the thickness of the Hele-Shaw cell. The presence of the Hele-Shaw cell not only fixes the position of the drop, but also introduces extra friction force to the flow field characterized by $k = \sqrt{12}R/d$ [2]. If one only considers the influence of the Hele-Shaw cell on the Marangoni flow boundary layer thickness δ, one finds that δ is very large (small) when k is very small (large) [2]. On the other hand, if one only considers the influence of the stratification, one finds that $\delta \sim R/Ra^{1/4}$ which is small (large) when the concentration gradient is large (small). When the above two factors are combined, the real boundary layer thickness δ should be the smaller one. Thus, when R is small (large) so that k is consequently small (large), the concentration gradient happens to be large (small), then we have $\delta \sim R/Ra^{1/4}$ ($\delta \sim R$ when k is large). Combined with the advection-diffusion equation, we obtain a unifying scaling theory which predicts the two instability criteria: $Ma/Ra^{1/4} > s_1$ and $Ma > s_2$, where s_1 and s_2 are constants to be determined. The two scaling criteria are found to fit well with the experimental results, see Fig. 1(c). Our findings may shed new light on the understandings of Marangoni flows in confined geometries.

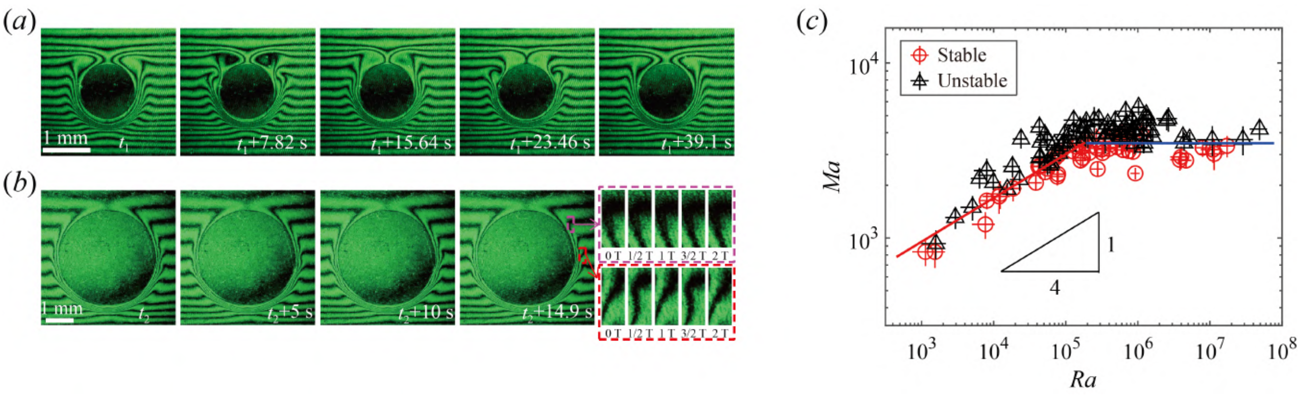

Figure 1: Snapshots of 100 cSt silicone oil drops in linearly stratified ethanol–water mixtures. (a) $R = 0.57\,\mathrm{mm}$, $\mathrm{d}w_\mathrm{e}/\mathrm{d}y = 107.9\,\mathrm{m}^{-1}$. The oscillation period is $T = 39.1\,\mathrm{s}$. (b) $R = 1.71\,\mathrm{mm}$, $\mathrm{d}w_\mathrm{e}/\mathrm{d}y = 44.5\,\mathrm{m}^{-1}$. The oscillation period is $T = 14.9\,\mathrm{s}$. (c) Phase diagram of the 100 cSt drops presented in the Ma vs. Ra parameter space. Red circles stand for stable flow fields and black triangles for unstable flow fields.

References

[1] D. Bratsun, K. Kostarev, A. Mizev, S. Aland, M. Mokbel, K. Schwarzenberger, and K. Eckert. *Adaptive micromixer based on the solutocapillary Marangoni effect in a continuous-flow microreactor.* Micromachines, **9**(11), 600, 2018.

[2] D. Boos, A. Thess. *Thermocapillary flow in a hele-shaw cell.* J. Fluid Mech. **352**, 305–330, 1997.

The multifractal structure of energy dissipation in multiphase turbulence

M. Crialesi-Esposito[1], A. Rivière[2] and S. Chibbaro[1,2]
[1] DIEF, University of Modena and Reggio Emilia, via Vivarelli 10, 41125, Modena, Italy
[2] Laboratory of Fluid Mechanics and Instabilities,
Ecole Polytechnique Fédérale de Lausanne, CH-1015 Lausanne, Switzerland
[3] Universitè Paris-Saclay, CNRS, LISN, 91400 Orsay, France

In recent years, an increasing number of observations have been reported on the nature of turbulence in multiphase flows where two phases are separated by a deformable interface. Among the many peculiar behaviors of this class of flows, two aspects remain largely unexplored: the formation of scales smaller than those observed in single-phase turbulence and the strongly intermittent nature of multiphase turbulence.

In this work, we study turbulence under homogeneous and isotropic conditions with high small-scale resolution, achieving $\eta_{K41}/\Delta x \approx 6$, where η_{K41} is the Kolmogorov scale and Δx is the grid spacing. We analyze sub-Kolmogorov velocity fluctuations and the associated dissipation regions. To characterize the geometrical structure of these flow patches, we perform a multifractal analysis, ultimately linking the intermittent nature of multiphase turbulence to the extension of dissipative regions at scales smaller than the Kolmogorov scale.

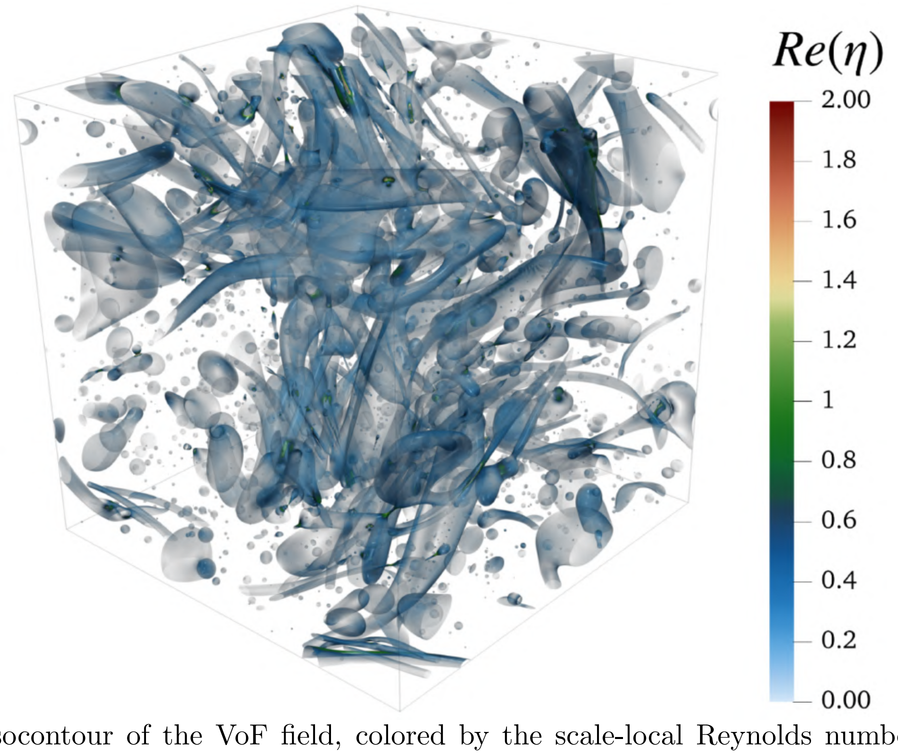

Figure 1: Isocontour of the VoF field, colored by the scale-local Reynolds number $Re(\eta)$ computed at the scale $\eta = \eta_{K41}/3$

Interface-Resolved DNS Studies of Flexible Fiber Dynamics in a Fluid Using an LBM-DEM Method

Junjie Chen[1], Zhaosheng Yu[1], Lian-Ping Wang[2], Yu Guo[1*]
[1] Department of Engineering Mechanics, Zhejiang University, Hangzhou, 310027, China
[2] Department of Mechanics and Aerospace Engineering, Southern University of Science and Technology, Shenzhen 518055, China
[*] Corresponding author: yguo@zju.edu.cn

Compared to rigid spheres and cylinders, flexible fibers exhibit more complex fluid-solid interactive dynamics. In this study, we develop an interface-resolved Direct Numerical Simulation (DNS) framework to model two-phase flows of finite-volume flexible fibers in a viscous fluid. The fibers’ deformation, motion, and contacts are computed using a bonded sphero-cylinder model based on the Discrete Element Method (DEM) [1], while the fluid flow is solved by the Lattice Boltzmann Method (LBM) [2]. The fluid-fiber interaction is fully resolved through an interpolated bounce-back scheme [2] with a high interface resolution, which ensures accurate determination of location of the fiber surface and consistent classification of lattice nodes. The developed method is validated against several benchmark problems, including flow past rigid bodies, fluttering of a confined fiber, fiber cantilever bending, and sedimentation of a flexible fiber. The results demonstrate accurate predictions of hydrodynamic forces, large deformation, and unsteady dynamics by the method. Finally, sedimentation of a single flexible fiber in a thin-sliced channel is investigated, where distinct settling and deformation modes are observed depending on the Reynolds number and fiber flexibility.

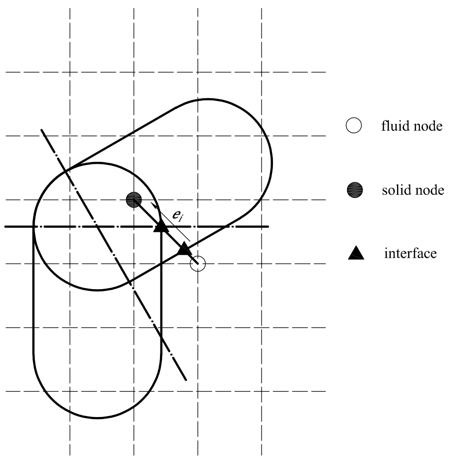

Figure 1: Illustration of the connection between a boundary fluid node and a solid node intersecting multiple sphero-cylinder elements.

References

[1] Y. Guo et al., AIChE Journal 67, e17296 (2021).

[2] Y. Liu, Y. Guo et al., J. Fluid Mech. 960, A25 (2023).

Modelling of elongated particles in channel flows with realistic rough walls

M. A. Taborda[1], B. van Wachem[1]
[1] Otto-von-Guericke University Magdeburg, Universitätspl. 2, Germany

The transport of inertial particles over rough boundaries is relevant to a wide range of natural and industrial processes, including fibrous suspensions, filtration, and sediment transport. While particle-wall interactions of spherical particles over smooth surfaces have been extensively studied, the combined influence of three-dimensional roughness and particle non-sphericity remains poorly understood. In particular, elongated particles, such as fibres, present complex orientation-dependent hydrodynamic forces and torques that significantly alter their near-wall dynamics compared to spherical particles. Moreover, the interaction mechanisms between rough walls and non-spherical particles differ fundamentally from those governing rough-wall interactions with spherical particles.

In this contribution, we will investigate the coupled effects of realistic 3D surface roughness and particle elongation on the transport, rotation, and wall interactions of such particles in a turbulent channel flow. The considered rough surface is generated using statistically controlled Gaussian-distributed surface heights with prescribed root-mean-square roughness and correlation lengths in both streamwise and spanwise directions based on experiments using stainless steel (Kussin and Sommerfeld, 2002). The resulting surfaces are incorporated into a CFD/DEM simulation framework, which enables fully resolved particle-wall interactions over realistic rough-wall geometries. Additionally, particle motion is computed using a two-way coupled approach that accounts for drag, lift, and hydrodynamic torque contributions, including orientation-dependent correlations for elongated non-spherical particles (Chéron et al., 2024).

The obtained results show that wall roughness magnifies the shape-dependent differences. Roughness elements locally modify the fibre-wall interaction, which is reflected in the particle concentration and particle velocity along the channel height (see Figure 1). Furthermore, elongated particles present reduced angular velocities and stronger alignment within the wall-parallel plane, while spheres maintain comparatively higher rotational velocities due to the absence of orientation-dependent damping mechanisms.

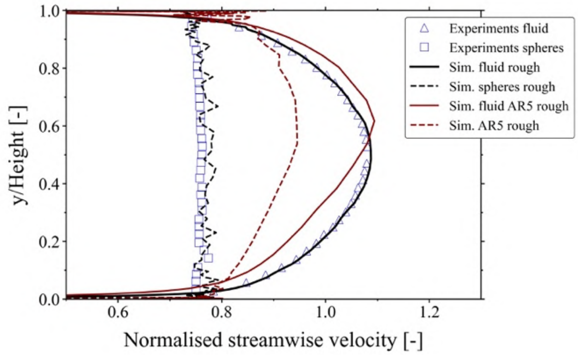

Figure 1: Comparison of simulation results against experiments. Spherical and

elongated particles with aspect ratio 5 are presented. lines correspond to fluid velocity and dashed lines correspond to particle velocity.

References

V. Chéron, F. Evrard, B. van Wachem. Drag, lift and torque correlations for axi-symmetric rod-like non-spherical particles in locally linear shear flows. *International Journal of Multiphase Flow*. 104692, 2024.

J. Kussin and M. Sommerfeld. Experimental studies on particle behaviour and turbulence modification in horizontal channel flow with different wall roughness. *Experiments in Fluids*, 33, 143-159, 2002.

Numerical Simulation of a Long Flexible Fibre in a Lid-driven Fluid Cavity

S. Radhakrishnakumar[1], U. Hampel[1,2] and G. Lecrivain[1]
[1] Helmholtz-Zentrum Dresden-Rossendorf, Institute of Fluid Dynamics, Dresden, Germany
[2] Chair of Imaging Techniques and Process Engineering, TU Dresden, Germany

The dynamic behaviour of flexible fibres in fluid flow play a crucial role in many industrial and biological applications, such as pulp processing, filtration, fibre-reinforced materials and microfluidic devices. While previous studies have explored deformation of flexible fibres in turbulent channel flows (Dotto (2020)), a detailed numerical study of the dynamic evolution of a single long flexible fibre suspended in a viscous lid-driven cavity is still lacking.

To address this, we employ a Lagrangian beam model (Lecrivain (2020)) in which the fibre is represented as a chain of spherical beads that undergo bending, twisting and stretching. The deformation is driven by hydrodynamic drag, while elastic forces maintain fibre integrity. The aim is to develop a numerical framework to identify key factors governing flow-induced coiling and subsequent de-coiling. As illustrated in Figure 1, an initially straight fibre deforms under the influence of the moving lid and eventually forms a stable coil. The expected outcomes include scaling relations for coiling time with respect to fibre length and flexibility, as well as the identification of parameter regimes leading to stable coiled states. This helps us understand fibre entanglement in confined flows, to prevent clogging in microchannels and optimise fibre dispersion in composite manufacturing.

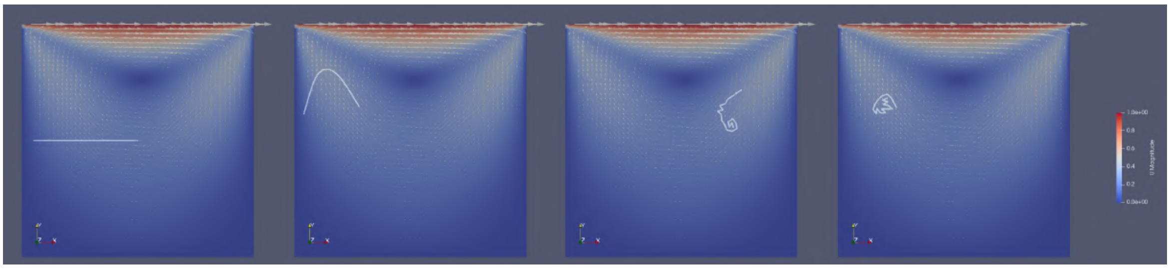

Figure 1: Evolution of a long flexible fibre in a lid-driven cavity. From left to right, the initially straight fibre is advected by the primary vortex generated by the moving lid and progressively deforms, leading to a coiled configuration.

References

D. Dotto, A. Soldati, and C. Marchioli. *Deformation of flexible fibers in turbulent channel flow.* Meccanica, Springer, **55**(2), 343–356, 2020.

G. Lecrivain, T.B.P. Grein, R. Yamamoto, U. Hampel, and T. Taniguchi. *Eulerian/Lagrangian formulation for the elasto-capillary deformation of a flexible fibre.* J. Comput. Phys., **409**, 109324, 2020.

Length effect on rigid fiber dynamics in turbulent channel flow

D. Sun[1], C. Brouzet[1] and J. Bec[1,2]
[1] Université Côte d'Azur, CNRS, INPHYNI, Nice, France
[2] Université Côte d'Azur, Inria, CNRS, Calisto team, Sophia Antipolis, France

Turbulent flows laden with anisotropic particles are commonly encountered in various natural phenomena and industrial processes (Voth and Soldati, 2017). In this work, we experimentally investigate the dynamic behaviors of three sets of polystyrene rigid fibers of different lengths transported by a turbulent channel flow ($\mathrm{Re}_\tau \approx 400$) and perform a one-to-one comparison with our numerical simulation results based on the slender body theory. The fibres we use are very long ($\ell/h = 0.25,\ 0.5,\ 1$, where ℓ is the length of fibers and h is the channel half height) and have moderate inertia ($\mathrm{St}^+ = 16,\ 21,\ 25$, where St^+ is the Stokes number based on the wall units). In addition, their terminal settling velocity is of the same order of magnitude as the wall friction velocity, which leads to their accumulation near the bottom wall (Baker and Coletti, 2022).

The effect of length on orientation, translational velocity and concentration profiles remains relatively weak, while it becomes significant for tumbling rate, as already reported in HIT (Oehmke et al., 2021). However, we show that the presence of the wall impacts the tumbling dynamics. Near the wall, due to geometric constraints, fiber mainly adopts a "kayaking" motion, tumbling in a plane parallel to the wall. Further from the wall, when fibers are able to orient along the wall-normal direction, they turn to a "pole-vaulting" mode (see Fig. 1). This induces a localized peak in tumbling rate, at a wall distance $\ell/2$. These two types of tumbling motion and their scalings will be discussed during the conference.

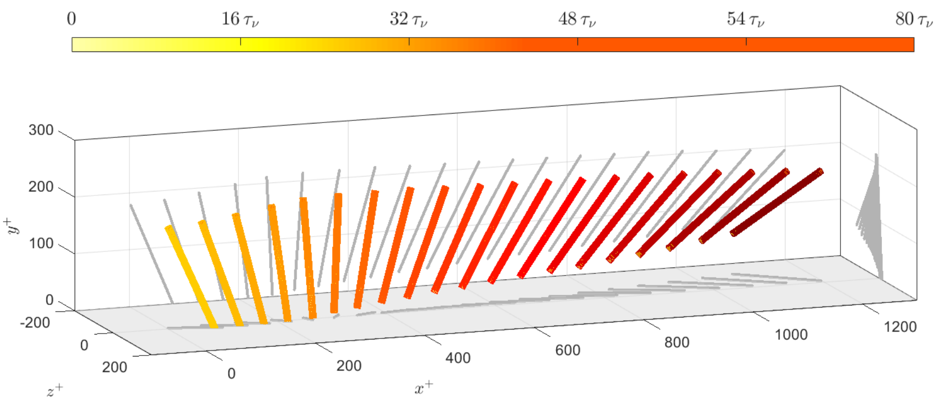

Figure 1: Tumbling of a fiber of length $\ell^+ = 200$, leading to an instance of pole-vaulting. Different colors correspond to various instant of time, expressed in viscous units.

References

L. J. Baker and F. Coletti. Experimental investigation of inertial fibres and disks in a turbulent boundary layer. *Journal of Fluid Mechanics*, 943:A27, 2022.

T. B. Oehmke, A. D. Bordoloi, E. Variano, and G. Verhille. Spinning and tumbling of long fibers in isotropic turbulence. *Phys. Rev. Fluids*, 6:044610, 2021.

G. A. Voth and A. Soldati. Anisotropic particles in turbulence. *Annual Review of Fluid Mechanics*, 49:249–276, 2017.

Fragmentation of slender fibres by inertial-range turbulence: quasi-static mechanics, hazard scaling and intermittency effects

A. Mazzino[1]
[1] DICCA & INFN, Univeristy of Genova , Via Montallegro 1, 16145 Genova, Italy

March 15, 2026

We study fragmentation of slender elastic fibres transported by homogeneous and isotropic turbulence, in the regime where the fibre length L lies in the inertial range and the fibre response is quasi-static (QS), i.e. the shape adjusts within one eddy-turnover time at scale L (Mazzino , 2026a). In this limit, the fibre behaves as an overdamped Euler–Bernoulli beam forced by the transverse velocity increment $\delta_L u$, which gives the characteristic curvature estimate

$$\kappa_L \sim \frac{\xi_\perp}{\gamma} L^2 \, \delta_L u, \tag{1}$$

where κ_L is the typical curvature, $\xi_\perp$ the transverse viscous drag coefficient, and γ the bending stiffness.

Comparing κ_L with the material fracture threshold κ_{frac} defines a critical length ℓ_c separating a subcritical regime, $L \ll \ell_c$, where breakup is rare, from a supercritical regime, $L \gg \ell_c$, where breakup occurs within $O(1)$ eddy turnovers. In the supercritical range, the breakup hazard $h(L)$ is set by the inertial-range turnover time $h(L) \sim \tau_L^{-1}$, $\tau_L \sim \bar{\varepsilon}^{-1/3} L^{2/3}$, with $\bar{\varepsilon}$ the mean kinetic-energy dissipation rate. Hence

$$h(L) \sim \bar{\varepsilon}^{1/3} L^{-2/3}. \tag{2}$$

Embedding this mechanically derived hazard into a binary self-similar population-balance model for the fibre-length number density $n(L)$, where $n(L)\, dL$ is the number of fibres in $[L, L + dL]$, yields in the stationary case

$$n(L) \sim L^{-4/3}. \tag{3}$$

This provides a first-principles route from inertial-range turbulence to a nontrivial fragmentation spectrum.

We finally assess the role of intermittency (Mazzino , 2026b). Intermittency enters through the statistics of $\delta_L u$ and mainly affects the subcritical and crossover regimes, where breakup is controlled by rare fluctuations. Results indicate that the supercritical scaling $h(L) \sim \tau_L^{-1}$ and the baseline spectrum $n(L) \sim L^{-4/3}$ remain robust, whereas intermittency enhances subcritical breakup and broadens the crossover around ℓ_c. The framework therefore links fibre mechanics, turbulent scaling, and fragmentation kinetics in dispersed multiphase flows.

References

A. Mazzino. *Turbulence-informed kinetic theory of inertial-range fibre fragmentation.* J. Fluid Mech., **1030**, A6, 2026.

A. Mazzino. *From impossible to likely: a new intermittency-driven channel for subcritical fibre breakage in turbulence.* Submitted, 2026.

Numerical investigation of drag enhancement by interfacial tension in Taylor–Couette turbulence

Jinghong Su[1], Yi-Bao Zhang[2], Junwu Wang[1] and Chao Sun[2, 3]

[1]College of Mechanical and Transportation Engineering, China University of Petroleum, Beijing 102249, P R. China
[2]Department of Energy and Power Engineering, Tsinghua University, Beijing 100084, China
[3]Department of Engineering Mechanics, School of Aerospace Engineering, Tsinghua University, Beijing 100084, China

Dispersed droplets can substantially increase drag in turbulent liquid–liquid flows, yet the underlying mechanism remains insufficiently understood. We investigate this problem in turbulent Taylor–Couette flow using three-dimensional direct numerical simulations with a modified multi-marker volume-of-fluid method designed to mitigate numerical coalescence at moderate droplet volume fractions. The simulations are conducted with the outer cylinder fixed and the inner cylinder rotating at constant angular velocity. The two phases are neutrally buoyant and have equal viscosity. The Reynolds number is fixed at Re = 5200, with droplet volume fractions up to 40% and a Weber number of approximately 8.

The simulations reproduce the experimentally observed monotonic increase of torque with increasing droplet volume fraction. By decomposing the angular-velocity flux into turbulent, viscous, and interfacial-tension contributions, we show that the drag enhancement is dominated by the interfacial-tension term, whereas the turbulent and viscous stress contributions remain nearly unchanged in the bulk-averaged sense. Focusing on the inner-cylinder boundary layer, we find that droplets undergo strong shear-induced deformation and streamwise stretching. This deformation produces an asymmetric interfacial-tension effect: the droplet “fore head” (closer to the inner cylinder) experiences interfacial tension predominantly opposing the local flow, while the “rear end” tends to experience interfacial tension in the flow direction. The net outcome is a hindering effect associated with the fore head that reduces local angular velocity, disrupts high-speed streaks, promotes low-speed streaks, and thereby increases near-wall viscous stress and overall torque. These findings highlight the crucial role of interfacial tension in near-wall momentum transport and provide guidance for improving two-phase turbulence models that often under-represent interfacial-tension effects.

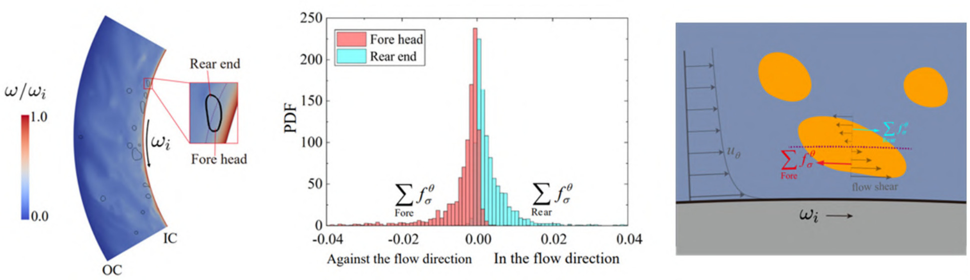

Figure 1: Mechanism underlying interfacial-tension-induced drag enhancement in Taylor–Couette turbulence.

Length Scales and Interphase Energy Transfer in Turbulent Gas-particle Flows

S. Schneiderbauer[1] and B. Hardy[2]
[1] Dep. of Particulate Flow Modelling, Johannes Kepler University, Linz, Austria
[2] Institute of Mechanics, Materials and Civil Engineering, UCLouvain, Belgium

Turbulent gas-particle flows exhibit energy decay mechanisms that differ fundamentally from those in single-phase turbulence because momentum exchange between phases can act as both a sink and a source of fluctuations. In dilute suspensions, particles preferentially accumulate in low-vorticity regions of the carrier flow. At moderate particle loadings, however, the particle phase behaves like a compressible continuum and can sustain fluctuations – up to and including self-generated turbulence – even when there is no surrounding fluid. Drag-mediated coupling can therefore drive persistent heterogeneities such as particle clustering.

We present theoretical concepts for turbulent multiphase flows with an emphasis on gas-particle systems, focusing on the relevant length scales and the associated pathways of energy transfer and decay that are critical for predictive, industrial-scale simulations. The discussion is supported by highly resolved simulations of unbounded fluidization in triple-periodic domains using a kinetic-theory based two-fluid model (Esgandari et al. (2025)).

Our simulations identify two plausible turbulent length scales, $\mathscr{L}_I = u_t^2/g$ and $\mathscr{L}_{II} = u_t^2/g, \mathrm{Fr}^{-2/3}$, where $\mathrm{Fr} = u_t^2/(g d_p)$ is the particle Froude number, u_t the terminal settling velocity. When the domain size is scaled with $\mathscr{L}_{II}$, both the integral length scale and the Taylor microscale increase linearly with $\mathscr{L}_{II}$. A domain-size sensitivity study further shows that the variance of particle volume fraction and the domain-averaged slip velocity converge in relatively small boxes, whereas accurate prediction of gas- and particle-velocity variances requires substantially larger domains due to wake dynamics downstream of particle clusters.

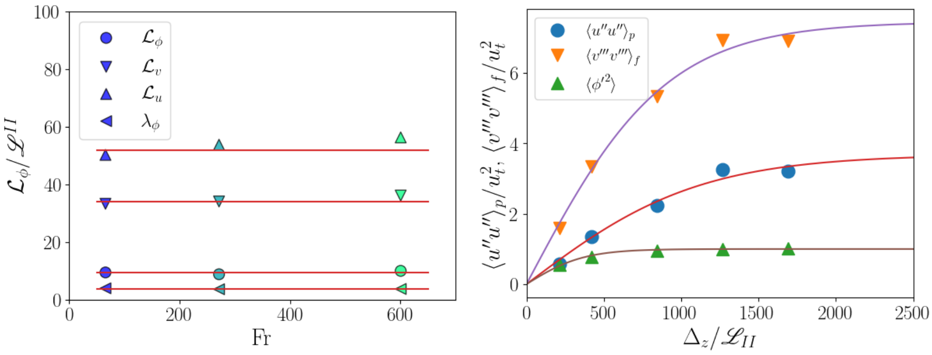

Figure 1: Normalized integral length scales ($\mathcal{L}$; left) and box size dependence of variances (right) of particle volume fraction ϕ, gas-phase velocity v and particle velocity u.

References

B. Esgandari, S. Bhat, J. Capecelatro, and S. Schneiderbauer. A comprehensive comparison of TFM and CFD-DEM in simulations of cluster-induced turbulence in unbounded fluidization systems. *Chemical Engineering Journal*, 523:167398, 9 2025.

A sharp interface multiphase method for shock-induced reactive droplets with phase change

Shucheng Pan [1,2], Jiaxi Song [1]
[1] School of Aeronautics, Northwestern Polytechnical University, Xi’an 710072, China
[2] Institute of Extreme Mechanics, Northwestern Polytechnical University, Xi’an 710072, China

The interaction between shock waves and reactive droplets undergoing phase change plays a crucial role in various engineering and scientific applications, such as combustion, fuel injection, and detonation processes. This study presents a numerical investigation of shock-induced reactive droplets with phase change using a recently developed conservative sharp-interface solver that accurately captures both chemical reactions and phase change effects. The solver captures complex multiphase phenomena, including droplet deformation, evaporation, and chemical reactions induced by the shock impact. A level-set method is employed to track the liquid-gas interface with high accuracy, ensuring proper treatment of the sharp discontinuities in thermodynamic and transport properties. The numerical results reveal the intricate coupling between shock dynamics, droplet breakup, and phase change, highlighting the role of reaction kinetics in modifying the droplet dynamics and phase change process. Comparisons with numerical and experimental data validate the accuracy and robustness of the proposed approach. The findings provide new insights into shock-induced droplet dynamics and contribute to the development of improved predictive models for reactive multiphase flows, as shown in Fig. 1.

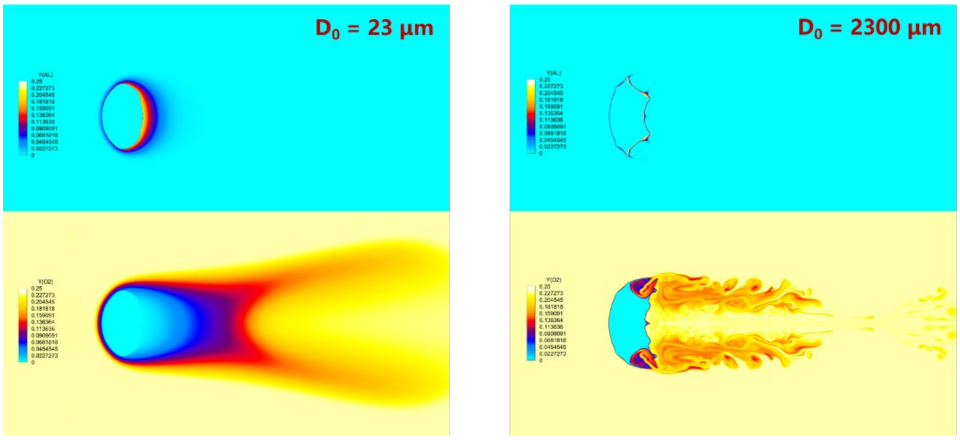

Figure 1. Numerical results of induced droplet dynamics for different size of the droplet.

References

J. Song; T. Long, and S. Pan. Three-dimensional numerical simulations of phase change effects on shock-droplet interactions. *Phys. Fluids*, **37**, 033358, 2025.

T. Long, J. Cai, and S. Pan. A fully conservative sharp-interface method for compressible multiphase flows with phase change. *J. Comput. Phys.*, **493**, 112501, 2023.

The dynamics of copepods in turbulence: how micro-swimmers can adapt their behaviour

E. Climent[1], F.-G. Michalec[2], O. Praud[1], M. Lorite-Diez[1], S. Cazin[1], and S. Souissi[2]
[1] IMFT, CNRS, Toulouse INP, Univ. Toulouse – France
[2] LOG, CNRS, Univ. Lille, ULCO – France

This study explores the swimming behaviour of the estuarine copepod *Eurytemora affinis* in response to turbulence, using 3D Lagrangian particle tracking velocimetry. Copepod ability to actively swim and adapt their behaviour in fluctuating hydrodynamic conditions[1,2] is critical for survival and ecological function (predator-prey dynamics, and vertical migration). The research investigates how copepods modulate their motility from calm water to controlled turbulence experienced in their natural habitats. Experiments were conducted in a large tank equipped with two oscillating grids to generate turbulence (Fig. 1 left). High-resolution cameras and laser illumination enabled simultaneous tracking of copepod trajectories and surrounding flow fields (Fig. 1 right). The study distinguishes between two fundamental swimming modes: slow cruising and rapid relocation jumps.

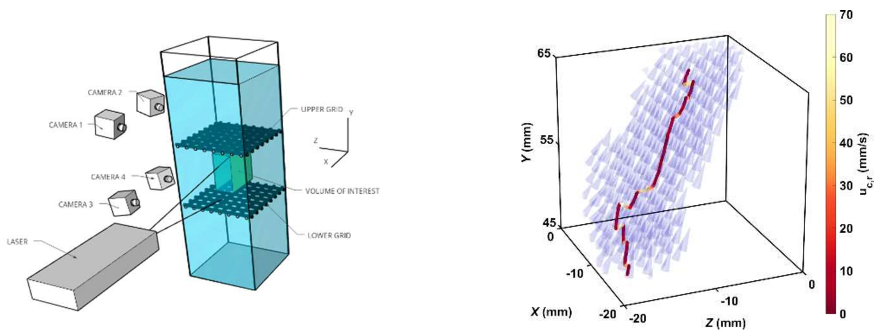

Figure 1: *Left* - Region of interest between the two oscillating grids.
Right – 3D trajectory of a copepod surrounded by the fluid velocity field from 3D PTV.

The relative velocity of copepods with respect to the flow was analyzed to decouple active swimming from passive advection, revealing adaptive strategies to turbulence. Under turbulent conditions, copepods increase their jump frequency without altering the amplitude or duration of jumps, allowing them to deviate from passive transport by the flow. In addition, we investigated how microplastics pollution impacts the swimming behavior of the copepods[3] in both calm water and turbulence. The research focuses on the smallest size fraction of polyethylene microplastics (5–10 µm). Exposure to microplastics (300 µg/L) for 12 hours led to a 25% increase in jump frequency in calm water, indicating hyperactive behavior. However, in turbulent conditions, microplastic exposure had minimal additional effects, suggesting turbulence masks microplastic-induced behavioural changes.

References

[1] Michalec, F.-G., Fouxon, I., Souissi, S., Holzner, M. - Zooplankton can actively adjust their motility to turbulent flow. *PNAS* **114**(52), 11199–11207 (2017)

[2] Michalec, F.-G., Praud, O., Cazin, S., Climent, E. - Experimental investigation of preferential concentration in zooplankton swimming in turbulence. *Eur. Phy. J. E* **45**(2), 12 (2022)

[3] Michalec, F.-G., Praud, O., Lorite-Diez M., Cazin, S., Climent, E., Souissi S. - The effect of microplastics on the swimming behavior of copepods. submitted to *Eur. Phy. J. E* (2026)

Swimmer-resolving simulations on the biogenic hydrodynamic transport of cruising copepods

R. Zhu[1], Y. Su[2], B. Vowinckel[1], E. Meiburg[3] and M. M. Wilhelmus[4]
[1] Institute of Urban and Industrial Water Management, Technische Universität Dresden, Dresden, 01062, Germany
[2] Mechanical and Industrial Engineering Department, University of Minnesota Duluth, Duluth, MN 55812, USA
[3] Department of Mechanical Engineering, University of California, Santa Barbara, Santa Barbara, CA 93106-5070, USA
[4] Center for Fluid Mechanics, School of Engineering, Brown University, Providence, RI 02912 USA

Mesozooplankton aggregations undergoing vertical migrations in the upper ocean have been hypothesized to have an important role in the redistribution of carbon, nutrients, and oxygen via biogenic hydrodynamic transport (BHT). While laboratory studies have demonstrated how swarm-induced hydrodynamic instabilities can drive large-scale transport in strongly stratified environments, measurements are usually performed with model organisms that differ in morphology and swimming mode from ecologically relevant marine species. To bridge this gap, we perform fully coupled, swimmer-resolved direct numerical simulations (DNS) using the squirmer model to represent copepod locomotion, focusing on the effects of the reduced gravity of the swimmers and the density stratification of the surrounding fluid. Our simulations reveal that both the excess weight of the organisms and the fluid stratification strongly constrain the net BHT for individual swimmers. We further examine how individual swimming behaviors modulate BHT during collective vertical migration within swarms. This study provides a critical step toward integrating lab-based models of marine mesozooplankton with remote sensing data to incorporate vertical migrations into global ocean models with realistic biogeochemistry and assess their ecological significance in actively sustaining local ecosystems.

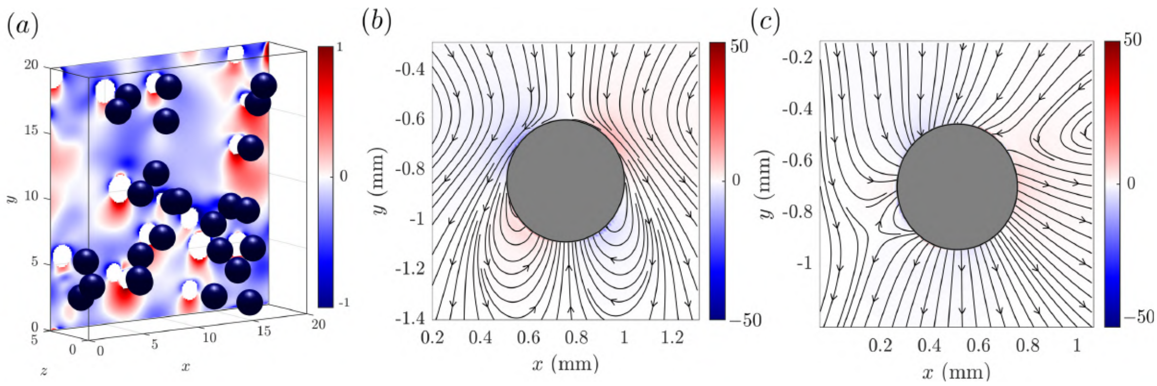

Figure 1: (a) The configuration of the simulations and a slice of the vertical velocity. (b-c) The simulation results for streamlines and vorticity fields (contours, unit s^{-1}) induced by individual swimmers (gravity direction is in the negative y direction). (b) an upward swimming with puller mode; (c) a downward swimming with pusher mode.

Lagrangian angular velocity of fluid elements in homogeneous isotropic turbulence

Yifei Chen[1], Zhiwen Cui[1], Peng Han[3] and Lihao Zhao[2]
[1] College of Mechanical and Vehicle Engineering, Hunan University, Changsha, China
[2] AML, Department of Engineering Mechanics, Tsinghua University, Beijing, China
[3] State Key Laboratory for Strength and Vibration of Mechanical Structures and School of Aerospace, Xi'an Jiaotong University, Xi'an, China

In present study, we investigate the Lagrangian angular velocity of fluid elements in homogeneous isotropic turbulence, defined as the rigid-body rotation of a fluid element along its trajectory. Exploiting the formal analogy between the evolution of the principal axes of fluid elements and those of inertialess triaxial ellipsoids, we demonstrate that Lagrangian angular velocity fundamentally differs from its Eulerian counterpart, defined as one-half of the local vorticity. Specifically, Lagrangian angular velocity admits a natural decomposition into two contributions: an Eulerian component and a shear-induced component arising from the coupling between element orientation and the local strain-rate tensor. To quantify these differences, we construct spherical probability density functions (PDFs) of the orientational distributions of Lagrangian and Eulerian angular velocities in a Lagrangian reference frame. The statistics reveal systematic discrepancies in directional alignment and in their dependence on local flow topology, indicating that strain-induced rotations play an important dynamical role. Furthermore, we introduce a vector-triangle representation that geometrically links the Lagrangian, Eulerian and shear-induced angular velocities. Three canonical vector-triangle configurations emerge, corresponding to Eulerian-dominated, strain-dominated and joint regimes, respectively, reflecting distinct local balances between fluid rotation and strain. These results provide new physical insight into the rotational dynamics of fluid elements in turbulent flows.

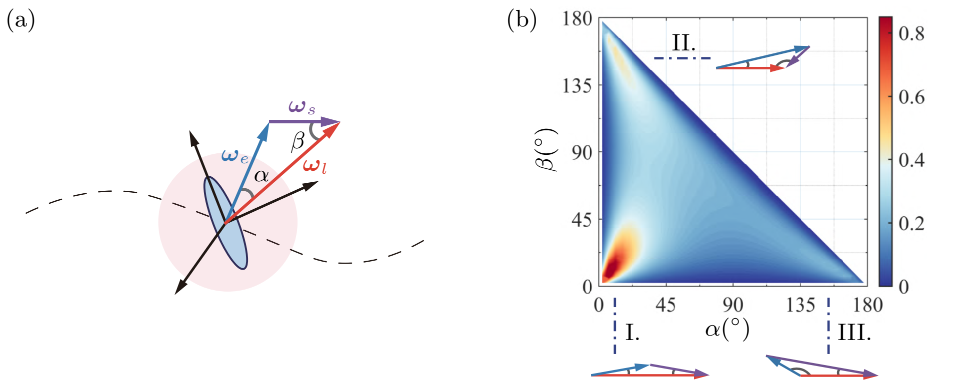

Figure 1: (a) Decomposition of the Lagrangian rotation $\boldsymbol{\omega}_l$ of a fluid element into the Eulerian rotation $\boldsymbol{\omega}_e$ and the shear-induced rotation $\boldsymbol{\omega}_s$, expressed in a Lagrangian reference frame along the particle trajectory. The angle between $\boldsymbol{\omega}_l$ and $\boldsymbol{\omega}_e$ is denoted by α, while that between $\boldsymbol{\omega}_l$ and $\boldsymbol{\omega}_s$ is denoted by β. (b) Joint PDF of α and β at $Re_\lambda = 90$. Three local maxima of the PDF identify three canonical vector-triangle configurations: (I) joint regime; (II) Eulerian-dominated regime; (III) shear-dominated regime.

Time-reversal-symmetry breaking in free-surface turbulence

Yaxing Li[1], Guotao Wu[1] and Filippo Coletti [2]

[1] Department of Engineering Mechanics, School of Aeronaustics and Astronaustics, Zhejiang University, Hangzhou 310027, PR China

[2] Department of Mechanical and Process Engineering, ETH Zurich, 8092 Zurich, Switzerland

The transport of mass, momentum and energy along the free surface bounding a turbulent liquid has long attracted the attention of scientists and engineers. Energy transfer is an essence of mixing process of turbulent flow. In three-dimensional turbulence, the irreversible flux of energy from large to small scales breaks time symmetry. It can be quantified by tracking the relative motion of Lagrangian tracers, i.e., the separation of particles in pair is temporally slower forwards than backwards at short times. Jucha et al. (2014) showed that the difference between forward and backward dispersion grows as t^3 by numerical and experimental observations. In this work, we track millions of trajectories of tracers, floating on the free surface with turbulence underneath to testify the time-symmetry breaking by statistically computing the mean-square separation of particles in forward and backward directions. The results display a ballistic dispersion at short times and diffusive dispersion at long times, either in forward or backward direction. We show that the two particles in pair separate faster backwards than forwards at relatively small scales, which is consistent with that in three-dimensional turbulence; whereas at relative large scales, it is opposite, which implies an inverse energy transfer from small to large scales, resembling the energy cascade of a two-dimensional turbulence.

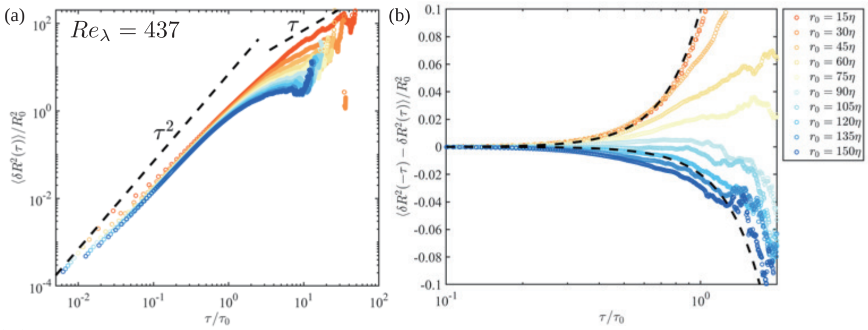

Figure 1: (a) The forward mean-square separation for various initial separations of particles in pair. (b) The difference between the backward and forward mean-square separation $\langle \delta R^2(-\tau) - \delta R^2(\tau)\rangle$, compensated by R_0^2.

References

J. Jucha, H. Xu, A. Pumir, and E. Bodenschatz. *Time-reveral-symmetry breaking in turbulence.* Phys. Rev. Lett., **113**, 054501, 2014.

G. Wu, Y. Li, and F. Coletti. *Localised inter-scale energy cascades in free-surface turbulence.* J. Fluid Mech., **1026**, A51, 2026.

Bubble-Generated Turbulent Convection in a Liquid Vessel

R. Shnapp[1]
[1] Mechanical Engineering Department, Ben-Gurion University of the Negev, Beer Sheva, Israel

The behavior of gas bubbles embedded liquids makeup a fascinating dynamical system due to the innate coupling between the two phases. One simple aspect of this is that, under gravity, buoyancy forces acting on the liquid-gas interface, cause bubbles to raise while pushing down the liquid surrounding them. In addition, normal and tangential stresses across the interface cause some liquid to be dragged as the bubbles ascend. Macroscopically, this manifests a convective, buoyancy-driven flow. While this fundamental phenomenon is hugely abundant both in nature and industry, understanding the flow fields generated therein is an ongoing undertaking of our community.

In this talk I would like to present the results of a recent inquiry into the flow generated in liquid containers by a localized bubble column at its periphery. Experiments were conducted with air bubble release into a water container covering approximately two orders of magnitude in the bubble-Rayleigh number, and the water velocity fields were measured with 3D particle tracking velocimetry. Two main phenomena are observed. First, a container-scale circulation cell is formed, akin to the well known cavity-flow; we propose a model relating the circulation Reynolds number and the bubble-Rayleigh number which captures the scaling law for this flow. Second, we observe turbulence emerging through two mechanisms—both small scale eddies formed in the bubbles' wakes, and as the rate of bubble generation is increased, a gradual transition from laminar to turbulent flow is observed in the main circulation cell. We analyze experimentally the appearance of turbulence in this flow and suggest the cause for its onset.

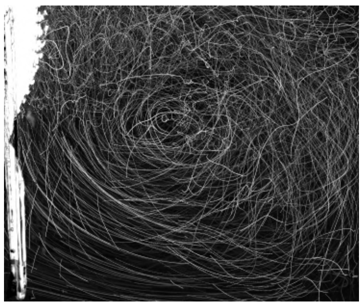

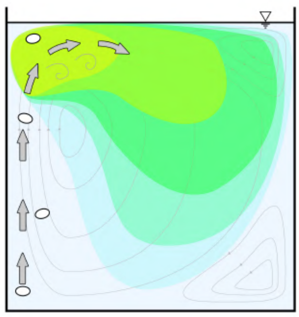

Figure 1: Left: Visualization of the flow structure through long-exposure imaging, with the bubble column on the left. Right: a conceptual map showing the convection of turbulent kinetic energy in the buoyancy-driven flow. *From: Shnapp and Holzner, J. Fluid Mech. (2024).*

References

R. Shnapp, and M. Holzner F. Bianco, S. Chibbaro, C. Marchioli, M. V. Salvetti, and A. Soldati. *Bubble-induced convection and flow instability in liquid vessels.* J. Fluid Mech., **996**, A2, 2024.

Preferential Flow Control by Non-Coalescing Multi-Bubble Systems in Pore-Doublet Channels

Caoxing Mo[1], Lijun Yang[1], Bingqiang Ji[1,2,3], Qingfei Fu[1,2,4] and Chiyu Xie[1,2,3]
[1] School of Astronautics, Beihang University, Beijing 100191, China
[2] Ningbo Institute of Technology, Beihang University, Ningbo, 315100, China
[3] State Key Laboratory of High-Efficiency Reusable Aerospace Transportation Technology, Beijing, 102206, China
[4] National Key Laboratory of Aerospace Liquid Propulsion, Xi'an 710100, China

Preferential flow commonly occurs in heterogeneous porous media due to variations in pore size and flow resistance. Foam injection has been proven effective for controlling preferential flow, but the underlying mechanisms remain unclear. In this study, we numerically investigate foam flow in a pore-doublet channel, a local representative unit of heterogeneous structures, using the multilayer volume-of-fluid method (Multi-VOF) method for non-coalescing multi-bubble systems. The gas saturation ratio between the two channels is defined to quantify preferential flow control. A phase diagram is constructed to show the impact of bubble size and capillary number (Ca), dividing flow into three regimes: larger-bubble, smaller-bubble, and transition. In the large-bubble regime, the breakup mechanism dominates, with larger Ca and bubble size increasing breakup probability and gas saturation in narrower channels. In both the transition regime and the smaller-bubble regime, the gas saturation ratio increases as Ca decreases. In the small-bubble regime, blocking and squeezing govern flow, causing gas saturation to rise slightly then decrease as bubble size decrease. In the transition regime, the bubble flow is primarily at the initial breakup state, then shifts to the non-breakup state as bubble size decreases, resulting in a rapid rise in the gas saturation ratio. There exists a critical bubble diameter at which flow shifts from breakup to non-breakup state, and it decreases as Ca increases. These findings clarify the dynamic mechanisms of preferential flow control by multi-bubble systems, with practical relevance for optimizing industrial processes such as energy recovery, environmental remediation, and targeted drug delivery.

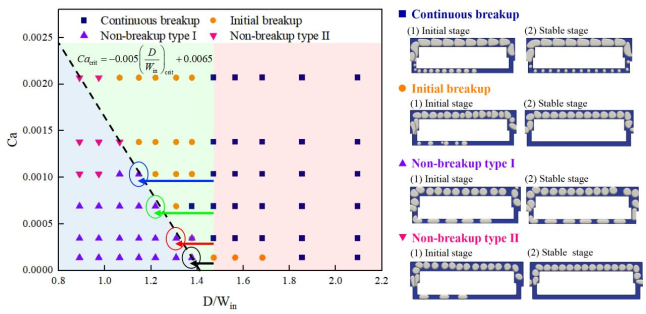

Figure 1: Phase diagram of the effect of bubble diameter D/W_{in} and Ca on the bubble breakup types.

Eliminating Spurious Currents in the Simulation of Hydrogen Microbubbles for Electrolysis

D.E.A. v.d. Eertwegh[1], J.A.M. Kuipers[1] and M.W. Baltussen[1]
[1] Eindhoven University of Technology, P.O. Box 513, 5600 MB Eindhoven, The Netherlands

The increasing penetration of renewable energy sources introduces strong intermittency in power production, creating an urgent need for efficient energy storage. Water electrolysis provides a viable pathway by converting excess electricity into green hydrogen. However, green hydrogen is currently 3–4 times more expensive than fossil-derived hydrogen (Curcio, 2025), largely due to inefficiencies in electrolyzer operation.

A major contributor to these inefficiencies is the overpotential, which can be decomposed into activation, ohmic, and concentration contributions. In water electrolysis, hydrogen bubbles nucleate and grow at the electrode surface, forming a partially insulating gas layer that increases both activation and ohmic overpotentials and alters local mass transport (Ross et al., 2025). Quantifying and controlling this bubble-induced performance loss requires accurate modeling of microbubble dynamics near the electrode.

The relevant bubbles are typically only 10–20 μm in diameter (Li et al., 2023), posing severe numerical challenges. In commonly used one-fluid formulations, spurious currents induced by surface tension discretization errors can exceed the physical rise velocities of these bubbles, rendering simulations unreliable. To address this issue, we develop a novel two-phase numerical method that treats the gas and liquid phases separately. The method reduces spurious currents to machine precision, achieving liquid-phase capillary numbers as low as 10^{-20}–10^{-17} when analytical curvature is employed. This enables physically accurate simulations of hydrogen microbubble formation and dynamics, providing a robust basis for understanding and ultimately reducing overpotential losses in water electrolysis.

References

E. Curcio, Techno-economic analysis of hydrogen production: Costs, policies, and scalability in the transition to net-zero, *Int. J. Hydrog. Energy*, **128**, 473-487, 2025.

K. Li, S.T. Matkarimov, W. Xiao, C. Liu and S. Yang, Fundamental study on the growth processes of interfacial microbubbles in air-supersaturated solution, *Colloids Surf. A Physicochem. Eng. Asp.*,**673**, 131879, 2023.

B. Ross, S. Haussener and K. Brinkert, Impact of Gas Bubble Evolution Dynamics on Electrochemical Reaction Overpotentials in Water Electrolyser Systems, *J. Phys. Chem. C*, **129**, 4383-4397, 2025.

Dynamics of a large spherical bubble in a turbulent flow

E. De Angelis[1], L. Campana[1] and F. Maluta[2] and G. Montante[2]
[1] University of Bologna, Department of Industrial Engineering, Forlì, Italy
[2] University of Bologna, Department of Industrial Chemistry, Bologna, Italy

Bubbly flows play an essential role in many technical applications. From an industrial point of view, design approaches based on Reynolds averaged Eulerian-Eulerian models are attractive due to their applicability to complex geometries and large scale equipment, despite current limitations Garcia et al. (2025). In order to assess some semi-empirical correlations for inter-phase forces commonly used in the context of RANS models, the current analysis will utilize knowledge of liquid-bubble interactions from Direct Numerical Simulations (DNS).

We have performed a series of DNSs of single deformable air bubbles, at various relevant diameters, rising in water because of buoyancy. The base flow is driven by an external stirring in a periodic domain, imposing three different Taylor Reynolds numbers. The full Navier-Stokes equations are solved using a finite difference method Rosti et al. (2020)that accommodates a fully deformable interface around the bubbles, as well as the inclusion of surface tension σ. The problem is described by the four dimensionless parameters; the Eötvös number ($Eo \equiv \rho_l g d_b^2/\sigma$) relating the buoyancy to surface tension forces and the Galilei number ($Ga \equiv \rho_l (g d_b^3)^{1/2}/\mu_l$) that is the ratio of buoyancy to viscous forces, and the density and viscosities ratio $r_\rho = \rho_b/\rho_l$ and $r_\mu = \mu_b/\mu_l$, with subscripts b denoting the dispersed phase (bubbles) and l the carrier phase (liquid).

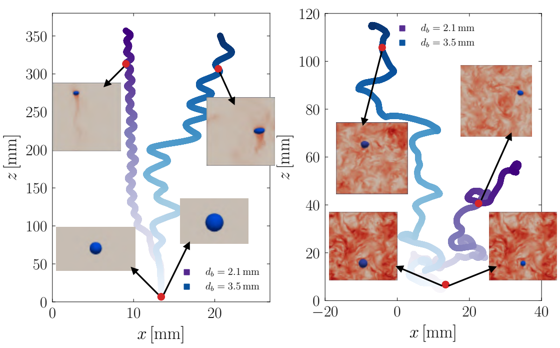

Figure 1: Bubble trajectories for two different diameters projected on the xz−plane; in quiescent fluid (left panel) and turbulent one (right panel). Colour map from light to dark indicates the increasing time.

As an example, Fig. 1 (left panel) shows the trajectories of single bubbles on the xz-plane. The smallest one, with a diameter of $d_b = 2.1$ mm, follows a predominantly straight path as it ascends. In contrast, a larger bubble ($d_b = 3.5$ mm) exhibits a more complex trajectory. The average vertical velocity observed aligns well with previous experimental measurements. A quite different behaviour is observed when turbulence is introduced, as shown in Fig. 1 (right panel). Here, the terminal velocity U_b is significantly diminished, leading to highly irregular trajectories in both cases. Specifically, for the smallest bubble ($d_b = 2.1$mm), its movement is greatly influenced by the turbulence, resulting in substantial alterations to its path.

References

M. Garcia-Villalba, T. Colonius, O. Desjardins, D. Lucas, A. Mani, D. Marchisio, O. K. Matar, F. Picano, S. Zaleski *Numerical methods for multiphase flows* International Journal of Multiphase Flow **191**, 105285, 2025.

M. E. Rosti, Z. Ge, S. S. Jain, M. S. Dodd and L. Brandt *Droplets in homogeneous shear turbulence* Journal of Fluid Mechanics **876**, 962-984, 2020.

Numerical simulation of powder melting and multiphase keyhole dynamics in laser powder bed fusion

Zhiyuan Yang[1], Shuai Wang[1,2] , Kun Luo[1,2] ,Jianren Fan[1,2]
[1] State Key Laboratory of Clean Energy Utilization, Zhejiang University, Hangzhou 310027, China
[2] Shanghai Institute for Advanced Study of Zhejiang University, Shanghai 200120, China

Laser powder bed fusion (LPBF) involves highly localized and transient thermal fluid dynamics, including discrete powder melting, molten pool evolution, and keyhole formation. Understanding the complex multiphase flow dynamics under intense recoil pressure is essential. In this study, a comprehensive numerical framework is developed by integrating the discrete element method (DEM) for dispersed powder bed deposition and computational fluid dynamics (CFD) for melt pool dynamics. The volume of fluid (VOF) method captures the dynamic topological changes of the complex gas-liquid interface during phase transitions. The multiphase model explicitly accounts for surface tension, Marangoni flow, Darcy effect, and evaporation-induced recoil pressure.

Results indicate that recoil pressure significantly alters the multiphase flow state, generating narrower, deeper melt pools with higher peak temperatures. Driven by localized vapor recoil pressure, molten liquid primarily flows downward along the keyhole's front wall toward its bottom, then subsequently moves toward the rear, forming a "J"-shaped keyhole and a strong internal clockwise vortex. These intense dynamics cause continuous keyhole depth fluctuations. Parametric analysis reveals that smaller laser spot diameters deepen keyholes and intensify dynamic fluctuations at the gas-liquid interface. These findings provide critical insights into the multiphase interaction mechanisms at material interfaces, offering guidance for defect control and process stability enhancement.

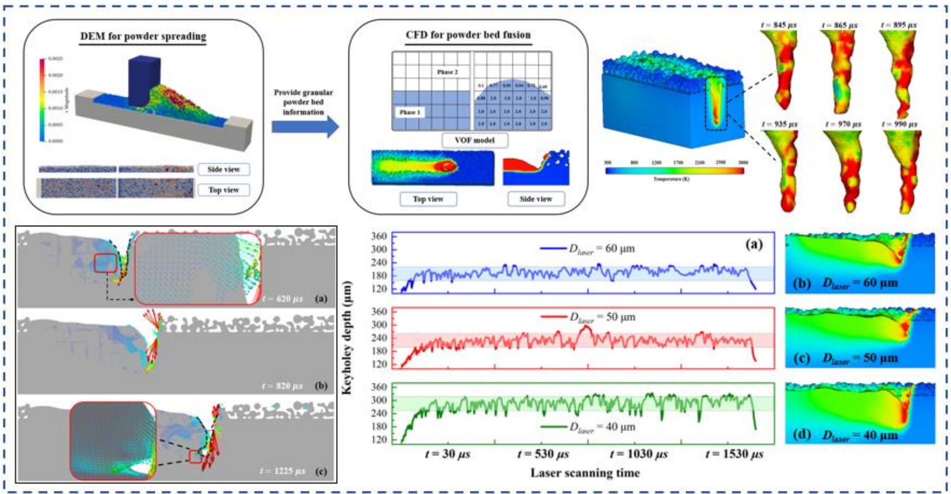

Figure 1: Multiphase flow in laser powder bed fusion process: modeling framework, result and parametric analysis. *From: Yang et al., P. T, (2025).*

Asymmetric particle transport in turbulent flows within concentric annular ducts

Chi Zhang[1,2], Taiyang Wang[1,2] and Yaomin Zhao[1,2]
[1] HEDPS, Center for Applied Physics and Technology,
School of Mechanics and Engineering Science, Peking University, Beijing 100871, China
[2] State Key Laboratory for Turbulence and Complex Systems,
School of Mechanics and Engineering Science, Peking University, Beijing 100871, China

We present the first direct numerical simulations of particle-laden turbulent flow in concentric annuli to investigate the effects of transverse curvature. Three radius ratios, $\alpha \equiv R_i/R_o$, where R_i and R_o denote the inner and outer wall radii, are considered, ranging from the planar limit ($\alpha = 1$) to strong curvature ($\alpha = 0.1$). Our results show that curvature yields an increasingly asymmetric concentration field, with enhanced outer-wall accumulation and, at strong curvature, pronounced inner-wall depletion. In addition, the particle concentration near the inner wall exhibits a previously unreported non-monotonic transient evolution. To elucidate the underlying transport mechanisms, we derive a radial particle transport equation in annular channels within a probability-density-function (PDF) framework (Johnson *et al.*, 2020). Building on this equation, we show that curvature induces a centrifugal drift and renders turbophoretic transport asymmetric; both effects intensify with increasing curvature, thereby amplifying the asymmetry. A Sturm–Liouville modal analysis of the transport equation then identifies the competition between asymmetric transport modes with different decay rates as the key mechanism driving the non-monotonic evolution, yielding a reduced-order model that accurately captures the concentration dynamics.

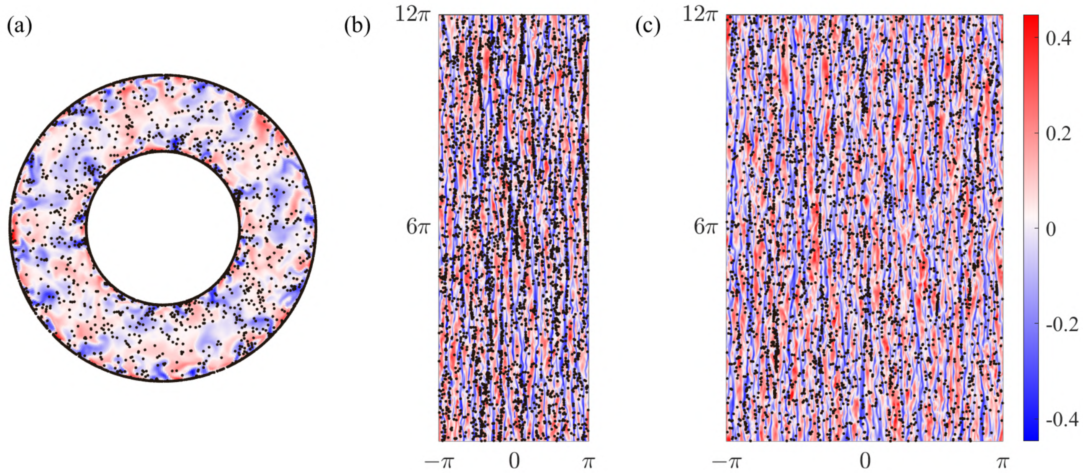

Figure 1: Instantaneous snapshots of particle-laden turbulence in an annular channel ($\alpha = 0.5$). Colours: streamwise velocity fluctuations; dots: particles. (a) Cross-section. (b) Near the inner wall. (c) Near the outer wall.

References

P. L. Johnson, M. Bassenne, and P. Moin. *Turbophoresis of small inertial particles: theoretical considerations and application to wall-modelled large-eddy simulations.* J. Fluid Mech., **883**, A27, 2020.

Numerical investigation of cohesive iron powder fluidization in metal energy storage systems via a coarse-grained CFD-DEM-SJKR framework

Bingchen Li[1], Junjie Lin[1, 2], Kun Luo[1, 2, *], Shuai Wang[1, 2], and Jianren Fan[1, 2]
[1] State Key Laboratory of Clean Energy Utilization, Zhejiang University, Hangzhou 310027, China
[2] Shanghai Institute for Advanced Study of Zhejiang University, Shanghai 200120, China

Iron-based particles have emerged as a promising medium for long-duration energy storage due to their high energy density and carbon-free oxidation. However, the efficient utilization of fine iron powders is often hindered by strong cohesive forces (Geldart A/C classification), which lead to poor fluidization quality. This study develops an advanced coarse-grained computational fluid dynamics-discrete element method (CFD-DEM) framework, integrating a simplified Johnson-Kendall-Roberts (SJKR) model to accurately and efficiently capture inter-particle cohesion. A physically consistent scaling law is derived to preserve cohesive contact mechanics, collision dynamics, and hydrodynamic similarity between the original and coarse-grained systems. The framework is rigorously validated against experimental data, demonstrating high fidelity in predicting minimum fluidization velocities across varying bed configurations. Results indicate that moderate gas velocities facilitate rapid solids mixing and stable fluidization, essential for uniform energy release. Conversely, excessive velocities trigger slugging, while increasing particle diameter shifts the system from agglomerate-dominated regimes to uniform structures. While this work establishes a robust hydrodynamic foundation, future research will extend this framework to incorporate complex heat and mass transfer models. Specifically, the coupling of chemical reaction kinetics will be explored to optimize the charging and discharging efficiency of iron-based energy storage systems under reactive conditions.

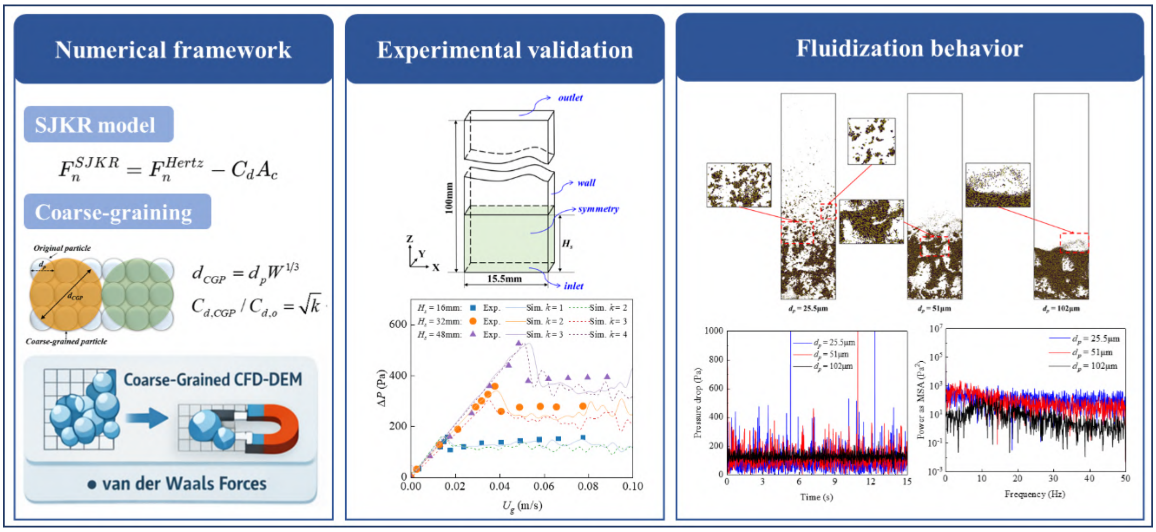

Figure 1: Graphical abstract of the proposed method for simulation of cohesive particles.

Wall-bounded turbulence driven by heat-releasing particles

Yuhang Du[1], Yantao Yang[2]
[1] School of Mechanical Engineering, Hebei University of Technology, Tianjin 300401, P. R. China
[2] State Key Laboratory for Turbulence and Complex Systems, and Department of Mechanics, School of Mechanics and Engineering Science, Peking University, Beijing 100871, P. R. China

In this work, we conduct Euler-Lagrange direct numerical simulations to investigate the thermal convection driven by heat-releasing particles, which absorb energy from an external source. The energy absorbed by particles is then released to heat the surrounding fluid, which drives the buoyancy flow motions in the domain. We first consider wall bounded convection driven by heat-releasing particles in which the gravity is normal to the wall. In this configuration, the particles accumulate into the boundary layer in the specific parameter space, while for other cases particles are constantly advected over the entire domain. Then we work on vertically wall-bounded turbulence interacting with heat-releasing particles. Two distinct regimes are observed. In the gravity-dominated regime, particles settle and entrain the fluid downward. In the buoyancy-driven regime, the heat released from particles induces upward fluid motion, which carries the particles upward. In the above two configurations, the competition between the gravitational effect on particles and the buoyancy effect on the fluid determine different flow regimes. These two effects are characterized by the Rayleigh number and Froude number respectively. The critical Froude number is identified for different Rayleigh numbers that allows us to distinguish between distinct regimes of the system.

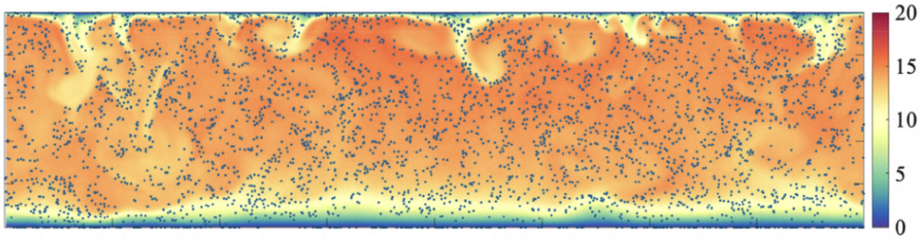

Figure 1: The instantaneous contours of temperature field and the particle distributions on the mid vertical plane for three cases with $Ra = 10^9$ and $Fr = 10$. *From: Du et al., Phys. Fluids, (2023).*

References

Y. Du and Y. Yang. *Effects of the gravitational force on the convection turbulence driven by heat-releasing point particles.* Phys. Fluids, **35**, 7, 2023.

Y. Du and Y. Yang. *Wall-bounded thermal turbulent convection driven by heat-releasing point particles.* J. Fluid Mech., **953**, A41, 2022.

Active control of bubbling fluidized bed by coupling deep reinforcement learning with reduced-order model

Xiaofei Li[1], Shuai Wang[1,2], Junjie Lin[1], Kun Luo[1,2,*] and Jianren Fan[1,2]
[1] State Key Laboratory of Clean Energy Utilization, Zhejiang University, Hangzhou 310027, China
[2] Shanghai Institute for Advanced Study of Zhejiang University, Shanghai 200120, China

Dense gas-solid flow in fluidized beds involves highly coupled physical, thermal, and chemical processes, making rapid prediction and real-time control particularly challenging. To address these challenges, this study innovatively develops a coupled framework integrating enhanced compressed sensing (ECS), time convolutional neural networks (TCN), reduced-order modeling (ROM), and deep reinforcement learning (DRL), termed ECS-TCN-ROM-DRL, for real-time prediction and control of global flow features in fluidized beds. Specifically, the ROM enables fast prediction of the flow field, while ECS establishes the mapping between sparse measurement points and the global flow field. The TCN captures the temporal evolution of system dynamics, and DRL actively controls the inlet gas velocity of a bubbling fluidized bed to optimize bubble behavior. The results demonstrate the ROM achieves a computational speedup of four orders of magnitude. The ECS-TCN-ROM-DRL framework reduces the average bubble volume by approximately 50%, while increasing the number of bubbles by up to 2.5 times, indicating significantly enhanced fluidization quality. The spatial-distribution DRL strategy yields superior optimization performance compared to the overall-velocity DRL strategy. Overall, this work provides a novel and effective implementation for real-time prediction and intelligent control within digital twin systems for fluidized beds.

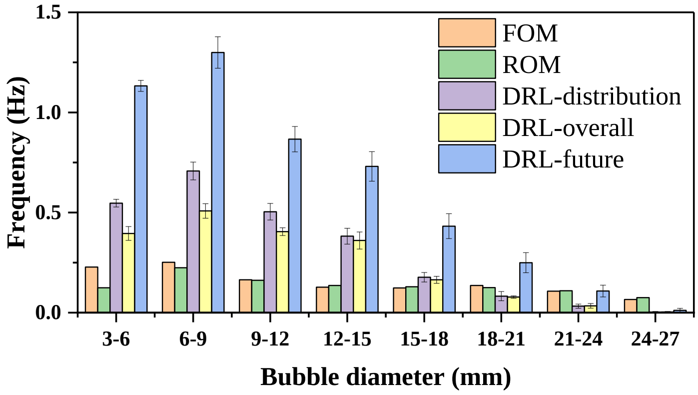

Figure 1 The bubble frequency of the DRL: FOM refers to the full-order model; DRL-distribution, DRL-overall, and DRL-future represent the distribution optimization, overall optimization, and forward optimization of the inlet velocity, respectively.

Release of ice-entrapped bubbles accelerates melting

J. Hu[1], F. Wang[1], Y. Du[1], E. Calzavarini[2] and C. Sun[1,3]
[1] Department of Energy and Power Engineering,
Tsinghua University, Beijing 100084, China
[2] Unité de Mécanique de Lille - J. Boussinesq (UML) ULR 7512,
Université Lille, F-59000 Lille, France
[3] Department of Engineering Mechanics, School of Aerospace Engineering,
Tsinghua University, Beijing 100084, China

Melting of glaciers, sea ice and ice shelves plays a pivotal role in the Earth's climate system. In most natural settings, glacier and sea ice are heterogeneous solids containing entrapped air bubbles and other inclusions, which are progressively released during melting but are rarely incorporated into current investigations of melt rates. Here, we numerically examine how bubble release from a melting ice layer alters the coupled melting-convection dynamics. The system is heated at a vertical sidewall, leading to development of a liquid layer adjacent to ice that propagates from right to left and drives buoyancy-driven convection. Results demonstrate that even a small bubble volume fraction within ice can significantly accelerate melting. This acceleration arises primarily from two mechanisms: First, the freely rising bubbles inject vertical momentum and kinetic energy into liquid. Moreover, bubbles penetrate the 4 °C isotherm, which separates upwelling from downwelling regions [*Wang et al., Phys. Rev. Fluids,* ***6****(9), L091501, 2021*], thereby enhancing mixing and heat transfer between upper warm and lower cold plumes. These results confirm the importance of bubble release as a previously overlooked process in theoretical modelling of sea ice melting rates.

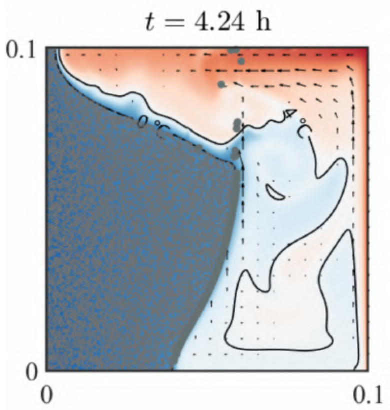

(a)

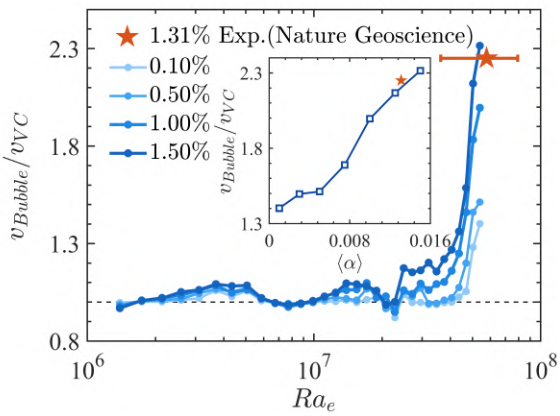

(b)

Figure 1: (a) Instantaneous temperature and velocity fields in a two-dimensional square box ($L = 0.1\,\text{m}$) with $\langle\alpha\rangle = 1.5\%$. The left wall is cold $T_c = -1\,°\text{C}$, and the right wall is hot $T_h = 10°\text{C}$. Solid grey points represent the bubbles. (b) Melting rate ratio v_{Bubble}/v_{VC} under different $\langle\alpha\rangle$ and effective Rayleigh number Ra_e, where v_{Bubble} and v_{VC} denote the melting rates of bubbly and bubble-free VC systems, respectively. The subfigure shows results for different $\langle\alpha\rangle$ under conditions with Ra_e similar to experimental results. The red solid pentagrams represent experimental results. *From: Wengrove et al., Nat. Geosci.,* ***16****(10), 871–876, 2023.*

Direct numerical simulation of boiling

A. Roccon[1,2]
[1]DPIA, University of Udine, 33100 Udine, Italy
[2]Inst. Fluid Mechanics and Heat Transfer, TU-Wien, 1060 Vienna, Austria

In this work, we propose and test the validity of a phase-field method tailored specifically for modeling boiling phenomena. The method relies on numerical solutions of the Navier-Stokes equations coupled with a phase-field method and the energy equation. The continuity and Navier-Stokes equations have been modified introducing a source term that accounts for phase change. Likewise, in the conservative Allen-Cahn equation (phase-field method) a source term that accounts for the volume is introduced. The system of governing equations is solved using a projection-correction method and equations are discretized using a second-order finite difference approach. Thanks to the numerical discretization employed, a constant coefficient Poisson equation for pressure is obtained, which can be efficiently solved using FFT-based direct solvers. The proposed method is validated against several benchmarks: an interface undergoing vaporization at a constant rate, the Stefan problem, the adsorption problem, and the growth of a 2D vapor bubble. For all the benchmarks, the present method well matches with analytical and archival literature results for a wide range of vapor-to-liquid density ratios, from $\rho_v/\rho_l = 1$ down to $\rho_v/\rho_l \simeq 5\times10^{-4}$ (where ρ_v identifies the vapor density and ρ_l the liquid density). Finally, the proposed method is used to investigate the growth of a vapor bubble in superheated liquid and the film boiling process, providing physical insights into these complex phenomena.

References

A. Roccon. *Boiling heat transfer by phase-field method.* Acta Mech. 236 (9), 5623-5638.

Simulating aeolian sand transport with a turbulence-informed stochastic particle force model

Yuqi Wang[1], Ruifeng Hu[1]
[1] Center for Particle-Laden Turbulence, College of Civil Engineering and Mechanics, Lanzhou University, Lanzhou, China

For the simulation of aeolian sand transport, most studies do not fully take into account the effect of turbulent fluctuations on particle motion. In some studies, the effect of turbulence is introduced by stochastically reconstructing the full flow velocity seen by a particle. However, this kind of method is limited to small point-like particles, but not applicable to large sand particles blown by strong winds. In this study, we leverage a new stochastic force model for finite-size particles in turbulence (Wang & Hu, *Int. J. Multiph. Flow*, 2025, vol.191, 105300) to simulate aeolian sand transport within the RANS CFD and DEM framework for the first time. This turbulence-informed stochastic force model establishes a relationship between the fluctuating force on sand particles and the turbulent kinetic energy and dissipation rate, thereby accounting for the effects of turbulence. The simulation results demonstrate that, after the stochastic force model is employed, the sand transport rate is significantly increased. The predicted distributions of the volume fraction and velocity of sand particles are in good agreement with experimental measurements.

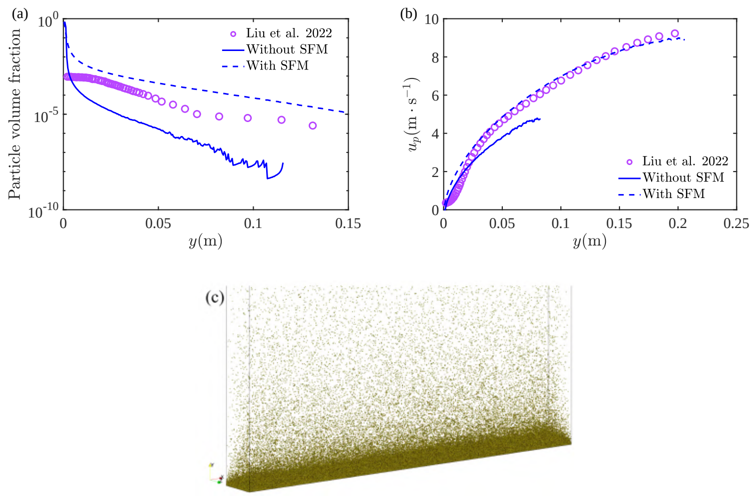

Figure 1: (a) Particle volume fraction and (b) streamwise particle velocity along the wall-normal direction, (c) instantaneous distributions of sand particles.

References

[1] Y. Wang, R. Hu. *A stochastic force model for a finite-size spherical particle in turbulence.* Int. J. Multiph. Flow, **191**, 105300, 2025.

[2] H. Liu, Y. Feng., X. Zheng. *Experimental investigation of the effects of particle near-wall motions on turbulence statistics in particle-laden flows.* J. Fluid Mech., **943**, A8, 2022.

Sediment transport in a half-channel turbulent flow: the effect of density

X. Jiang[1], P. Mirbod[2], C. Manes[1] and L. Brandt[1]
[1] Department of Environmental, Land and Infrastructure Engineering (DIATI), Politecnico di Torino, 10129 Torino, Italy
[2] Mechanical and Industrial Engineering Department, University of Illinois, USA

In this work, we conducted particle-resolved direct numerical simulations of half-channel turbulence laden with particle sediments. Spherical particles with the size 5% of the channel height are considered at a fixed bulk volume fraction $\phi = 18\%$, with the particle-to-fluid density ratio, $\gamma = \rho_p/\rho_f$, varying from 1.05 to 4.0. With the increase of the density contrast, the flow regime transitions from the suspension flow (for light particles) to the turbulent flow over static, particle sediments (for heavy particles). The particle volumetric flux increases with the decreasing density ratio, suggesting more efficient transport of particles of lighter weight. However, we find a non-monotonic variation of the pressure drop to maintain a constant flow rate of the mixture, indicating the non-monotonic change in the overall drag. In particular, the drag is always greater than the single-phase turbulence; the degree of drag enhancement first rises with γ and peaks at an intermediate density ratio $\gamma = 2$, and then decreases as γ further increases. The stress budget analysis demonstrates that the drag enhancement is mainly attributed to the turbulence augmentation in the upper half of the channel, manifested by the greatest contribution from the Reynolds stress at $\gamma = 2$. Further examining on the mean fluid velocity, we find a proper logarithmic scaling of the velocity profile by introducing an effective wall location, δ_{pw}. This quantity also varies non-monotonically with the density ratio, accounting for the non-monotonic drag enhancement. For light particles ($\gamma = 1.05$), the effective wall location is of the order of one particle diameter, reminiscent of the suspension flow of neutrally-buoyant particles. In the other limit of heavy particles ($\gamma \geq 2.5$), particles are compactly packed at the channel bottom with rare re-suspensions, like the flow over a porous wall; δ_{pw} is estimated by the bulk volume of the particles and the packing fraction. For the intermediate density ratio, however, particle sediments remain to exist at the channel bottom, while a considerable number of particles are re-suspended to great height, leading to an elevation of the effective wall location. We also identify the ripple-like structures near the surface of the sediment at $\gamma = 2$, which modulate the coherent structures of the turbulent flow. Particle arrangement within the sediment bed also varies with the particle weight, demonstrated by the particle packing fraction and statistical distribution of contacting neighbors.

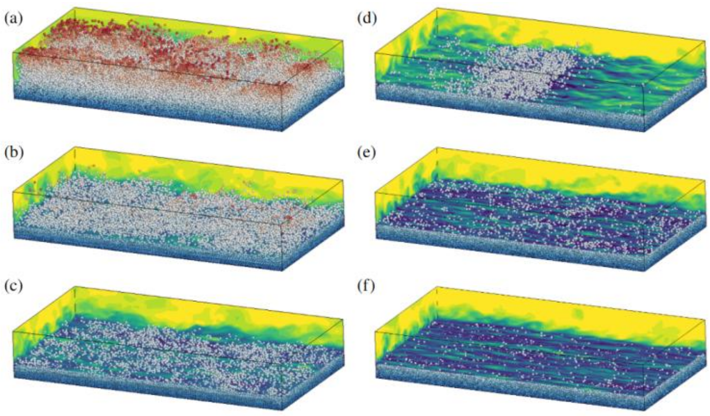

Figure 1: Snapshots of the particle-laden flows for the cases with different particle-fluid density ratios: (a) γ = 1.05, (b) γ = 1.2, (c) γ = 1.5, (d) γ = 2.0, (e) γ = 2.5, (f) γ = 4.0.

Numerical study of the randomness of single particle entrainment in wall turbulence on rough bed

Ping Wang[1] Yicong Zhu[1]

[1] Key Laboratory of Mechanics on Disaster and Environment in Western China, The Ministry of Education of China, Department of Mechanics, Lanzhou University, Lanzhou 730000, PR China

The initiation conditions of sediment particles by fluid is the first step in the formation and development of wind-blown sand flows. Both experiments and numerical simulations have observed particle transport phenomena occurring below the aforementioned average entrainment thresholds. This suggests that the entrainment thresholds for individual particles at low flow speeds do not align with the traditional statistical entrainment thresholds. To deeply investigate the complexity of fluid entrainment of a single particle, this study primarily examines the influence of particle bed arrangement and the indirect interactions between entrainable particles by DNS four-way coupled with DEM. For the former, the incipient particle is placed in two types of 'pockets' within a hexagonally arranged fixed particle bed, where there are either one ('top rolling' as shown in Figure 1 (a)) or two bed particles ('saddle rolling' as shown in Figure 1 (b)) acting as obstacles in front of the entrainable particle. For the latter, the number of movable particles on the fixed bed surface is gradually increased, thereby progressively reducing the spacing between them.

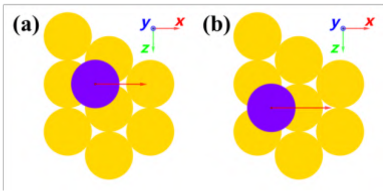

Figure 1: Two types of 'pockets' the entrainable particle located: (a) saddle rolling, (b) top rolling.

The simulation results indicate that for 'saddle rolling', the particle is mainly entrained from the saddle between the two particles. For the case of 'top rolling', at lower Shields numbers, the particle undergoes spanwise displacement and is entrained from the lateral saddle, while at higher Shields numbers, the particle is entrained directly by passing over the top of the bed particle. Meanwhile, the entrainment threshold for single-particle in 'saddle rolling' is significantly higher than in the 'top rolling'. Furthermore, as the number of entrainable particles gradually increases, the threshold Shields number for single-particle entrainment gradually increases. This can be attributed to the reduction of the average flow velocity at that height caused by the larger number of particle and the decreasement of the turbulent structures by the arrangement of particles. They all make it more difficult for 'events' to entrain particles. These findings indicate that, under the same Shields number conditions, the entrainment of single particles also exhibits considerable randomness.

References

T. Pähtz, O. Durán. The cessation threshold of nonsuspended sediment transport across aeolian and fluvial environments. *Journal of Geophysical Research: Earth Surface*, 123 (8), 1638–1666, 2018.

X. H. Zhao, M. Valyrakis, T. Pähtz, Z. S. Li. The role of coherent airflow structures on the incipient aeolian entrainment of coarse particles. *Journal of Geophysical Research: Earth Surface,* 129 (5), e2023JF007420, 2024.

Wave-induced transport of neutrally buoyant particles over a shallow rippled seabed: Insights from DNS

K. Jagadeesan[1], M. Mazzuoli[1] and A. G. Kidanemariam[2]
[1] University of Genoa, Via Montallegro 1, Genoa, 16145, Italy
[2] University of Melbourne, Grattan Street, Parkville, Victoria, 3010, Australia

We perform direct numerical simulations (DNS) of a progressive surface gravity wave over a rippled sea bottom, using an in-house pseudo-spectral finite difference method. The study is aimed at predicting the transport of pollutant micro-particles in the coastal environment. The Navier Stokes equations are solved in the transformed computational space obtained using a non-orthogonal algebraic transformation (Xuan and Shen, 2019). We consider non-breaking waves in the deep-to-shallow transitional zone, where the waves significantly interact with the bottom and affect its morphodynamics. In dimensional terms, the wave is characterized by wavelength $\lambda_w = 5.6\,\mathrm{m}$, with a steepness of about 2.5% and flow depth of $h = 0.7\,\mathrm{m}$; this results in a Reynolds number of approximately 5200, based on the bulk velocity and h. The ripples at the bottom are characterized by wavelength of $\lambda_b = 0.112\,\mathrm{m}$ and a steepness of 10%, that are representative of vortex ripples.

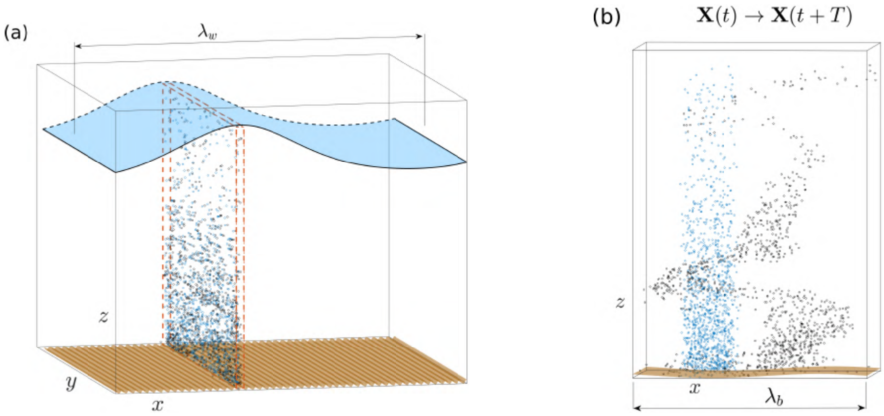

Figure 1: Lagrangian particle positions obtained over one wave period T, from the DNS. Particle positions $\mathbf{X}(t)$ are shown on the scale of (a) the surface wave or; (b) a single bottom ripple.

The mass transport velocity is obtained from the Lagrangian tracking of randomly-injected passive fluid tracers (cf. Figure 1). In particular, the Lagrangian flow properties are used to investigate the interaction between the wave-induced orbital motion and the wave boundary layer at the bottom. The present contribution also gives new insights on the vorticity dynamics close to the rippled bed and on the effects of the vortices on the net mass transport and potentially also on the transport of sediments.

References

A. Xuan and L. Shen. *A conservative scheme for simulation of free-surface turbulent and wave flows.* J. Comput. Phys., **378**, 18–43, 2019.

The current study is supported by "Ministero dell'Università e della Ricerca" under PRIN project "MARINE DUST" no. 202247MA8A (CUP D53C24003780001) while the computational resources are provided by CINECA (project no. IsB28_SEAWAVES) and EuroHPC JU (project no. EHPC-REG-2023R03-114).

Wall-resolved large-eddy simulation of electrification of wind-blown sand flows

X. Tan[1], H. Zhang[1] and X. Zheng[2]
[1] Center for Particle-laden Turbulence, Lanzhou University, Lanzhou 730000, PR China
[2] Research Center for Applied Mechanics, Xidian University, Xi?an 710071, PR China

We develop a wall-resolved large-eddy simulation model for the electrification of wind-blown sand flows at the wind-tunnel scale, formulated within an Eulerian–Lagrangian point-particle framework at a friction Reynolds number of $Re_\tau = 5200$. Instantaneous fields reveal correlated, self-organized turbulent structures in the wind velocity, particle distribution and electric field. Large-scale particle clustering in the outer region is closely associated with very-large-scale motions (VLSMs). Statistical analyses show a pronounced size-dependent charging effect, with positively charged particles being significantly larger than negatively charged ones. The mean charge-to-mass ratio increases in magnitude with height, and the three components of the electric field exhibit markedly different turbulent structures, reflecting their distinct generation mechanisms. Sand electrification substantially modifies particle transport by enhancing near-surface outward and sweep events, while reducing particle mass loading and horizontal fluxes. These changes alter the mean airflow and air-particle slip velocities, enhance streamwise and wall-normal particle fluctuations, and suppress spanwise fluctuations. Moreover, electrical effects weaken the overall turbulence modulation by particles, redistribute turbulent kinetic energy towards the near-surface region, and shift particle-induced energy dissipation to lower wall-normal locations. Spectral analyses further demonstrate that the enhancement of outer-layer VLSMs is closely associated with amplified turbulent production at the corresponding wall-normal locations and spatial scales, while electrical effects broaden the range of wall-normal locations and spatial scales over which particle feedback influences turbulence.

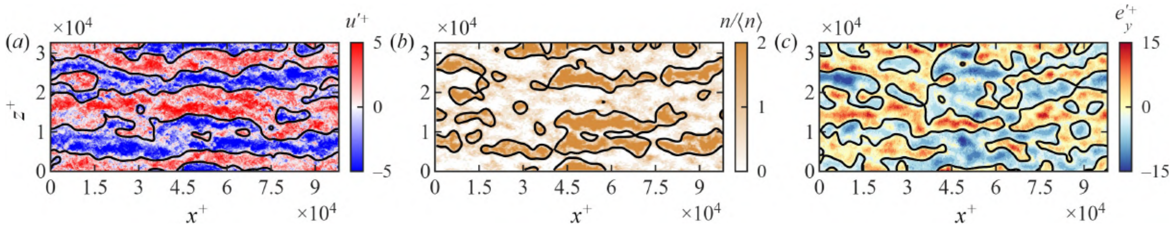

Figure 1: Instantaneous snapshots for the normalised (a) streamwise fluid fluctuating velocity, (b) particle number density, and (c) wall-normal fluctuating electric field.

References

Zheng, X.J., Huang, N. & Zhou, Y.H. 2003 Laboratory measurement of electrification of wind-blown sands and simulation of its effect on sand saltation movement. *J. Geophys. Res.-Atmos.* **108**, 4322.